Cytokine super-families affect adult stem cells: IL-6 and the skeletal muscle niche.

Paul Steyn

Thesis presented in partial fulfillment of the requirements for the degree of Master of Physiological Sciences at the University of Stellenbosch

Supervisors: Prof. Kathryn H. Myburgh and Dr. Robert M. Smith

March 2011

I, the undersigned, hereby declare that the work contained in this thesis is my own original work and that I have not previously in its entirety or in part submitted it at any university for a degree

……..

Signature

……..

Date

Abstract

Background: IL-6 belongs to a cytokine super-family known to affect cell proliferation, although other family members are better characterized. Proliferation promoting factors (IL-6) compete with differentiation promoting factors (myogenic regulatory factors: MyoD and myogenin) to affect cell cycle. Cell cycle progression is assessed by determining the proportion of cells shifting from arrest to chromatin synthesis and mitosis phases (G0/G1 and S and G2/M respectively).

Methods: This study assessed the effects of IL-6 on cell cycle progression and proliferation *vs.* differentiation of C2C12 skeletal myoblasts. Physiological doses (10 or 100 pg/ml) were compared to a high dose (10 ng/ml), with exposure lasting 48 hours (addition of IL-6 dose to proliferation medium at 0 and 24 hours). Acute signaling downstream of the IL-6 gp130 receptor was assessed after the first exposure.

Results: Propidium iodide analysis of nuclear material using flow cytometry indicated shifts in forward scatter. Both Low and Medium doses shifted a greater proportion ($p<0.05$) of cells from G0/G1 to S and G2M phases at 24 hours and all doses resulted in the same shift ($p<0.05$) at the 48 hour time point. However, the High dose significantly ($p<0.05$) increased myogenin expression at the 48 hour time point. Microscopy indicated that confluence was prevented by low seeding density and did not influence the result. Cells harvested at 5 minutes post stimulation indicated that all doses significantly increased STAT3 phosphorylation. 10 minutes post stimulation the High dose group sustained elevated levels of STAT3 phosphorylation.

Conclusions: Low and medium doses of IL-6 increase proliferation in a muscle satellite cell line by activating cell division and allowing myoblasts to remain in the active cell cycle. High doses of IL-6 increase differentiation by mediating upregulation of myogenic regulatory factors and this is thought to be due to prolonged STAT3 activation. Physiological control of myoblast behaviour by cytokines is evident and such control would be influenced by the severity of the endogenous cytokine response to various stimuli.

Uittreksel

Agtergrond: IL-6 behoort aan n sitokien super-familie bekend vir die affektering van sel verspreiding, alhoewel ander familie lede beter gekenmerk is. Bevordering van verspreiding faktore (IL-6) kompeteer met bevordering van differensiasie fatore (myogenic regulatory factors: MyoD en myogenin) om die sel siklus te affekteer. Sel siklus progressie word geassesseer deur die bepaling van die proporsie selle wat verskuif van arrestasie na chromatien sintese en mitose fases (G0/G1 en S en G2/M onderskeidelik).

Metodes: Hierdie studie het die effekte van IL-6 op die progressie van die sel siklus geassesseer asook die proliferasie *vs.* differensiasie van C2C12 skelet spier satelliet selle. Fisiologiese dosisse (10 en 100 pg/ml) was vergelyk tot n hoog dose (10 ng/ml), met blywende blootstelling van 48 uur (byvoeging van IL-6 dose tot verspreidings medium op 0 and 24 uur). Akute sein stroomaf van die IL-6 gp130 reseptor was ook geassesseer na die eerste blootstelling.

Resultate: Propidium iodide analise van kern materiaal deur vloei sitometrie het voorwaarts verskuiwing aangedui. Beide Laag and Medium doses het n groter proporsie ($p<0.05$) selle verskuif van die G0/G1 tot die S en G2M fases na 24 uur en alle dosisse het gelei in die selfde verskuiwing ($p<0.05$) by die 48 huur tyd punt. Alhoewel die Hoog dose myogenin uitdrukking aansienlik ($p<0.05$) verhoog het na 48 uur. Mikroskopie het aangedui dat samevloeiing voorkom was deur n lae loting digtheid en dit het nie resultate geaffekteer nie. Selle wat geoes was 5 minute na stimulasie het aangedui dat alle dosisse STAT3 fosforilasie laat toeneem het. 10 minute na stimulasie het die Hoog dose groep volgehoue vlakke van STAT3 fosforilasie besit.

Gevolgtrekkings: Laag en Medium dosisse van IL-6 verhoog verspreiding in n spier satelliet sel lyn deur die aktivering van sel deling en deur selle toe te laat om in die aktiewe sel siklus te bly. Hoog dosisse van IL-6 verhoog differensiase deur bemiddelende opstoot van myogenic regulatory factors en die gedagte is dat dit bewerkstellig word deur aanhoudende aktivering van STAT3. Fisiologies beheer van satelliet selle deur sitokiene is duidelik en die beheer sal beinvloed word deur die erns van die endogene sitokien reaksie op verskillende stimuli.

Acknowledgements

First and foremost I would like to thank my parents for the never-ending support.

Thank you to Dr. Rob Smith and Prof. Kathy Myburgh for excellent insight and guidance.

Thank you to all my colleagues in the Muscle group as well as all my other colleagues in the department.

Thank you to the NRF for financial support.

List of Abbreviations

ANOVA	Analysis of Variance
bHLH	basic Helix Loop Helix
DMEM	Dulbecco's Modified Eagle's Medium
ECL	Enhanced Chemiluminescence
ESC	Embryonic Stem Cell
FITC	Fluorescein Streptavidin
gp130	glycoprotein 130
HGF	Hepatocyte Growth Factor
IκBα	NFκB Inhibitory subunit
ICC	Immunocytochemistry
IGF	Insulin-like Growth Factor
IL-6	Interleukin-6
IL-6R	Interleukin-6 Receptor
JAK	Janus Kinase
LIF	Leukemia Inhibitory Factor
M-phase	Mitosis-phase
MHC	Myosin Heavy Chain
MRF	Myogenic Regulatory Factor
NFκB	Nuclear Factor Kappa B

PBS	Phosphate Buffered Saline
PCNA	Proliferating Cell Nuclear Antigen
pSTAT3	phosphorylated STAT3
PVDF	Polyvinylidine Fluoride
S-phase	Synthesis-phase
SDS-PAGE	Sodium Dodecyl Sulphate Polyacrylamide Gel Electrophoresis
SEM	Standard Error of the Mean
Ser	Serine
STAT3	Signal Transducer and Activator of Transcription
TBS-T	Tris Buffered Saline-Tween 20
tSTAT3	total STAT3
TNF-α	Tumor Necrosis Factor Alpha
Tyr	Tyrosine
uSTAT3	unphosphorylated STAT3
VCAM1	Vascular Cell Adhesion Molecule 1

List of Tables

List of Figures

Figure 16: Immunocytochemical Analysis of Control group visualizing the expression of PCNA (A), Myogenin (B), PCNA & Myogenin (C) and PCNA, Myogenin and DAPI (D) at 48 hours.

Figure 17: Immunocytochemical Analysis of High IL-6 treatment group visualizing the expression of PCNA (A), Myogenin (B), PCNA & Myogenin (C) and PCNA, Myogenin and DAPI (D) at 48 hours.

Figure 18: Immunocytochemical Analysis of Medium IL-6 treatment group visualizing the expression of PCNA (A), Myogenin (B), PCNA & Myogenin (C) and PCNA, Myogenin and DAPI (D) at 48 hours.

Figure 19: Immunocytochemical Analysis of Low IL-6 treatment group visualizing the expression of PCNA (A), Myogenin (B), PCNA & Myogenin (C) and PCNA, Myogenin and DAPI (D) at 48 hours.

Figure 20: Immunocytochemical Analysis of Control group visualizing the Mitochondria (A), pSTAT3 (B), Mitochondria & pSTAT3 (C) and Mitochondria, pSTAT3 and DAPI (D) at 5 minutes. Arrows provided to indicate the same group of cells in each image.

Figure 21: Immunocytochemical Analysis of High IL-6 treatment group visualizing the Mitochondria (A), pSTAT3 (B), Mitochondria & pSTAT3 (C) and Mitochondria, pSTAT3 and DAPI (D) at 5 minutes.

Figure 22: Immunocytochemical Analysis of Medium IL-6 treatment group visualizing the Mitochondria (A), pSTAT3 (B), Mitochondria & pSTAT3 (C) and Mitochondria, pSTAT3 and DAPI (D) at 5 minutes.

Figure 23: Immunocytochemical Analysis of Low IL-6 treatment group visualizing the Mitochondria (A), pSTAT3 (B), Mitochondria & pSTAT3 (C) and Mitochondria, pSTAT3 and DAPI (D) at 5 minutes.

Figure 24: Immunocytochemical Analysis of Control group visualizing the Mitochondria (A), pSTAT3 (B), Mitochondria & pSTAT3 (C) and Mitochondria, pSTAT3 and DAPI (D) at 10 minutes.

Figure 25: Immunocytochemical Analysis of High IL-6 treatment group visualizing the Mitochondria (A), pSTAT3 (B), Mitochondria & pSTAT3 (C) and Mitochondria, pSTAT3 and DAPI (D) at 10 minutes.

Figure 26: Immunocytochemical Analysis of Medium IL-6 treatment group visualizing the Mitochondria (A), pSTAT3 (B), Mitochondria & pSTAT3 (C) and Mitochondria, pSTAT3 and DAPI (D) at 10 minutes.

Figure 27: Immunocytochemical Analysis of Low IL-6 treatment group visualizing the Mitochondria (A), pSTAT3 (B), Mitochondria & pSTAT3 (C) and Mitochondria, pSTAT3 and DAPI (D) at 10 minutes.

Figure 28: Immunocytochemical Analysis of Control group visualizing the Mitochondria (A), pSTAT3 (B), Mitochondria & pSTAT3 (C) and Mitochondria, pSTAT3 and DAPI (D) at 15 minutes.

Figure 29: Immunocytochemical Analysis of High IL-6 treatment group visualizing the Mitochondria (A), pSTAT3 (B), Mitochondria & pSTAT3 (C) and Mitochondria, pSTAT3 and DAPI (D) at 15 minutes.

Figure 30: Immunocytochemical Analysis of Medium IL-6 treatment group visualizing the Mitochondria (A), pSTAT3 (B), Mitochondria & pSTAT3 (C) and Mitochondria, pSTAT3 and DAPI (D) at 15 minutes.

Figure 31: Immunocytochemical Analysis of Low IL-6 treatment group visualizing the Mitochondria (A), pSTAT3 (B), Mitochondria & pSTAT3 (C) and Mitochondria, pSTAT3 and DAPI (D) at 15 minutes.

Figure 32: Immunocytochemical Analysis of Control group visualizing the Mitochondria (A), pSTAT3 (B), Mitochondria & pSTAT3 (C) and Mitochondria, pSTAT3 and DAPI (D) at 30 minutes.

Figure 33: Immunocytochemical Analysis of High IL-6 treatment group visualizing the Mitochondria (A), pSTAT3 (B), Mitochondria & pSTAT3 (C) and Mitochondria, pSTAT3 and DAPI (D) at 30 minutes.

Figure 34: Immunocytochemical Analysis of Medium IL-6 treatment group visualizing the Mitochondria (A), pSTAT3 (B), Mitochondria & pSTAT3 (C) and Mitochondria, pSTAT3 and DAPI (D) at 30 minutes.

Figure 35: Immunocytochemical Analysis of Low IL-6 treatment group visualizing the Mitochondria (A), pSTAT3 (B), Mitochondria & pSTAT3 (C) and Mitochondria, pSTAT3 and DAPI (D) at 30 minutes.

Figure 35E: Immunocytochemical Analysis of Control group as well as High and Low IL-6 treatment group visualizing the Mitochondria (red), pSTAT3 (green) and the nucleus DAPI (D) at 5, 10, 15 and 30 minutes.

Figure 36: Representation of phosphorylated STAT3 expression after IL-6 treatment. (n=3, Mean±SEM)

Figure 37: Representation of total STAT3 expression after IL-6 treatment. (n=3,Mean±SEM)

Table of Contents

1. Introduction

1.1 Satellite cells

These cells are responsible for the repair of muscle fibers after muscle injury induced by trauma or unaccustomed strenuous exercise and during diseased states within the skeletal muscle (Webster and Blau 1990; Cooper, Butler-Browne et al. 2006). Satellite cells are also responsible for muscle growth and some aspects of muscle adaptation (Goldberg, Etlinger et al. 1975; Rosenblatt, Yong et al. 1994; Gallegly, Turesky et al. 2004; Anderson 2006). Since their discovery (Cooper and Konigsberg 1961), satellite cells have been extensively studied and characterized for these postnatal roles and their roles in embryonic muscle development. Satellite cells are also present within many vertebrates (Asakura 2003; Redshaw, McOrist et al. 2010) and are referred to by many different names including skeletal muscle myoblasts as well as muscle progenitor cells. The study of these cells could give valuable insight into mechanisms of muscle repair as well as muscle adaptation.

1.1.1 The Origin of satellite cells

The vertebrate skeletal muscles are derived from the mesodermal precursor cells, which originate from the somites, which are cells located in the dorsal part of the dermomyotome (DM). The epaxial dermomyotome, next to the neural tube and notochord, gives rise to the deep back muscles whereas the rest of the muscles in the body and the limbs derive from the hypaxial extremity of the dermomyotome (Buckingham, Bajard et al. 2003). During the development of the embryo the specification of these mesodermal precursor cells is controlled by positive and negative signals from surrounding tissue. In order for the specification to occur, the basic helix-loop-helix (bHLH) factors must form heterodimers with the myogenic regulatory factor family (MRF) (Seale and Rudnicki 2000; Otto, Collins-Hooper et al. 2009). Examples of MRFs with bHLH motifs are MyoD and Myf5 and these are present in proliferating myogenic cells, referred to as myoblasts These proliferating myoblasts will then exit the cell cycle in order to differentiate into myocytes that express the “late” MRFs myogenin, MRF4 as well as the contractile protein myosin heavy chain (MHC). It is evident form this early stage that MRFs play a big role in the determination of the satellite cell’s cell cycle fate. They will exit the cell cycle and migrate laterally to form the first muscle mass, the myotome (MT). Pax3 is responsible for myogenesis in the lateral myotome. The mononucleated myocytes will then fuse to each other to form a multinuclear syncytium and

these will mature into functional muscle fibers that possess the ability to contract. During this whole process a handful of myoblasts do not differentiate and they will be found on the surface of individual skeletal muscle fibres in a quiescent state (Asakura, Seale et al. 2002). These are referred to as satellite cells and are responsible for muscle repair as well as muscle adaptation.

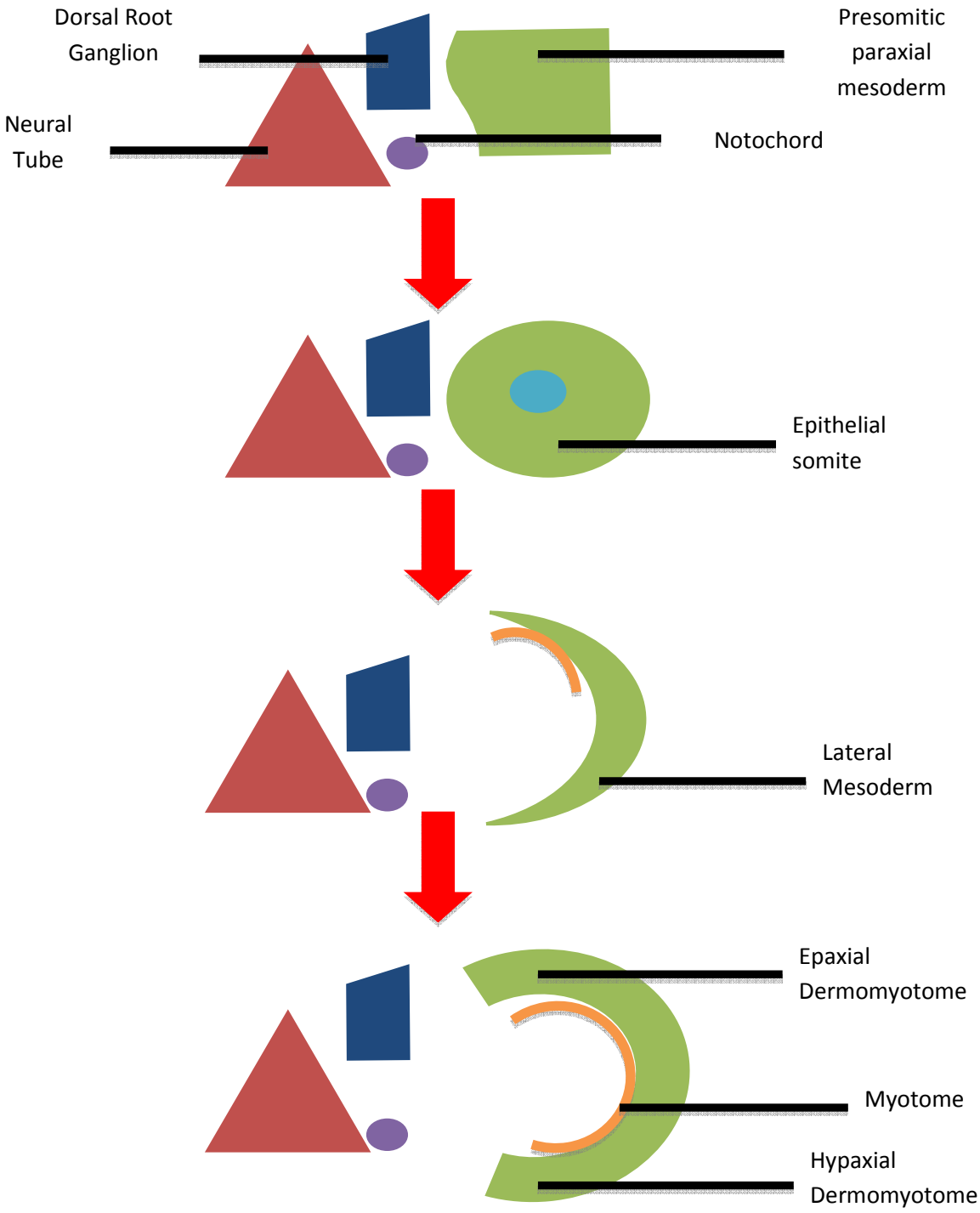

Figure 1: Cross sectional view of muscle formation during somitogenesis where the presomitic paraxial mesoderm gives rise to the epithelial somite and lateral mesoderm. The mesoderm is converted to the dermomyotome as well as the myotome, which is the origin of the skeletal muscle satellite cells. (Adapted from Buckingham, Bajard et al. 2003)

1.1.2 Morphology and location

Satellite cells are found above the sarcolemma and below the basal lamina of mature skeletal muscle fibers (Cooper, Butler-Browne et al. 2006)(Fig 2.) within depressions of the skeletal muscle caused by the presence of the satellite cells (Holterman and Rudnicki 2005). This location is ideal for the activation of these cells as the cell can easily move from its quiescent position and become activated. These cells are mononuclear with a small amount of cytoplasm (Asakura 2003). Few organelles are present and heterochromatin levels are higher than that of euchromatin (Holterman and Rudnicki 2005). Satellite cell population will be at its highest at birth (Dhawan and Rando 2005). Activated satellite cells exhibit an altered morphology. The cell's cytosolic fraction will have a larger volume and cell extensions will start to form to facilitate movement. There will be an increase in the appearance of organelles and the level of heterochromatin will decrease (Hawke and Garry 2001). This movement and subsequent activation of the satellite cells is vital in the repair and maintenance of skeletal muscle integrity.

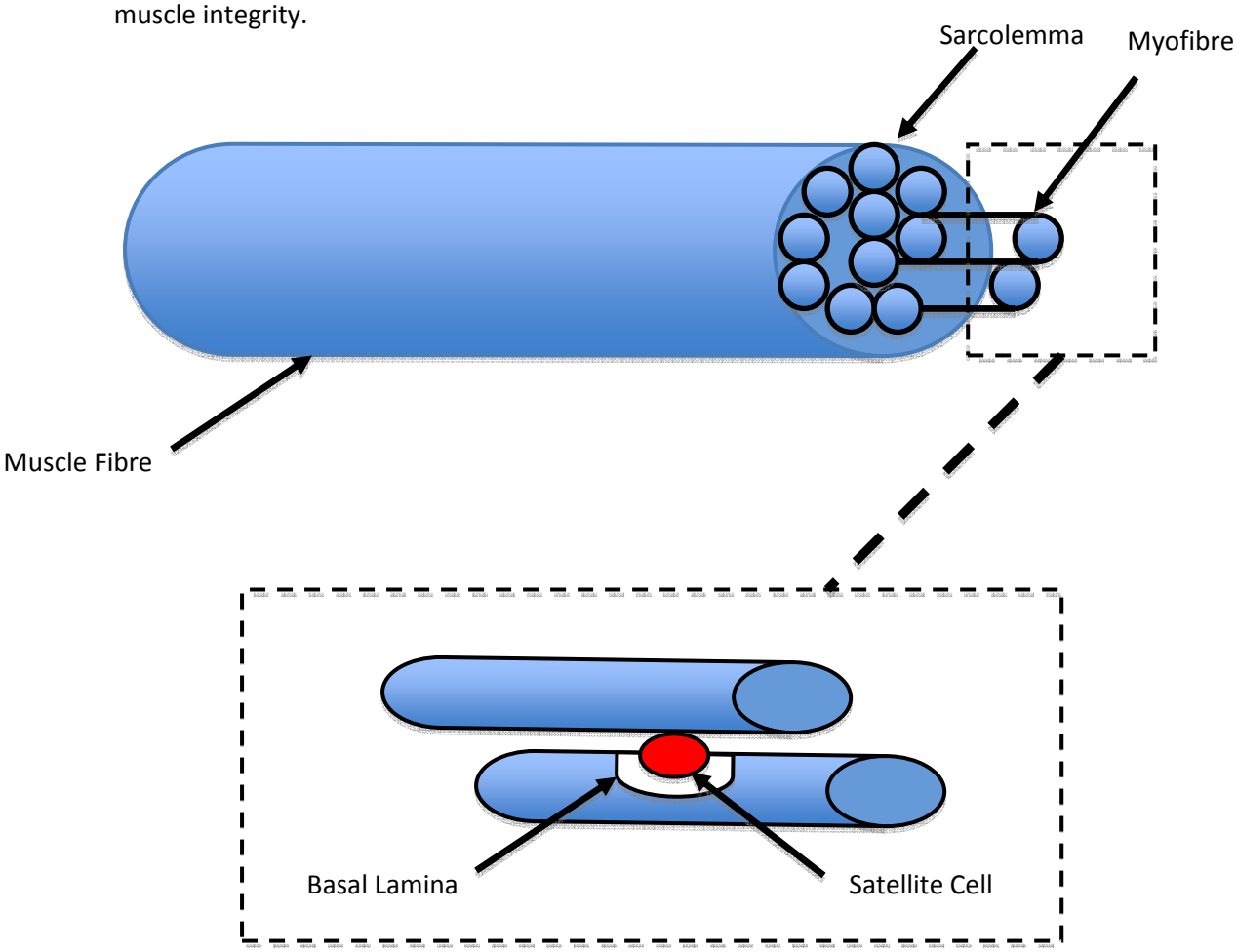

Figure 2: Cross sectional view of a skeletal muscle fibre indicating the relative position of a satellite cell above the sarcollemma and below the basal lamina

1.1.3 Satellite cell life cycle

In their position above the sarcolemma and below the basal lamina of myofibres the satellite cells are usually quiescent. Activation of satellite cells can occur as a result of injury or regular muscle growth. Once the cell is activated it is separated from under the basal lamina. The activated myoblasts start to proliferate rapidly in order to increase their numbers. A small number of newly formed satellite cells will return to the quiescent state in order to replenish the satellite cell pool (Charge and Rudnicki 2004). Cells that do not return to quiescence will undergo differentiation to form specialized muscle cells. The specialized muscle cells will aggregate and start to fuse in order to form myotubes consisting of multiple, specialized muscle cells. The newly formed myotubes will migrate to the site of injury or growth and fuse with the previously formed myofibres. Alternatively, individual myoblasts will fuse to the existing fibres (Dhawan and Rando 2005).

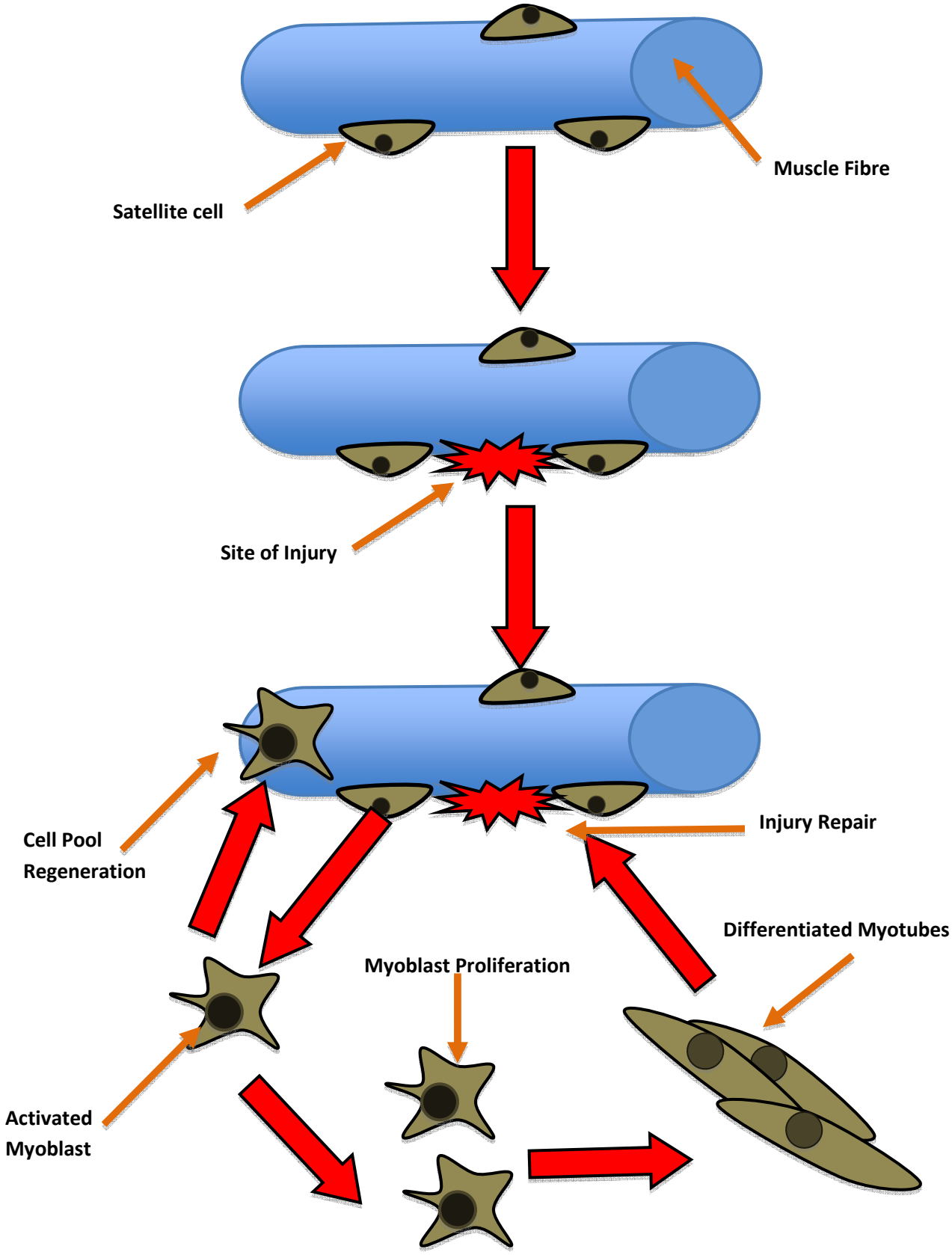

Figure 3: When injury occurs within the muscle fibre, the satellite cell is removed from its quiescent state and becomes activated. The activated cells will undergo proliferation and a certain amount of newly formed cells will return to quiescence to replenish the cell pool. Newly formed myoblasts will also become specialized and differentiate into myotubes in order to repair the site of injury

1.2 Markers of satellite cells

At the early stages of satellite cell discovery, it was only possible to identify satellite cells by means of ultramicroscopic criteria. Recently many proteins expressed by satellite cells have been discovered and have been utilized to identify these cells. These include proteins capable of controlling the exit of satellite cells from the cell and are referred to as myogenic regulatory factors (MRFs).

In a normal muscle state, the satellite cells are dormant or quiescent. Quiescent cells express Pax7 (Seale, Sabourin et al. 2000), M-cadherin (Irintchev, Zeschnigk et al. 1994) as well as CD34 and Myf5 (Beauchamp, Heslop et al. 2000) along with caveolin 1 (Volonte, Liu et al. 2005), c-met (Cornelison and Wold 1997) and VCAM1 (Cornelison and Wold 1997). The role and importance of each of these factors will now be discussed. It will also be mentioned how specific they are for satellite cells, or whether they need to be used with other markers or other criteria in order to identify the satellite cells more clearly.

Pax7 is the most unique marker of quiescent satellite cells. Pax7 is a transcription factor, which localizes to the nuclei, where it is situated in discreet peripheral locations (Seale, Sabourin et al. 2000). The importance of this is that the number of cells that actively express Pax7 can be correlated with the number of quiescent satellite cells. Vascular cell adhesion molecule 1 (VCAM1) mediates the cell-to-cell interactions by binding to the α4β1 integrin molecule (Cornelison and Wold 1997). VCAM1 expression is found in skeletal muscle cells in adults and acts as a marker, although it is also expressed in vascular endothelium hence its name. VCAM1 will only be seen in quiescent satellite cells and can be utilized in flow cytometry to identify the quiescent cells. M-cadherin is a calcium-dependent adhesion molecule that can be found in the quiescent cells, but not in differentiated myotubes (Irintchev, Zeschnigk et al. 1994). This is also important in the identification of satellite cells. It has been found that cells expressing m-cadherin also express the CD34 marker and that when m-cadherin is not expressed, CD34 is also absent (Beauchamp, Heslop et al. 2000). This may suggest a functional expression relationship between these proteins. Myf5 is a factor responsible for gene regulation. Myf5 possesses the basic-helix-loop helix structure. This motif provides a platform for the effective control of genes and is also capable of regulating genes downstream from this motif. It is not only a myogenic factor but is also responsible for the control of early somitogenesis prior to myoblast specification (Ancey, Menet et al. 2003).

Satellite cells become activated and start to proliferate when muscle injury occurs as well as during growth and muscular remodeling. Proliferating satellite cells express high amounts of the MRFs, MyoD and Myf5, as well as proliferating cell nuclear antigen (PCNA). PCNA levels are increased in cells that are actively proliferating (Schafer 1998). PCNA is a subunit of the DNA polymerase δ. The expression of PCNA is mostly seen in the synthesis phase of the cell cycle (Tauber, Lichnovsky et al. 1996; Ishido, Kami et al. 2004). MyoD can be seen as a pro-differentiation marker as it is seen in cells progressing from proliferation to differentiation.

After proliferation, the cells differentiate and the myoblasts fuse in order to form new myofibres. The protein products of MyoD are required for the induction of myogenin, which will ultimately lead to the onset of differentiation. The differentiation phase is characterized by a high level expression of the MRFs, myogenin and MRF4 (Kitzmann and Fernandez 2001; Wei and Paterson 2001; Rudnicki, Le Grand et al. 2008). As reviewed by Charge and Rudnicki, these signal the irreversible withdrawal of satellite cells from the cell cycle and terminal differentiation (Charge and Rudnicki 2004). The newly formed myoblasts or myotubes will associate with the damaged fibres to complete regeneration.

Although satellite cells are capable of performing many cell divisions, they differ from immortal myogenic cell lines, because just like normal diploid cells they only possess a limited capacity for division. After a short number of divisions these cells enter irreversible growth arrest, named senescence. The limited number of divisions of these cells is known as the “Hayflick limit” (Hayflick and Moorhead 1961). The reason for the limited division of these cells is as a result of the absence the telomerase enzyme. This will lead to telomere exhaustion and the regulatory enzymes in the DNA repair mechanism will recognize the DNA as foreign and degradation of the DNA will occur (Kadi and Ponsot 2010). This is of importance as a decrease in satellite cell numbers will lead to muscle dysfunction and hindered muscle repair.

Table 1: Satellite Cell molecular markers (Adapted from Fouche 2007, unpublished)

Molecular Marker	Satellite cell state	Reference
CD34	Quiescent	(Baron, Copizza et al. 2004)
CD56	Quiescent, activated and proliferating	(Hawke and Garry 2001; Baron, Copizza et al. 2004)
MNF	Quiescent, activated and proliferating	(Garry, Yang et al. 1997)
Pax7	Quiescent, activated and proliferating	(Olguin and Olwin 2004)
c-met	Quiescent, activated and proliferating	(Cornelison and Wold 1997)
M-cadherin	Quiescent, activated and proliferating	(Cornelison and Wold 1997)
VCAM-1	Quiescent, activated and proliferating	(Hawke and Garry 2001; Baron, Copizza et al. 2004)
PCNA	Activated and Proliferating	(Johnson and Allen 1993)
Desmin	Activated and Proliferating	(Bockhold, Rosenblatt et al. 1998)
Myf5	Activated and Proliferating	(Cornelison and Wold 1997)
MyoD	Activated and Proliferating, committed to differentiation	(Cornelison and Wold 1997)
myogenin	Terminal differentiation	(Hawke and Garry 2001; Baron, Copizza et al. 2004)
MHC	Terminal differentiation	(Hawke and Garry 2001; Baron, Copizza et al. 2004)
MRF4	Terminal differentiation	(Hawke and Garry 2001; Baron, Copizza et al. 2004)

1.3 The cell cycle

The typical cell cycle can be divided into four main stages namely G1, S, G2/M and the M phase (McKay, Toth et al. 2010).
In the G1 phase of the cycle, cell division is initiated. This usually occurs as a result of the cell reacting to growth signals or mitogens. The G1 phase is usually associated with the differentiating process of the cell and can act as a good direct measure of the proportion of cells proliferating and preparing for differentiation. This is the phase in which most of the cells will be found. In the S-phase DNA is newly synthesized in preparation for another cell division. This phase is mostly associated with the proliferation step in the activated satellite cell's cell cycle. In the G2/M phase the newly synthesized chromosomes are checked for defects in the DNA synthesis and the chromosomes will be aligned.
In the M phase the chromosomes will be attached by spindles in order to effectively separate the DNA equally among the daughter cells (Alm and Oredsson 2009).
It is possible for cells to exit the cell cycle and undergo differentiation and by doing so move into the G0 phase.

In studies that focused on the cell cycle and its progression, the fractions of cells in specific phases are scrutinized and by doing so it was possible to determine whether a certain growth factor stimulates differentiation or the proliferation of the specific cells. When a growth factor is administered that is known to increase differentiation there will be a significantly higher fraction in the G1 phase and a lower fraction in the S and G2/M phase when compared to the control group (Jayaraman and Marks 1993). When a cytokine is administered that is known to increase proliferation, a G1/S cycle progression will occur. In this process the fraction of cells in the G1 phase will be decreased as more cells will enter S and G2/M phase and this can be attributed to increased proliferation (Chakravarthy, Abraha et al. 2000).

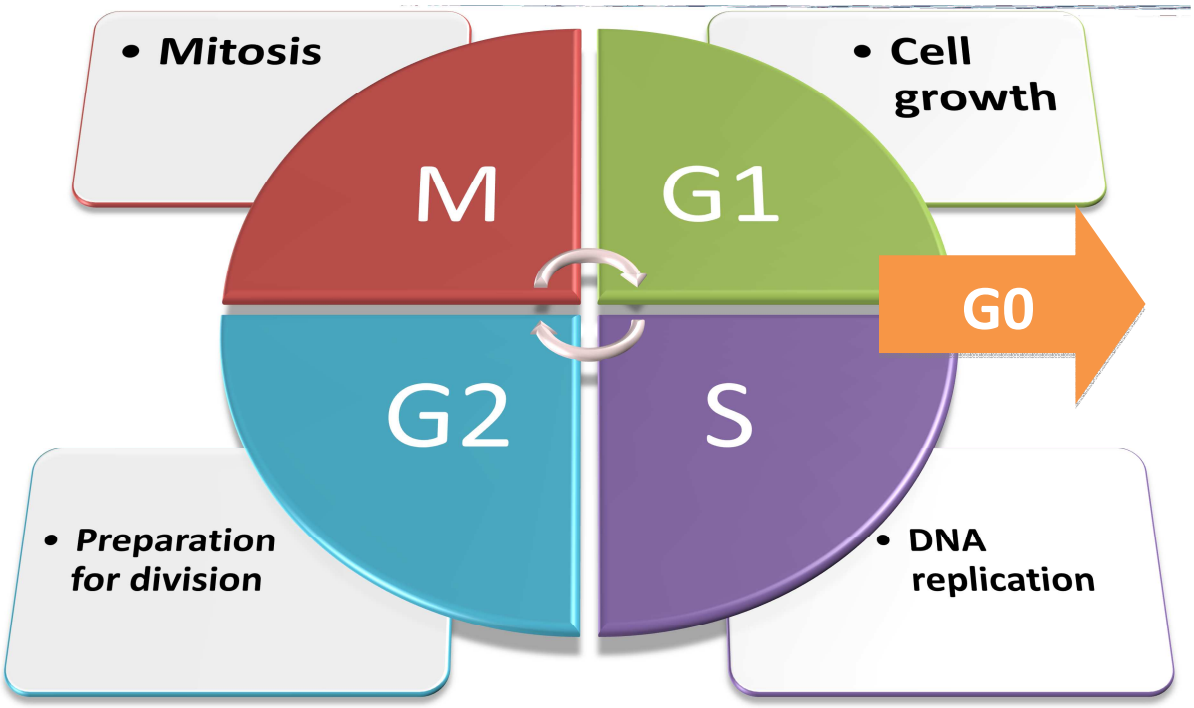

Figure 4: The satellite cell cycle can be divided into four stages. The G1 phase is associated with cell growth. In order for cells to undergo mitosis, DNA content has to be doubled and this occurs in the S phase. In the G2 phase the duplicated chromosomes align in preparation for mitosis, which occurs in the M phase. When cells exit the cell cycle in order to undergo differentiation they will movie into the Go phase

1.3.1 Regulation of the cell cycle

There are many markers of satellite cells that are responsible for differentiation or proliferation, but there are molecules upstream of these that control the satellite cell cycle. The myogenic regulatory factor, MyoD as well as the cyclin dependent kinases control the progression of cells through the cell cycle (Dhawan and Rando 2005).

MyoD plays a pivotal role in the progression of the cell cycle, thus its expression fluctuates throughout the cell cycle. When the satellite cells are in the S-phase of the cell cycle MyoD levels are low whereas its levels are elevated in the differentiation associated G1 phase. When cells exit the cell cycle, MyoD levels increase to facilitate differentiation by upregulation of the cyclin-dependent kinase inhibitor p21, cyclin D3, Rb and myogenin (Kitzmann and Fernandez 2001). p21 promotes differentiation by preventing cell cycle progression, whereas Rb prevents cells from entering the S-phase of the cell cycle by seizing transcriptional activity of the E2F family (Chellappan, Hiebert et al. 1991).

In order for activated satellite cells to return to quiescence they need to undergo arrest. This is accompanied by a decrease in MyoD expression, a downregulation of M-cadherin as well as the induction of the Rb family member p130. The growth-suppressive molecules p130 and p27 are found in quiescent cells and they are thought to be induced by the disintegrin, ADAM12 (Cao, Zhao et al. 2003). These growth-suppressive molecules are responsible for the repression of genes associated with the S-phase.

All of these molecules act in unison to assert strict control over the proliferation, differentiation as well as the quiescence of satellite cells and in order to effectively control the progression of satellite cells through the cycle, it is vital to regulate the expression and activity of these molecules.

1.3.2 Known mitogens of the satellite cell cycle

Satellite cells lend themselves to control by a wide array of growth factors and cytokines. In order for a certain molecule to be regarded as a mitogen it must be able to effectively manipulate the cell cycle, and be able to steer the relevant cells into the proliferative or the differentiation direction.

1.3.2.1 Tumor necrosis factor-α (TNF-α)

TNF-α is a pro-inflammatory cytokine synthesized and secreted by active macrophages and also plays a controlling role in muscle repair (Li and Schwartz 2001). It is capable of mediating

the inflammatory response as well as the apoptotic and muscle protein catabolic response (Tracey and Cerami 1992). Myocytes are also capable of producing TNF-α. When muscle injury occurs TNF-α diffusion to the site of injury is increased. The levels of TNF-α concentration also increase in the skeletal muscle after strenuous exercise (Ostrowski, Rohde et al. 1999). However, this is usually quite low. In order for muscle regeneration to proceed effectively, a high concentration of TNF-α must be present. Primary myoblasts cultured in TNF-α supplemented media (2-6 ng/ml) showed an increase in proliferation and an increase in the progression of cells from the G1 to the S phase of the cell cycle (Li 2003). TNF-α is also capable of activating quiescent satellite cells and by doing so will allow the cells to enter the cell cycle. TNF-α can thus be regarded as a cytokine that will enhance satellite cell proliferation as well as their activation.

Doses of TNF-α ranging from 0.01-1 ng/ml, have been shown to perform a dose-dependent halt in myogenin protein synthesis by in skeletal myoblasts (Broussard, McCusker et al. 2003). A previous study performed in our department found that chronic TNF-α doses ranging from 0.5 to 10 ng/ml negatively regulate markers of differentiation in a dose dependent manner within skeletal muscle myoblasts (Fouche 2007. Unpublished).

TNF-α concentrations found in muscle have been fairly well studied and the ability of these different concentrations to affect cell cycle progression of skeletal muscle myoblasts is well characterized.

1.3.2.2 Insulin-like growth factor-I (IGF-I)

IGF-I is a growth factor that has also been implicated in the effective control of the satellite cell cycle as well as proliferation. IGF-I is a polypeptide growth factor, which is homologous to insulin. IGF-I plays a crucial role in embryogenesis as well as organogenesis (Velcheti and Govindan 2006). Studies have been performed where the IGF-I transgene was constitutively expressed in mice in order to assess its effects on the satellite cells (Chakravarthy, Abraha et al. 2000). It was found that these satellite cells were capable of doubling their population five times more than the wild type cells. The action of IGF-I is mediated by means if the PI3K/Akt pathway which is independent from MAPK activity. These cells were also able to progress the transition of the cell cycle from the G1 to the S phase, which indicates an increased proliferative capability of these cells over expressing the IGF-I and this has lead to the belief that IGF-I is a cytokine that enhances the proliferation of satellite cells.

1.3.2.3 Hepatocyte growth factor (HGF)

HGF is responsible for increasing proliferation within skeletal myoblast (Gal-Levi, Leshem et al. 1998; Leshem, Spicer et al. 2000; Miller, Thaloor et al. 2000). HGF also possesses a basic helix-loop-helix (bHLH) protein motif and it is the expression of this protein that is responsible for the facilitation of proliferation. HGF also asserts control over proliferation through SHP2, a protein tyrosine phosphatase and in the absence of this phosphatase, proliferation is halted and differentiation is set underway (Li, Reed et al. 2009). Interestingly, treatment of satellite cells with high concentrations of HGF (50 ng/ml) inhibits proliferation and this phenomenon will be discussed in later chapters in relation to IL-6.

1.3.2.4 Interleukin-6 super-family

The IL-6 super-family of cytokines includes IL-11, LIF (leukemia inhibitory factor), oncostatin M, CT-1 (cardiotrophin-1), CLC (cardiotrophin-like cytokine) as well as CNTF (ciliary neurotrophic factor)(Heinrich, Behrmann et al. 2003).

The IL-6 family share similar receptor complexes, which include the 130-kDa membrane glycoprotein, gp130, vital for signal transduction. The IL-6 family assembles their receptor complexes in a similar manner as well. IL-6 binds to IL-6R and this IL-6/IL-6R complex then associates with the gp130 subunit, allowing it to homodimerize (Taga and Kishimoto 1997).

Although the IL-6 family has similar receptor complexes the members have varied effects on the cell cycle progression of satellite cells.

A vast amount of studies have assessed the effects of LIF on satellite cell proliferation and the majority have found that LIF increases proliferation within skeletal myoblasts (Megeney, Perry et al. 1996; White, Davies et al. 2001; Spangenburg and Booth 2002; Jo, Kim et al. 2005). LIF is thought to produce an increase in Janus-activated Kinase (JAK) 2 phosphorylation, which could be reversed by a specific inhibitor of JAK2, tryphostin AG490. This increase in JAK2 causes a downstream increase in signal transducers and activators of transcription (STAT3) phosphorylation as well as STAT3 transcriptional activity (Spangenburg and Booth 2002) and this signaling pathway is thought to facilitate proliferation.

Oncostatin M has been shown to inhibit the proliferation of skeletal muscle cells by blocking the cell cycle progression from G0/G1 to the S phase (Kim, Jo et al. 2008). Oncostatin M reduces the levels of cyclin D1 through ubiquitin/proteasome proteolysis and this thought to be regulated by the activation of STAT3

Cardiotrophin-1 has been implicated as a regulator of skeletal muscle differentiation. Cardiotrophin-1 suppresses the activity of MRFs as well as suppressing the promoter activation of myogenin, which is a pro-differentiation molecule. It is also capable of activating the signal transducer and activator of transcription 3 (STAT3) signaling pathway. It has also been shown to play a key role in the regeneration as well as the hypertrophy of skeletal muscle in rats (Nishikawa, Sakuma et al. 2005).

Human Vascular Smooth Muscle Cell (VSMC) proliferation is inhibited by the family member IL-11 is a growth factor that has been shown to inhibit the proliferation of human Vascular Smooth Muscle Cells (VSMC) (Zimmerman, Selzman et al. 2002). The addition of IL-11 to VSMC cells halted basic fibroblastic growth factor (bFGF)-induced proliferation. IL-11 also arrested the expression of the two NF kappa B-dependent cytokines, IL-8 and IL-6.

Many members of the IL-6 super-family are very well characterized and each of the these member's effect on proliferation and differentiation has been well studied. The effect of one member of this family, IL-6, on cell cycle progression has not been determined and the literature currently available seems to be contradictory or lacking.

1.4 Interleukin-6

It has been suggested that the cytokine Interleukin-6 (IL-6) could also be a mitogen. Very few studies have been done regarding this and the role of IL-6 on satellite cell cycle progression is yet to be determined. One study has been performed where the synergistic effects of TNF-α in conjunction with IL-6 was tested (Al-Shanti, Saini et al. 2008). The treated C2C12 cells showed a marked ability to induce proliferation by facilitating the G1 to S phase progression.

1.4.1 Sources of IL-6

IL-6 is a glycoprotein with a molecular mass of 21 to 28 kDa with a WSXWS motif in the C-terminal and a distinct pattern of cysteine residues in the N-terminal. It consists of four long α-helices that form a straight protein structure(Heinrich, Behrmann et al. 2003). Its production is dependent on the lymphoid as well as the non-lymphoid cells. IL-6 production is induced in T-cells or T-cell clones by their mitogens or specific antigens. IL-6 production can also be induced by viruses in fibroblasts or the central nervous system (Jacques, Bleau et al. 2009). Peptide factors like IL-1, TNF and platelet-derived growth factor (PDGF) can induce the production of IL-6 (Wang, Zhu et al. 2010). Although it was considered that these were the main sources of IL-6 it was found that one of the main sources of IL-6 found in muscle is produced by the muscle fibres themselves (Tseng, Su et al. 2010).

1.4.2 The IL-6 receptor

The receptor that binds IL-6 consists of two molecules namely the 80 kDa IL-6 binding protein (α chain) and the 130 kDa gp130 signal transducer. IL-6 does not bind directly to the gp130, but binds to the α chain and creates a complex with a high-affinity for the gp130 molecule. This receptor belongs to the type 1 cytokine receptor super-family that is characterized by conserved four cysteine residues and a tryptophan-serine-X-tryptophan-serine motif, which is located outside the transmembrane domain. The cytoplasmic domain of the IL-6R is not necessary for IL-6 mediated signal transduction (Heinrich, Behrmann et al. 2003). When IL-6 binds to the receptors, the ligand is internalized and this is mediated by the signal transducer subunits (Heinrich, Behrmann et al. 1998). This internalization of the ligand appears to be independent of the formation of the IL-6/IL-6R complex and that the endocytosis of the gp130 subunit is constitutive (Thiel, Dahmen et al. 1998). This is important as this internalization could affect the sensitivity of the receptor to IL-6.

When IL-6 binds to IL-6Rα and gp130, it induces the formation of a hexamer consisting of two members each. IL-6 has three receptor binding sites namely around Arg-179 on the D helix with affinity for the binding of IL-6Rα, secondly at residues composed from helix A and C is the binding site for one gp130 and thirdly centered around the N-terminal end of helix D is the binding site for the other gp130. The residues around Asn-230 and His-280 of the IL6-Rα are prominent in the interaction between the IL6-Rα and the gp130 molecule(Asakura 2003).

The gp130 subunits of the IL-6 receptor have been known to be susceptible to regulation. The expressed levels of gp130 within smooth muscle cells have been shown to be restricted, however when treated with IL-6 a marked increase in gp130 mRNA as well as surface protein expression was observed (Klouche, Bhakdi et al. 1999). When muscle fibres are exposed to bouts of physical exercise, the contracting muscle fibres produce and release IL-6. An increase in IL-6 receptor mRNA as well as cell membrane bound IL-6 accompany the bout of physical exercise. This exercise induced increase in IL-6 receptor elements is thought to occur via an IL-6 independent mechanism because IL-6 receptor mRNA elevation is also seen in IL -6 knock out mice exposed to exercise (Keller, Penkowa et al. 2005).

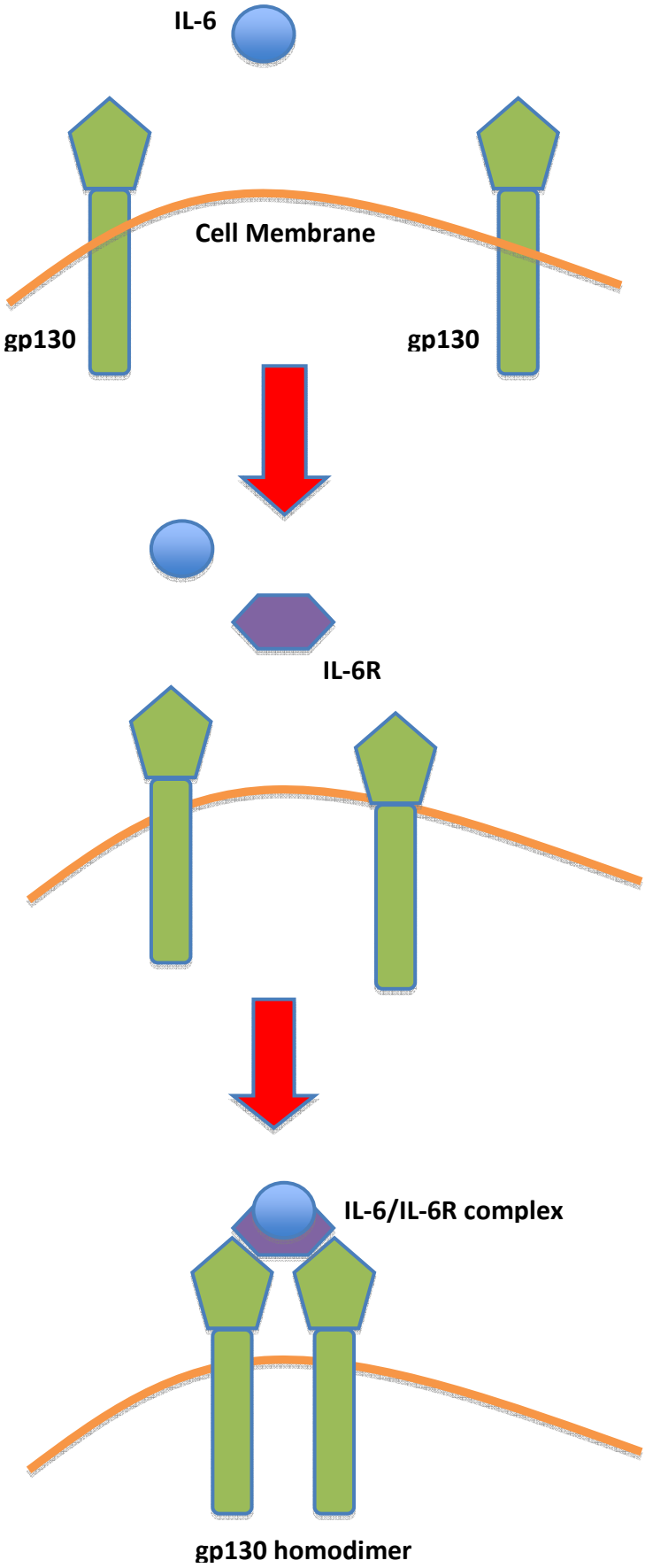

Figure 5: When IL-6 is present within the cell niche it leads to the formation of the IL-6 receptor complex. The gp130 (glycoprotein130) subunits are found traversing the cell membrane and will associate in the presence of IL-6 to form a homodimer. In order to completely form the IL-6 receptor, IL-6 must associate with IL-6R molecule to form the IL-6/IL-6R complex

1.4.3 The activity of Interleukin-6

Interleukin-6 can be referred to as a pleiotropic cytokine. This means that it can result in many distinct and seemingly unrelated effects, all as a result of this single cytokine. The processes that it regulates are widespread and it is vital for the execution of these processes.

1.4.3.1 Immune responses

The B cells play a key role in the recognition of antigens which would lead to the differentiation of the B cells into cells capable of producing and secreting specific antibodies. IL-6 is one of the factors that act on B cells in order for them to produce antibodies when exposed to the Epstein-Barr virus-transformed B-cell lines (Kishimoto, Hirai et al. 1978). Recombinant IL-6 is also responsible for acting on B cells on an mRNA level to produce secretory immunoglobulins (Kikutani, Taga et al. 1985). IL-6 is also a key player in the IL-4 dependent production of IgE as well as the specific production of antibodies to lipopolysaccharides.

This cytokine is also necessary for the activation, growth and differentiation of T-cells. IL-6 also induces serine esterase as well as perforin. Since these molecules are required for mediating target cell lysis, IL-6 could be involved in this aspect of differentiation of cytotoxic T cells (Takai, Wong et al. 1988). Within the immune system the role of IL-6 in influencing proliferation and differentiation is well known

1.4.3.2 Acute-phase response

IL-6 is responsible for the production of many proteins that are involved in the acute phase response, such as fibrinogen, α1-antichymotripsin, α1-acid glycoprotein as well as haptoglobin within the human hepatoma cell line HepG2 (Karlsson, Yarmush et al. 1998). When IL-6 is administered in rats, a typical acute-phase response is produced with an increase in IL-6 induced mRNAs and associated proteins (Geiger, Andus et al. 1988). Elevated serum levels of IL-6 have been reported in patients with fever after severe burns as well as patients undergoing a surgical procedure (Gauglitz, Song et al. 2008). In the absence of IL-6 the inflammatory acute-phase response is severely compromised in mice when infection or injury is induced (Penkowa, Moos et al. 1999).

All these studies as well as numerous others are proof that IL-6 is a key regulator of the acute-phase response during injury and other diseased states, but very few have assessed why it is that an IL-6 deficiency decreases repair of injured muscle.

1.4.3.3 Exercise and strenuous activity

It is a very well known fact that plasma concentrations are dramatically affected by strenuous exercise. A 100 fold increase in IL-6 has been observed in exercising individuals but normally the increase is not as dramatic but still very prominent (Febbraio and Pedersen 2002). An increase in IL-6 is usually accompanied by elevated levels of other anti-inflammatory cytokines such as IL-10. Many cytokines are increased during exercise, but IL-6 is the most marked and it precedes the production of many of the other cytokines. The increase in IL-6 is not a linear event over time, but has an exponential manner of elevation (Ostrowski, Hermann et al. 1998).

For a long period of time it was thought that the source of IL-6 increase during exercise was as a result of an immune response due to damage in the muscle (Nieman, Nehlsen-Cannarella et al. 1998) or the sensitization of the immune cells in response to exercise stress. Monocytes are responsible for increases in IL-6 during exercise, but the immune response theory was disproved as the IL-6 mRNA of monocytes did not increase, hence the response could not be attributed to these cells (Moldoveanu, Shephard et al. 2000). It was found that it was the skeletal muscle itself that was secreting the IL-6, but many cells in the skeletal muscle are capable of IL-6 production including myoblasts, endothelial cells, resident macrophages, infiltrating monocytes as well as smooth muscle cells (Moldoveanu, Shephard et al. 2000).

1.4.4 Physiological concentrations of IL-6

The concentration of IL-6 within skeletal muscle is extremely varied and can be altered by exercise as well as diseased states. The concentration of IL-6 in muscle at rest has been found to range from 1-8 pg/ml (Gray, Clifford et al. 2009; Robson-Ansley, Cockburn et al. 2010).

Post exercise plasma levels of IL-6 rise from baseline levels to a range of 6-120 pg/ml (Gray, Clifford et al. 2009; Robson-Ansley, Cockburn et al. 2010) depending on the severity of exercise. Interstitial levels of IL-6 have been known to reach 4 ng/ml (Langberg, Olesen et al. 2002; Rosendal, Sogaard et al. 2005).

Sepsis is a state where the levels of IL-6 are exceedingly elevated locally at the source of sepsis as well as in circulation. Concentrations of IL-6 in this state can range from 2 to 215 ng/ml in survivors and the level in non-survivors can reach in excess of 400 ng/ml (Damas, Ledoux et al. 1992).

A wide range of IL-6 concentrations can be observed within muscle and these levels are regularly altered in various conditions and because of this we have chosen to mimic these conditions in vitro to assess the effect on satellite cells.

Table 2: Physiological skeletal muscle concentrations of IL-6

IL-6 Concentration	Presence	Model	State	Reference
1-8 pg/ml	Plasma	Human	Rest	(Gray, Clifford et al. 2009; Robson-Ansley, Cockburn et al. 2010)
6 pg/ml	Plasma	Human	Mild exercise	(Gray, Clifford et al. 2009)
120 pg/ml	Plasma	Human	Strenuous exercise	(Gray, Clifford et al. 2009)
4 ng/ml	Interstitial	Human	Strenuous exercise	(Langberg, Olesen et al. 2002)
2-215 ng/ml	Plasma	Human	Non-lethal sepsis	(Damas, Ledoux et al. 1992)
400 ng/ml	Plasma	Human	Lethal sepsis	(Damas, Ledoux et al. 1992)

1.4.5 JAK/STAT signaling through the IL-6 receptor

For quite a number of years it was not known how cytokine receptors relay the effects of a cytokine binding. Eventually it was found that the Janus family tyrosine kinases were involved in signal transduction of cytokines and hormones. The JAK family of tyrosine kinases consists of JAK1, JAK2, JAK3 as well as Tyk-2. The signal transducer and activator of transcription (STAT) was also implicated in the relay of cytokine signaling. The STAT family has seven members: STAT 1-4, 5a, 5b as well as STAT6 (Levy and Darnell 2002).

JAK1, JAK2 and Tyk-2 constitutively associate with the gp130 molecule of the IL-6R when IL-6 is bound. This leads to the tyrosine phosphorylation of the JAK members. IL-6 is also known to activate STAT3, STAT1 and STAT5 by tyrosine phosphorylation produced by the JAK molecules. When the STAT3 molecules are phosphorylated they dimerize. These dimerized STAT3 molecules are moved to the nucleus where they will activate genes involved in the IL-6 mediated response. The gp130 molecule has 277 amino acids residues in its cytoplasmic domain, which also contains two conserved motifs among the cytokine receptor family, named Box1 and Box2 (Bromberg and Darnell 2000). The gp130 area closest to the membrane contains the Box1 and Box2 and these are sufficient for the activation of the JAK molecules by gp130. The human gp130 has 6 tyrosine residues in its cytoplasmic domain that are open for phosphorylation.

The phosphorylation of STAT3 is dependent on the second tyrosine (Tyr705) from the membrane termed Y2. The membrane-proximal region of gp130, consisting of 133 amino acids, has been implicated in the generation of signals for growth arrest, macrophage differentiation and the activation of STAT3 (Bromberg and Darnell 2000). The relay of IL-6 signaling is not only dependent on the phosphorylation of Tyr705 and in order to achieve maximal transcriptional activation the Serine 727 (Ser727) residue of STAT3 needs to be phosphorylated as well (Wen, Zhong et al. 1995). The two patterns of STAT3 phosphorylation seem to assert its influence on specific components of the cell.

Although the majority of activated STAT3 is found within the cytoplasm and nucleus, it has been proposed that STAT3 is responsible for the control of respiration in mitochondria. STAT3 phosphorylated at the Ser727 residue have been encountered in the mitochondria (Myers 2009) and an interaction with Complex I/II of the Electron Transport Chain has been suggested (Wegrzyn, Potla et al. 2009).

Tyrosine 705-induced STAT3 phosphorylation signals growth arrest as well as differentiation. IL-6 has also been shown to enhance the growth of M1 macrophage cells when STAT3 is suppressed. It is thus clear that IL-6 can generate growth-enhancing signals, growth arrest and differentiation-inducing signals all at the same time within various cells. One of the main roles of STAT3 in IL-6 induced signaling seems to be the progression of differentiation in M1 macrophages (Minami, Inoue et al. 1996). This is of particular relevance to the context of this thesis as muscle injury influences both satellite cells and macrophages.

Two distinct signals are necessary for gp130-induced cell growth. A cell cycle progression signal that is dependent on the Y2 second tyrosine is necessary as well as an anti-apoptotic signal that is dependent on the third tyrosine residue, Y3, which is mediated by STAT3 through Bcl-2 induction. A study has shown that STAT3 activation is involved in the IL-6 dependent T-cell proliferation through the prevention of apoptosis without the need for Bcl-2 (Takeda, Kaisho et al. 1998). This could suggest a possible role of IL-6 mediated STAT3 activation and proliferation of satellite cells. A study of this type has not been performed but could shed valuable light on the role that IL-6 plays in the proliferation of satellite cells.

1.4.5.1 Localization of STAT3

As mentioned above, in order for STAT3 to regulate transcription the molecule must be phosphorylated at its Tyr705 residue. In order to assess the translocation of pSTAT3 within muscle cells, subjects were exposed to intense resistance exercise. Muscle biopsy samples were harvested at 2, 4, and 24 hours into recovery following a single bout of maximal leg extension exercise. A rapid and transient activation as well as nuclear translocation of pSTAT3 was observed by immunocytochemistry, which was highest 2 hours post exercise. Transcriptional activity downstream of STAT3 activation also peaked 2 hours post exercise which included increased mRNA levels of the negative regulator of STAT3, SOCS3 (Trenerry, Carey et al. 2007). Although this study is useful in characterizing STAT3 activation after strenuous exercise, it only focused on muscle fibres, but did not pay specific attention to the satellite cells themselves. The main interest of this study was hypertrophy and the signaling involved. The protocol utilized would not have resulted in injury, thus the STAT3 signaling in muscle injury could not have been assessed.

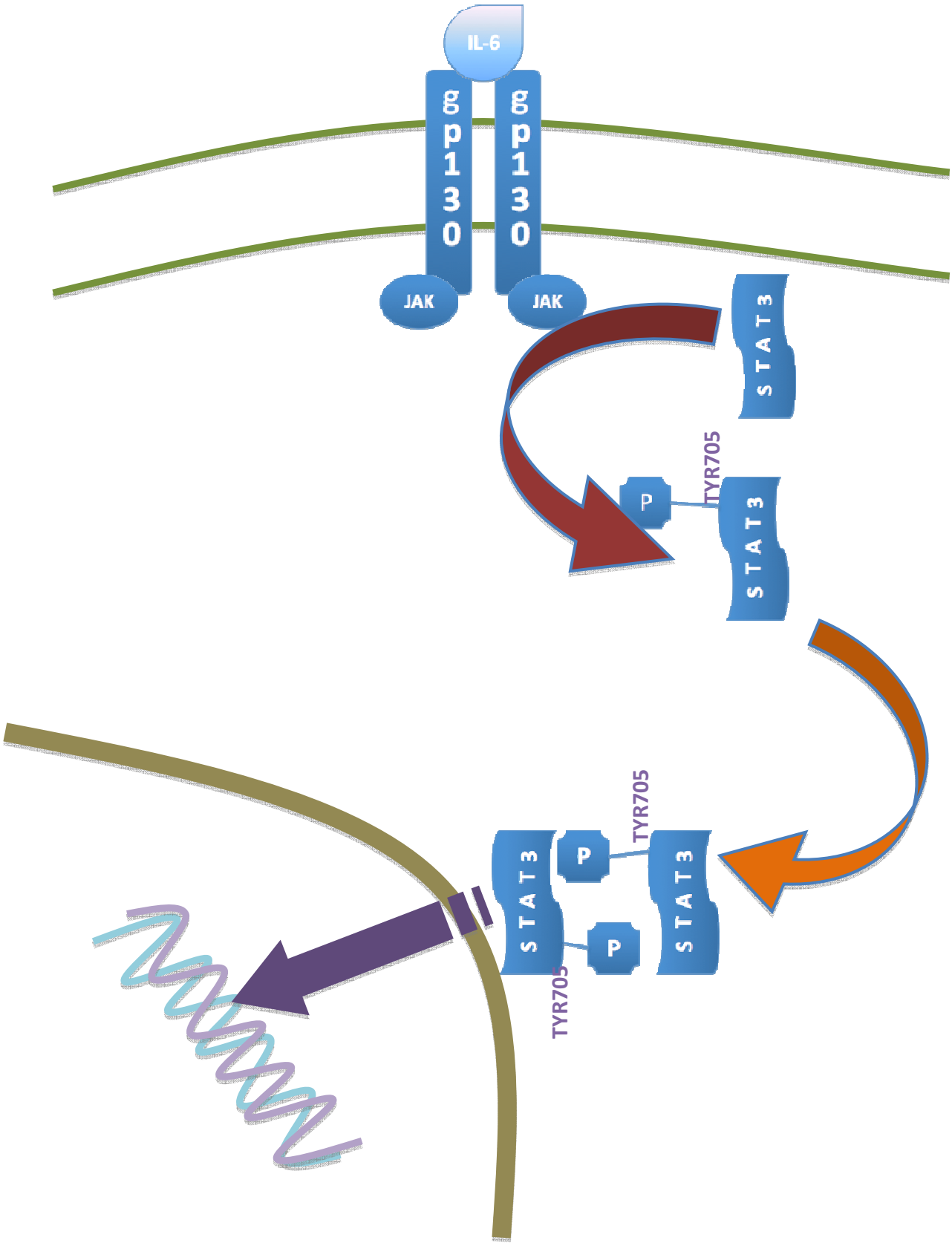

Figure 6: IL-6 relays it signal through the JAK/STAT pathway. After the formation of the IL-6 receptor, Janus Kinase (JAK) associates with the receptor. JAK is responsible for the activation of STAT3 (Signal Transducer and Activator of Transcription) by its phosphorylation at the Tyr705 residue. Two activated STAT3 molecules will homodimerize and translocate to the nucleus to activate transcription

1.4.6 STAT3 transcriptional activity

In order for STAT3 to regulate transcription it needs to translocate to the nucleus and bind to a certain sequence in the cell's DNA. These sequences vary substantially, but they have certain elements in common. STAT proteins bind to palindromic (base pairs that read the same forward as backward) elements. The binding elements of STAT3 have a general structure of TT(N)5AA. A TT-AA motif with 5bp spacing is associated with general STAT, whereas a TT-AA motif with 4bp spacing selectively binds to STAT3 (Seidel, Milocco et al. 1995).

For STAT3 to properly regulate transcription, direct components are required to associate with STAT3. These components are referred to as coactivators. The coactivators associated with STAT3 are the CREB-binding protein (CBP/p300), nuclear receptor coactivators (NCoAs) and p300/CBP-associated factor (p/CAF). NCoAs functionally interact with STAT3 through association with p300/CBP at its p300/CBP domain AD1. Transcriptional activity potential of STAT3 is greatly increased by these associations. Histone acetyltransferases (HAT) are responsible for directly linking chromatin modification to gene activation as well as histone binding. The CBP/p300 requires HAT activities to activate transcription and is the reason for the prevalence of multiple HAT components in the complex (Korzus, Torchia et al. 1998).

In order for STAT3 to regulate transcription a chaperone molecule is needed to guide the DNA binding ability of STAT3. The preservation of STAT3 signaling is dependent on the heat shock protein 90 (Hsp90). Mouse embryonic stem cells treated with IL-6 showed co-precipitation of Hsp90 and STAT3 within cytoplasmic complexes. This implies a positive interaction between these two molecules before nuclear translocation occurs. The STAT3 DNA-binding domain and Hsp 90 are thought to be closely associated and this association is depleted in the presence of geldanamycin, a highly specific Hsp90 inhibitor (Sato, Yamamoto et al. 2003). Another chaperone thought to be involved in STAT3 signaling is Hop. Co-precipitation of Hsp90 and STAT3 was accompanied by the precipitation of Hop and a cytoplasmic co-localization of Hop with Hsp90 and STAT3 was also found through immunocytochemistry in mouse embryonic stem cells (Longshaw, Baxter et al. 2009). These studies performed prove that the Hsp90/Hop complex is paramount in STAT3 nuclear translocation.

STAT3 proteins bind to a vast array of promoter sequences and so doing regulate many genes. Activated STAT3 recognizes an element in the cell cycle regulatory gene, p21, and its functional binding increases mRNA expression of this gene (Chin, Kitagawa et al. 1996). STAT3 is also responsible for the expression of proteins associated with cell cycle regulation namely cyclin D1 and cyclin E1. Many genes associated with the regulation of cell survival have STAT3

binding elements in their promoter regions and these include the direct targets of STAT3, Bcl-2, Fas and Bcl-xL. Other transcriptional factors under the control of STAT3 are c-Fos, c-Jun and c-myc (Hirano, Ishihara et al. 2000).

As mentioned before, within skeletal muscle progenitor cells, the MRFs are major transcription factors. It is therefore necessary to understand if they have interactions with other transcription factors such as STAT.

MyoD can be regarded as a pro-differentiation molecule. It was found that STAT3 inhibits the activity of MyoD by direct interaction (Kataoka, Matsumura et al. 2003). It was also found that MyoD in turn inhibited the DNA binding capabilities of STAT3 and by doing so inhibited STAT3-mediated cell growth and survival. It could also be possible that MyoD would halt STAT3 activity by depriving STAT3 of its transcriptional cofactors. These results show that the balance between MyoD and STAT3 activities are vital in the determination of myoblast cell cycle fate.

This interaction between STAT3 and MyoD has also been implicated in the induction of myogenesis (Yang, Xu et al. 2009). Direct evidence was found that STAT3 is essential for differentiation when the administration of a STAT3 RNAi decreased the expression of the differentiation marker, MHC. As mentioned above, a direct interaction between STAT3 and MyoD was found as both coimmunoprecipitated together.

It is evident that STAT3 and MyoD form a crucial interaction that is responsible for the control of proliferation as well as differentiation of myoblast. These studies had contradictory results and do not explain how a STAT3 and MyoD interaction could control both proliferation as well as differentiation. It is crucial to characterize this interaction in order to fully understand muscle regeneration.

As discussed above, it is well known that IL-6 is responsible for downstream phosphorylation of STAT3, which activates many genes along with the STAT3 gene itself. This would create a greater potential for STAT3 phosphorylation in the cytoplasm as more STAT3 proteins are expressed.

IL-6 is also responsible for the increase in unphosphorylated STAT3 or uSTAT3, which results in a second wave of gene expression, like RANTES, IL-6, IL-8 and MRAS that do not respond directly to the pSTAT3 (Yang, Liao et al. 2007). The uSTAT3 is responsible for signalling which is completely different from that used by pSTAT3. The uSTAT3 is able to form a unique transcription factor complex when it binds to unphosphorylated NFκB (uNFκB), in competition

with IκB. The uSTAT3/ uNFκB complex will accumulate in the nucleus with help of the uSTAT3 which will activate a subset of κB-dependent genes like RANTES.

RANTES is an important mediator of acute and chronic inflammation, with a possible involvement in immunopathological disorders. This study showed that the effect of IL-6 induced STAT formation has not yet been completely described and it is possible that uSTAT3 might play a role in many different pathways and gene expression. IL-6 will result in an increase in uSTAT3 and this will lead to IL-6 gene expression. This will cause another feed forward effect as seen with STAT3 and a self perpetuating cycle.

IL-6 can signal through various pathways in order assert control over the cell cycle thus it is important to study the signalling mechanisms of IL-6 in order to fully characterize its effect on proliferation and differentiation.

1.4.7 Control of cytokine signalling

Cytokine signaling lends itself to regulation in which the strength of the cytokine signal is controlled.

The IL-6 super-family is responsible for the induction of one these cytokine signal regulators, suppressors of cytokine signaling 3 (SOCS3) (Dalpke, Opper et al. 2001; Croker, Krebs et al. 2003). The SOCS family member, SOCS3, focuses on the suppression of the JAK/STAT signaling pathway, a pathway utilized by the IL-6 super-family. As reviewed by Krebs et al, SOCS3 modulates the JAK/STAT signaling pathway by inactivation of the Janus kinases, blocking the ability of STAT3 to bind to receptor sites as well as the ubiquitination of signaling proteins (Krebs and Hilton 2001). This control of the JAK/STAT signaling is thus essential for the suppression of the gp130-mediated signaling pathway, a pathway that is vital in the signaling of IL-6 (Krebs and Hilton 2001; Lang, Pauleau et al. 2003).

The signaling molecule, Wnt5a, plays an important role in the signal relay of the IL-6 super-family. This super-family signals through the JAK/STAT pathway and Wnt5a is pivotal in the expression and phosphorylation of STAT3 in this pathway (Lang, Pauleau et al. 2003; Fujio, Matsuda et al. 2004). STAT3 is responsible for the transcription of Wnt5a. The expressed Wnt5a signals through the beta-catenin pathway which up-regulates the mRNA for Stat3 and the knockdown of Wnt5a leads to a subsequent decrease in the levels of STAT3 (Hao, Li et al. 2006; Dissanayake, Olkhanud et al. 2008). This demonstrates that the activation and translocation of STAT3 relies heavily on Wnt5a.

STAT3 is a known regulator of satellite cell self-renewal as well an inhibitor of differentiation and the effective regulation of STAT3 signaling by Wnt5a could play a regulating role in the determination of satellite cell cycle fate.

1.5 The IL-6 super-family and control of the proliferation-differentiation transition

It has been hypothesized that the growth factors released by activated monocytes are able to increase proliferation of myoblasts. These growth factors in turn stimulate IL-6 production by the myoblasts. Monocytes also secrete IL-6 and are thought to increase the proliferation of myoblasts (Cantini, Massimino et al. 1995). The exact effect of IL-6 on skeletal muscle myoblasts is a controversial subject and a general consensus has not been reached. The main areas of uncertainty include questions around the ability of IL-6 to act independently of TNF-α as major cytokine influencing myoblasts and whether this influence is limited to proliferation or if differentiation of myoblasts is also influenced. Previous studies focused either on the proliferative or differentiation capabilities of IL-6. Finally, few studies in myoblasts have investigated signaling mechanisms that might explain the IL-6 effects observed.

IL-6 is thought to have an additive modulating effect on TNF-α. The incubation of C2C12 differentiated myotubes in the presence of 100 ng/ml TNF-α resulted in a significant increase in IL-6 mRNA. An increase in protein accumulation as well as an increase in the rate of protein synthesis has been attributed to the presence of IL-6 in C2C12 skeletal myotube cultures (Alvarez, Quinn et al. 2002).

A positive temporal interaction between TNF-α and IL-6 has been studied where maximum beneficial effects on myoblasts were found when the cells were treated with TNF-α (10 ng/ml) for 24 hours prior to IL-6 dosage (2.5 ng/ml). The combination significantly increased total cellular protein as well as the shift of cells to the S-phase of the cell cycle (Al-Shanti, Saini et al. 2008). Although the major focus of this study was on the synergistic effects of TNF-α and IL-6 and not just a focus on IL-6, this study was useful in characterizing the effect of IL-6 on the proliferation and cell cycle progression of myoblasts. However, the doses of IL-6 studied were not across a wide range and it is well known that the concentrations of IL-6 in muscle vary dramatically. The effects of the IL-6 dose was also only assessed for 24 hours thus the effects were not known at later time points. This may have been for two reasons: a) there are great technical difficulties when culturing C2C12 cells over longer period of time in terms of

spreading the doses over time and b) that the authors did not consider the physiological conditions they were mimicking.

In a third study, the effects of IL-6 on adult human myoblasts were assessed in culture, where they were exposed to medium supplemented with IL-6 (10 ng/ml). The IL-6 treatment significantly increased myoblast numbers but the treatment also increased the expression of MyoD, a pro-differentiation protein (Wang, Wu et al. 2008). This study was useful as it showed that IL-6 does not only have a proliferative effect but seems to have an effect on myoblast differentiation as well. This study considered with previous studies by Alvarez et al. 2002 and Al-Shanti et al. 2008, show two contradictory results and leaves some doubt over the effect of IL-6 on proliferation and differentiation.

Overexpression of IL-6 increases the extent of myogenic differentiation. The ablation of IL-6 in myoblasts decreases the expression of differentiation-associated genes such as myogenin and the administration of IL-6 (2 ng/ml) to myoblasts markedly increases the expression of this of pro-differentiation protein (Baeza-Raja and Munoz-Canoves 2004). Few studies have considered measuring the effect of IL-6 on the later MRFs, which would more definitively indicate differentiation, as opposed to MyoD, which is present in myoblasts that are still proliferating and needs to reach critical levels for cell cycle exit (Megeney, Kablar et al. 1996; Datta, Min et al. 1998; Jin, Kim et al. 2007; Goudenege, Pisani et al. 2009). However, another study, not focused on IL-6, has added some evidence.

The calcitonin gene-related peptide (CGRP) and IL-6 are also thought to have an additive affect on differentiation. Rat myoblasts cultured for 10 days in the presence of IL-6 showed an earlier and increased mRNA expression of the pro-differentiation markers myogenin and Myf-5. Myoblast cultures in the presence of CGRP as well as IL-6 expressed the specific mRNAs more rapidly when compared to the addition of CGRP or IL-6 alone (Okazaki, Kawai et al. 1996).

Another study also appears to definitively promote the understanding that IL-6 is an essential growth regulator. In young mice, growing myofibres as well as associated satellite cells actively produce IL-6 (Serrano, Baeza-Raja et al. 2008). When IL-6 expression is blunted genetically in these mice, hypertrophy is adversely affected in vivo. Although this could be considered even further evidence of a lack of stimulation of differentiation, this effect could also be as a consequence of abrogated satellite cell proliferation or as a result of a decrease in myonuclear accumulation.

From the studies mentioned it is evident that there is strong evidence for the implication of IL-6 in both proliferation and differentiation.

Table 3: Studies on the effect of IL-6 on proliferation and differentiation

Experimental model	Dosage	Findings	Interpretation	Reference
TNF-α and IL-6 on C2C12 myoblasts	TNF-α (10 ng/ml) IL-6 (2.5 ng/ml)	Increase in proliferation and cellular proteins	Synergistic effect of TNF-α and IL-6 to increase proliferation	(Al-Shanti, Saini et al. 2008)
IL-6 on adult human myoblasts	IL-6 (10 ng/ml)	Increase in myoblast numbers and MyoD	IL-6 increases proliferation with possible differentiative effect	(Wang, Wu et al. 2008).
IL-6 (2 ng/ml) on C2C12 myoblasts	IL-6 (2 ng/ml)	Increase in myogenin expression	IL-6 increases differentiation	(Baeza-Raja and Munoz-Canoves 2004).
IL-6 abrogated in mice		Hypertrophy adversely affected	IL-6 affects differentiation and proliferation	(Serrano, Baeza-Raja et al. 2008)

A previous study performed by our department assessed the affect of IL-6 dosage on MyoD expression in skeletal myoblasts (Qwemesha, G. 2008. Unpublished). A significant increase was recorded in MyoD expression when cells were treated with high doses (10 ng/ml) of IL-6. This insinuates that varying doses of IL-6 elicit a response in C2C12 cells and could possibly have an effect on proliferation and differentiation. It is important to not only study the MRFs, but also the signaling pathways associated with IL-6 and how MRF expression is regulated. The JAK/STAT pathway as well as the p38/NFκB could be a candidate pathway in the control of MRF expression.

The JAK/STAT pathway has been prominent in the literature with regard to its effects on the cell cycle of various cell lines (Beadling, Guschin et al. 1994; Danial, Pernis et al. 1995; van der Bruggen, Caldenhoven et al. 1995; Miller and Bell 1996) including myoblasts. The knockout of any part of this pathway has lead to lethality within mice (Parganas, Wang et al. 1998). The phosphorylation of STAT3 has been suggested to play a key role in embryonic stem cell renewal. LIF is well known to enhance stem cell self renewal and the absence of LIF hinders the expression levels of STAT3 and Hsp90 as well as negatively affecting the complex formed between these two molecules (Setati, Prinsloo et al. 2010). The phosphorylation, dimerization and translocation of STAT3 is thought to play a pivotal role in maintaining the pluripotent ability of embryonic stem cells. The suppression of the co-chaperone Hop by means of siRNA lead to the depletion of STAT3 mRNA, a decrease in pSTAT3 dimerization as well as an extranuclear accumulation of STAT3. The knockdown of Hop resulted in a loss of embryonic stem cell pluripotency as well as a loss in ability to form embryoid bodies with a basement membrane (Longshaw, Baxter et al. 2009).

It was shown that LIF (10 ng/ml) induces satellite cell proliferation and was accompanied by a considerable increase in the transcriptional activity of STAT3 assessed by means a luciferase reporter plasmid. Not only did LIF induce proliferation, there was also marked increase in JAK2 and STAT3 phosphorylation. The cytoplasmic STATs were activated by phosphorylation to form phosphorylated STAT3 (pSTAT3), and it was assumed that pSTAT3 dimers would be translocated to the nucleus (Spangenburg and Booth 2002). The knockdown of STAT3 has also shown a decrease in LIF-induced myoblast proliferation (Sun, Ma et al. 2007).

In addition to LIF, IL-6 also acts via the gp130 molecule and the STAT molecules. Studies found that there was a link between the STAT3 pathway and satellite cell proliferation (Spangenburg and Booth 2002) and play a role in controlling the proliferation of fibroblasts (Fredj, Bescond et al. 2005). The model clearly shows an increase in the proliferation of cardiac fibroblasts and proliferation was significantly decreased in the presence of an anti-IL-6 or anti-gp130 antagonists. Of relevance here, a marked increase in the phosphorylation of STAT molecules was noticed in the presence of IL-6, which indicates a downstream effect of IL-6 through the gp130 molecule and STAT. This implies that the proliferation of fibroblasts is dependent on IL-6, as well as the gp130 subunits of the IL-6 receptor.

It has been suggested that proliferation of myoblasts occurs through the JAK1/STAT1/STAT3 pathway (Sun, Ma et al. 2007). The knockdown of JAK1 in myoblasts promotes myogenic differentiation as well as a marked reduction in proliferation. The absence of JAK1 accelerates

initiation of the pro-differentiation proteins MyoD, MEF2 as well as an increased MEF2-dependent gene transcription. It is well known that LIF promotes myoblast proliferation and retards differentiation and this is thought to occur through the JAK1/STAT1/STAT3 signaling pathway.

The levels of STAT3 and pSTAT3 were studied in regenerating skeletal muscle in order to determine the progression of muscle regeneration (Kami and Senba 2002). It was found that at the early stage of regeneration, the activated STAT3 proteins were detected in the nuclei of the activated satellite cells and these continued to be active in proliferating myoblasts isolated from injured muscle fibres. When the muscle regeneration progressed, the level of activated STAT3 was decreased in differentiated myoblasts and myotubes. These findings lead to the conclusion that the activation of STAT3 was induced in proliferating myoblasts. Activated STAT3 and its effects on proliferation has also been seen in the transformation of fibroblasts (Bromberg, Wrzeszczynska et al. 1999) as well as uncontrolled proliferation seen in various tumors (Garcia and Jove 1998).

However, the JAK2/STAT2/STAT3 has been implicated in the differentiation of myoblasts (Wang, Wang et al. 2008). Therefore, it is still unclear whether the activation of STAT3 is responsible for proliferation or differentiation. The levels of STAT3 and pSTAT3 were also quantified in regenerating skeletal muscle in order to determine their relation to proliferation (Sun, Ma et al. 2007).

The expression of IL-6 is induced in differentiating C2C12 cells and this is thought to be dependent on the p38/NFκB interaction (Baeza-Raja and Munoz-Canoves 2004; Al-Shanti and Stewart 2008). The p38 MAPK as well as the nuclear factor kappa B (NFκB) signaling pathways have been shown to regulate skeletal muscle myogenesis. Activation of p38 is seen in differentiating myocytes whereas NFκB is present in both proliferating and differentiating myoblasts. The activation of NFκB is dependent on p38 in the differentiation process.

These studies show that IL-6 does play a role in the proliferation and differentiation of satellite cells through its signaling pathways and further characterizing of IL-6's signaling pathways is necessary.

1.6 Satellite cells in pathophysiology

Satellite cells play a pivotal role in the regeneration of damaged muscle fibres as well as sustaining an effective satellite cell pool. Close regulation of the satellite cell is necessary in order to maintain proper muscle function and regeneration. A decrease in proliferative capacity or a diminished satellite cell pool, may give rise to diseased states within muscle fibres.

Sarcopenia is a condition encountered in aging individuals. The condition is characterized by a loss in muscle mass and strength which leads to impaired functional capacity leading eventually to disability and the loss of independence. The causes of sarcopenia could be as a result of improper diet or a decline in physical activity. At the muscular level the cause of decreased muscle mass could be as a result of a decline in the number of satellite cells or a change in the satellite cell niche leading to incapacity to become activated and proliferate in order to form new muscle fibres. An age-related decline in satellite cell numbers has been reported in the rat anterior tibialis (Sajko, Kubinova et al. 2004). The preservation of the satellite cell pool appears to be maintained in individuals into their seventh decade of life (Petrella, Kim et al. 2006), but the pool seems to diminish thereafter (Kadi, Charifi et al. 2004). Another cause of sarcopenia could be as a result of DNA destabilization during terminal differentiation of skeletal myoblasts. It has been suggested that reactive oxygen species (ROS) is produced during the differentiation process of muscle fibres. ROS impairs DNA base excision repair by negatively affecting DNA ligases, which leads to DNA single-strand breaks (Narciso, Fortini et al. 2007).

The pathology or dysfunction may arise external to muscle tissue, with circulating factors subsequently affecting satellite cells. Obesity has been implicated in many disorders including heart and liver failure. There appears to be a negative correlation between obesity and muscle fiber size. A metabolic syndrome rat model was utilized to determine the effect of obesity on satellite cell proliferation and this was accomplished by BrdU incorporation of myoblasts. The results found, suggested that obesity causes a marked decrease in satellite cell proliferation and this is thought to be the underlying cause of low muscle mass (Peterson, Bryner et al. 2008).

The issue then arises that in the above-mentioned examples, IL-6 will be a major factor synthesized or released, but the extents will differ between these conditions.

1.7 Summary and Rationale

It is evident that satellite cells play a crucial role in the regeneration of damaged muscle as well as muscle renewal. In order for these cells to become activated, the associated sarcolemma must be disturbed. The disrupted sarcolemma also leads to the migration of additional satellite cells from their position underneath the basal lamina to the site of most damage. Once the cells are activated, proliferation is set underway in order to gain cell numbers. A regulated number of satellite cells reinstate their original, quiescent position below the basal lamina, which replenishes the satellite cell pool. The remaining activated cells participate in the differentiation process to form myotubes. The myoblasts and completed myotubes migrate into the site of injury and effectively repair the damaged sarcolemma. This process is the cornerstone of muscle repair and the preservation of the satellite cell pool.

The satellite cell cycle follows a predicted pattern, which is constituted by varying phases. The G0/G1 phase is a growth phase characterized by differentiation of cells. Alternatively, divided cells can pass through the G0/G1 phase and resume the cell cycle for another round of proliferation. The S-phase of the cell cycle is associated with DNA synthesis and active proliferation, whereas mitosis of satellite cells is seen in the G2/M phase.

Satellite cells are susceptible to cell cycle control by means of cytokines and growth factors named mitogens. A well-known mitogen of satellite cells is IL-6. The prevalence of IL-6 in the skeletal muscle niche is extremely varied and concentrations fluctuate according to specific conditions, which include exercise, inflammation and infection as well as other diseased states. The sources of IL-6 in muscle are also diverse and include diffusion from the circulation to the interstitial fluid, macrophages near the niche as well as the muscle cells or even satellite cell themselves.

The cytokine, IL-6, signals through the gp130 subunits of the IL-6 receptor. Downstream targets of IL-6 include JAK1, JAK2, STAT1, STAT2 and STAT3. The Janus kinases (JAK) are responsible for the phosphorylation and resultant activation of the Signal Transducer and Activator of Transcription (STAT) 3. In order for STAT3 to assert control over transcription it needs to translocate to the nucleus to gain access to DNA binding sites. The activation and translocation of STAT3 is a rapid process occurring during the minutes after IL-6 induction binding to its receptor and even minutes after its translation.

Phosphorylated STAT3 (pSTAT3) asserts control over a large array of genes paramount to the control of the cell cycle. Myogenic regulatory factors (MRF) are proteins whose expression

asserts control over the cell cycle and include MyoD and myogenin. The proliferating cell nuclear antigen (PCNA) is found in the nucleus and is a cofactor of DNA polymerase delta. PCNA helps increase the processivity during DNA replication. MyoD and myogenin are proteins conspicuous in the differentiation process, whereas PCNA is prominent in proliferation. MyoD signals late proliferation/early differentiation and terminal differentiation is marked by myogenin expression. Activated pSTAT3 effectively suppresses the expression of MyoD, but MyoD is also capable of suppressing the DNA binding capability of pSTAT3. MyoD is capable of binding to pSTAT3, which results in the inactivation of pSTAT3 within the nucleus.. Myogenin gene transcription is dependent on MyoD, thus MyoD protein expression precedes that of myogenin.

The satellite cell mitogens, LIF and TNF-α, are well characterized but the exact effect of IL-6 on the cell cycle is still unknown. Previous studies performed concerning IL-6 and its effect on cell cycle progression is contradictory. The majority of studies only focus on one specific concentration of IL-6 but it is well known that IL-6 concentrations in the muscle vary greatly. Previous studies also only focused on either the proliferation or differentiation effects of IL-6 but never both.

The characterization of IL-6 signaling as well as cell cycle control is imperative since IL-6 is prominent in the majority of diseased states within muscle. Frailty conditions like sarcopenia are characterized by decreased muscle mass and strength as well as a diminished satellite cell pool and a lower incidence of muscle repair. The proper description of IL-6‘s influence on the satellite cell cycle could present a pharmacological treatment for frailty.

1.8 Aims of the study

1. Set up a proliferating cellular model with varying physiologically relevant doses of
    - Control
    - High
    - Medium
    - Low
2. Assess the effect of IL-6 dosage on proliferation and differentiation
    - Cell cycle analysis
3. Assess the expression and localization of myogenic transcription factors
    - MyoD
    - myogenin
    - PCNA
4. Assess the expression and localization of STAT3
    - pSTAT3
    - tSTAT3

1.9 Hypothesis

Varying concentrations of IL-6 have diverse effects on the cell cycle progression of skeletal muscle satellite cells

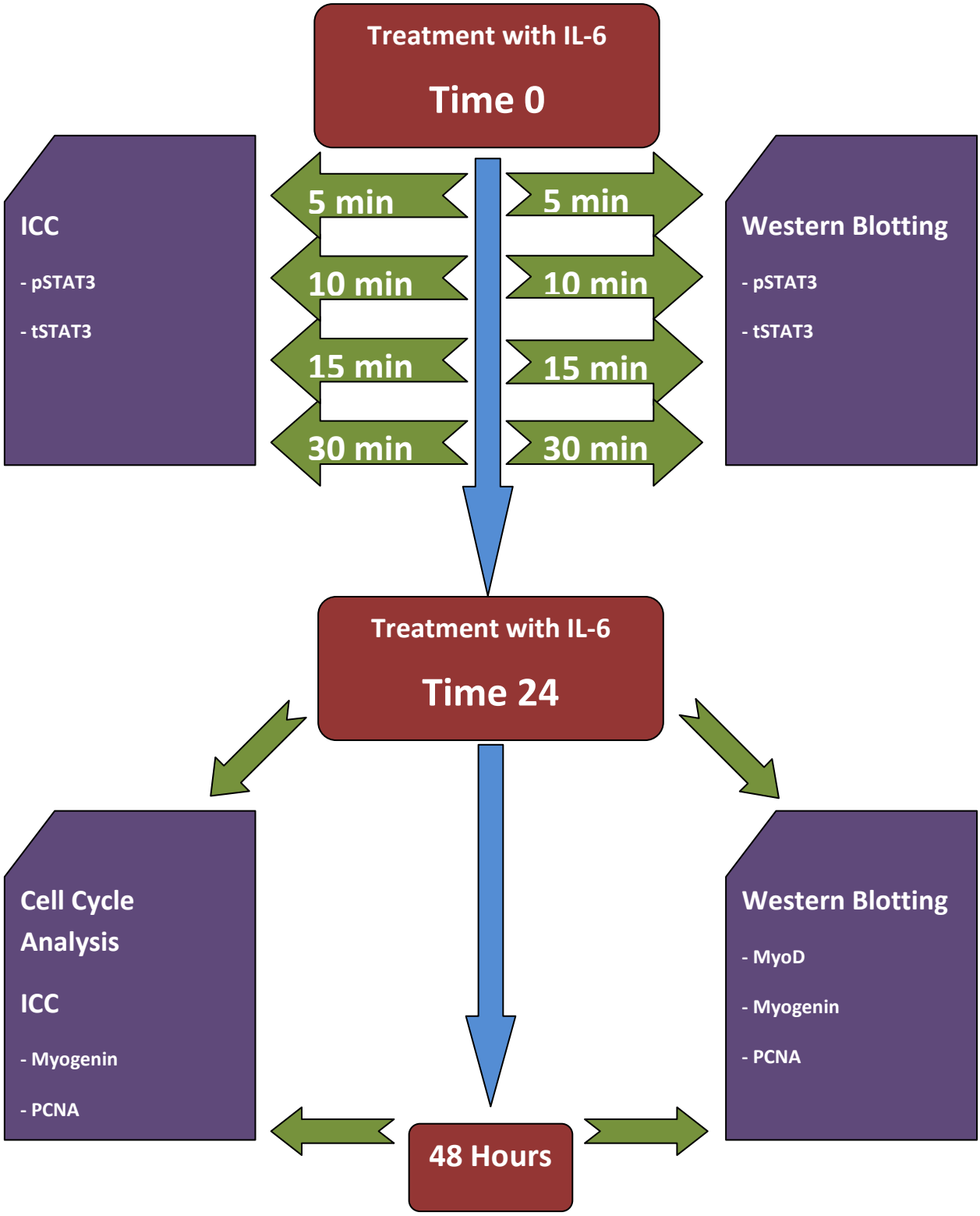

Figure 7: IL-6 treatment Study Design (pSTAT3 = Phosphorylated Signal Transducer and Activator of Transcription 3, tSTAT3 = Total Signal Transducer and Activator of Transcription 3, PCNA = Proliferating Cell Nuclear Antigen, ICC=Immunocytochemistry)

2. Materials and methods

All chemicals used were of analytical grade.

All chemicals supplied by Sigma-Aldrich (Pty) Ltd, Aston Manor 1630, South Africa unless otherwise stated.

The C2C12 murine skeletal muscle cell line was acquired from the European Collection of Cell Cultures (ECACC).

2.1 IL-6 treatment protocol

Cultured satellite cells were treated with High (10 ng/ml), Medium (100 pg/ml) and Low (10 pg/ml) doses of IL-6 and the first supplementation was regarded as Time 0 (for Schematic see Fig. 7). Fresh IL-6 supplemented medium was administered 24 hours after the first treatment and this was regarded as Time 24. The cells were allowed to grow for another 24 hours and this was regarded as Time 48.

Cell cycle analysis, Western blotting and Immunocytochemistry were performed using cells harvested at Time 24 and 48.

Western blotting and Immunocytochemistry were performed using cells harvested at 5, 10, 15 and 30 minutes after the first supplementation of IL-6.

2.2 Preparation of rhIL-6

Stock (10 µg/ml): 10µg rhIL-6 (PeproTech, Rehovot, Israel, #400-06, MW = 21,7 kDa) was added to 1000µl sterile Phosphate Buffered Saline (PBS). The solution was incubated at room temperature for 10 min, aliquoted into labelled Eppendorf tubes (10µl per Eppendorf tube), frozen and at the start of the experiment appropriately diluted:

High concentration (10 ng/ml): Dilute stock solution 1:1000

1µl Stock (10 µg/ml) rhIL-6 was added to 999µl PM

Medium concentration (100 pg/ml): Dilute High concentration 1:100

10µl High concentrated rhIL-6 medium was added to 990µl PM

Low concentration (10 pg/ml): Dilute Medium concentration 1:10

100µl Medium concentrated rhIL-6 medium was added to 900µl PM

2.3 Cell culture

2.3.1 Preparation of proliferation medium

C2C12 cells were cultured in Dulbecco's Modified Eagle Medium (DMEM, Batch # 038K2345) supplemented with 1% (v/v) Penicillin/Streptomycin (PenStrep, Highveld Biological (PTY) LTD, Johannesburg, South Africa, Batch # CN3286), 10% (v/v) Foetal Bovine Serum (FBS, GIBCO™, Paisley, Scotland, Batch # 41F5180F) and 6.8% (v/v) L-Glutamine (20mM, Batch # 068K2352). The resultant solution shall henceforth be referred to as Proliferation Medium (PM).

2.3.2 Cell passaging

Cell passaging was performed when the cells covered 70 % of the growth surface available. This occurrence is referred to as confluency. Old medium was discarded from T75 flasks and the cells were rinsed with preheated, sterile Phosphate Buffered Saline (PBS) at 37°C to remove traces of old medium. Trypsin-EDTA (1X, Batch # 048K2421) was added to the cells in order to digest appendages and dislodge cells from the growth surface. Cells were incubated in a heated shaker at 37°C for 5 minutes. Preheated (37°C) PM was added to deactivate the Trypsin. Cells were then transferred to a conical tube and centrifuged for 3 minutes at 325*G* (Digicen 20, Serial # 040377/05) at room temperature.

2.3.3 Cell counting

To determine the number of cells gathered from passaging, a haemocytometer (MarienFeld, Germany, Neubauer Improved) was utilized. For the experiment, cells were cultured in sterile, six well plates (Grenier bio-one Cellstar ®, Kremsmunster, Austria, Batch # 657160) containing 40 000 cells per well to prevent over confluency. Cells were incubated in a humidified incubator (SL, Shel Lab CO_2 Incubator) at 37°C with 5% (v/v) CO_2.

2.3.4 Cell harvesting for flow cytometric analysis

Cells were harvested as described in the cell passaging protocol. Cells were resuspended in citrate buffer consisting of 250 mM Sucrose (UnivAR, $C_{12}H_{22}O_{11}$, # 588150, Mr = 342.30), 40mM Trisodium citrate (B&M Scientific, $Na_3C_6H_5O_7.2H_2O$, # LOB-0680 Mr = 294.10) and 0.5%

(v/v) DMSO ($(CH_3)_2SO$, # D2650, Mr = 78.13) adjusted to a pH of 7.60 (Consort C830, Serial # 69519). Cells were stored at - 80°C.

2.3.5 Protein harvesting

In order to harvest cells for protein analysis, medium was decanted from the six well plates and the wells washed with ice cold PBS. RIPA-buffer containing 50mM Tris (hydroxymethyl) aminomethane ($NH_2C(CH_2OH)_3$, # 201-064-4, Mr = 121.14), 2.5mM TRIS-HCL 1M (#T2913), 1% (v/v) NP-40 (# NP40S), 0.5% (v/v) Na-deoxycholate (# DA5670), 0.25% (w/v) ethylenediaminetetraacetic acid (EDTA, ($C_{10}H_{14}N_2Na_2O_8 \cdot 2H_2O$, # 205-358-3, Mr = 372.24), 5 mM Sodium fluoride (NaF, # 231-667-8, Mr = 41.99), 4 µg/ml SBTI (# T-9003), 0.1mM Phenylmetyl sulfonyl fluoride (PMSF, $C_7H_7FO_2S$, # 206-350-2, Mr = 174.19), 1 µg/ml Leupeptin hydrochloride ($C_{20}H_{38}N_6O_4 \cdot HCl$, # L9873, Mr = 463.01) was added to wells. The cells were forcefully removed from the growth surface. The cell suspension containing protein were placed in Eppendorf tubes and sonicated (ViniSonic 300, Serial # V1256 200830) for 5 seconds and placed on ice for 10 minutes to disrupt cell membranes. The cell lysates were then centrifuged for 10 minutes at 1800*G* (ALC Multispeed Refrigerated Centrifuge PK121R, Serial # 30103759) at 4°C and the resultant supernatant held the applicable proteins. The supernatant was pipetted into new Eppendorfs and stored at -80°C until further analyses were carried out.

2.4 Protein quantification

2.4.1 Bradford reagents

Reagents were prepared according to the Bradford protein determination method (Bradford 1976).

2.4.2 Lysate protein quantification

Small volumes of each sample were used to determine the total protein content. After the Bradford method was performed the solutions were placed in cuvettes and spectrophotometrically (Cary 50 Conc UV visible spectrophotometer, Vorna Valley, RSA, Serial # EL00034073) analysed. The Absorbance readings were compared to a standard curve in order to determine protein concentrations.

2.4.3 Sample preparation

A specific volume of the sample was isolated in order to contain a total of 20 µg of protein. A pre-made sample buffer containing 10% (v/v) mercaptoethanol (Batch # 09524MH) was added to the proteins. Samples were frozen at -80°C.

2.5 Western blotting

2.5.1 Gel preparation

Cell lysate samples were separated on polyacrylamide gels by sodium dodecyl sulphate polyacrylamide gel electrophoresis (SDS-PAGE). The BIO RAD PowerPac Basic™ (Serial # 041BR19278) was used for gel preparation and electrophoresis. A 10% Loading gel was prepared for proteins ranging between 20 and 50 kDa in size and an 8% Loading gel was prepared for proteins ranging from 70 to 100 kDa. A 4% Stacking gel was layered on top of the Loading gel.

2.5.2 Gel electrophoresis

A Tris base/SDS running buffer was added to cover the wells of the gel. Protein marker (peQGold Protein Marker IV, peQLab, # 48770) and samples were loaded into the wells carefully to prevent sample from exiting its specific well. For the first phase of the electrophoresis run, power was set at a constant voltage of 100V and 400mA for 10 minutes to allow the samples to pass the loading gel. The second phase run was at constant amperes of 400mA and 200V and ran for 50 minutes.

2.5.3 Semi-dry transfer

Gels were placed in a transfer sandwich containing 2 squares of extra thick blotting paper (BIO RAD Protean XL size, # 1703969) and one 0.45 µm PVDF membrane (Pall Corporation, # T010981 submersed in Tris/Glycine Buffer (BIO RAD, # 161-0071). Proteins on the gel were transferred to the membrane by running the apparatus at 15V and 0.5A for one hour (BIO RAD Trans-Blot® SD Semi-dry transfer cell, Serial # 221BR30734)

2.5.4 Membrane probing

After the proteins were successfully transferred to the membrane, the membrane was removed from between the blotting paper squares. Membranes were washed using a shaker

platform belly dancer (Stoval Life Science Corporation, Breensboro, NC, USA, Patent # 4,702,610) (with 1% (v/v) TBS-Tween buffer). To prevent non-specific binding, membranes were blocked with 5% (w/v) non-fat milk powder dissolved in 1% (v/v) TBS-Tween buffer. Membranes were incubated with either mouse MyOD (Dako, Glostrup, Denmark, Ref: M3512, Lot 00002861), myogenin (F5D) (Santa Cruz, # G0510), PCNA (Santa Cruz, sc-7907, # G0910) or rabbit Phosphorylated-STAT3 (Cell Signalling, Danvers, MA, USA, Lot 6, # 9131S), STAT3 (Cell Signalling, Danvers, MA, USA, Lot 3, # 9132) primary antibodies overnight at 4°C with constant agitation**.** After the primary antibodies were allowed to bind, the membrane was washed on the shaker platform with 1% (v/v) TBS-Tween three times. The membrane was incubated in either anti-mouse [Anti-mouse IgG Horseradish Peroxidase linked (GE Healthcare UK Limited, Ref: NIF825, # 358607)] or anti-rabbit [Anti-Rabbit Donkey IgG Horseradish Peroxidase linked (GE Healthcare UK Limited, # 362613)] secondary antibodies for 1 hour at room temperature with constant agitation and again washed three times with 1 % (v/v) TBS-Tween buffer.

Table 4: Western Blotting Primary Antibody Specifications and Dilutions

1 °Antibody	Manufacturer	Description	Dilution
MyoD	Santa Cruz	Mouse Monoclonal	1:1000
myogenin	Santa Cruz	Mouse Monoclonal	1:1000
PCNA	Santa Cruz	Mouse Monoclonal	1:1000
P-STAT3	Cell Signaling	Rabbit Polyclonal	1:1000
T-STAT3	Cell Signaling	Rabbit Polyclonal	1:1000
β-actin	Cell Signaling	Rabbit Polyclonal	1:1000

Table 5: Western Blotting Secondary Antibody Specifications and Dilutions

2°Antibody	Manufacturer	Description	Dilution
Anti-Mouse	Cell Signaling	Donkey HRP conjugated	1:5000
Anti-Rabbit	Cell Signaling	Donkey HRP conjugated	1:5000

2.5.5 Protein visualization

After incubation with the secondary antibody the Amersham™ ECL™ Western Blotting Detection Reagents were warmed to room temperature (GE Healthcare, Buckinghamshire, UK, # 56, Pack: W364982). The detection reagent substrates were added together in equal volumes and administered to the area of the membrane where the protein of interest was located. The membrane was transferred to a light blocking Hypercassette™ (Amersham Biosciences UK Limited, England, Batch # 0803). The Hypercassette™, containing the membranes, was taken into a dark room**.** Hyperfilm™ (GE Healthcare LTD, Buckinghamshire, HP84SP, UK) was cut in order to cover the area of interest on the membrane. The Hypercassette™ was closed and the film was left to develop. Bands of proteins were developed to appear in shades of gray and not become bleached leading to black bands. The film containing bands was fixed by means of an X-ray fixer to protect it from light bleaching.

2.5.6 Densitometric analysis

The developed hyperfilms were digitally scanned (hp scanjet 3500c, Serial #Q2800A) in 256 gray scale after development. Densitometric analysis was performed by ImageJ Software (1.43μ, Wayne Rasband, National Institutes of Health, USA).

2.5.7 Membrane stripping

Proteins bound to PVDF membranes could be reprobed with a different antibody, in which case previous antibodies were stripped from the membrane by a 0.2 M NaOH (Merck, # MH6M561954, Mr = 40.00) washing step for 5 minutes with agitation at room temperature.

2.6 Flow cytometry

2.6.1 Cell cycle analysis

Cell samples suspended in citrate buffer were removed from the -80°C freezer and allowed to thaw. Samples were treated in accordance with the Vindelov protocol (Vindelov, Christensen et al. 1983). The Vindelov protocol incorporates trypsin inhibitors and detergents to gain a clean sample. RNase is also added to remove single-stranded RNA and leave only DNA. Finally, Propidium Iodide is added to intercalate with the DNA and by doing so the cell DNA can be quantified by means of fluorescence. The solution was placed on ice for 15 minutes, with the eppendorfs wrapped in foil, and cell cycle fractions were analysed by a Flow Cytometer (BD FACSAria™ Cell Sorter, Serial # P9990037, BD Biosciences, San Jose, CA 95133 USA).

If IL-6 asserts control over the cell cycle, there has to be a shift from one phase to another of the cell cycle. An example of a phase shift can be seen in Figure 8.

The scatterplots obtained show the size and granularity of cells analysed. The X-axis represents the forward scatter (FSC-A) channel, which shows the extent of propidium iodide staining (granularity) within each cell. The Y-axis represents the side scatter (SSC-A) channels, which shows the size of cells analysed.

Histograms were obtained from the analysis of scatterplots. In the histograms the Y-axis represents cell numbers and the X-axis shows the granularity of cells analysed, which gives an indication of chromatin density within the cells. Diploid cells' DNA was labeled by the intercalating propidium iodide stain. The two distinct, red peaks of the G0/G1 and G2/M phase can be observed in the histograms. Cells in the G0/G1 phase have less DNA content and thus lower granularity when compared to the G2/M phase. Peaks in scatter plots are assumed to be Gaussian (bell-shaped) curves. The S-phase is extrapolated from the start of the S-phase bell shape to the end of the G2/M curve. In this example, cells have shifted to the S-phase when a High cytokine dose was administered. This is clearly seen as a higher number of cells in the S-phase of the cell cycle. Histograms were obtained from the analysis of scatter plots by the ModFIT software package.

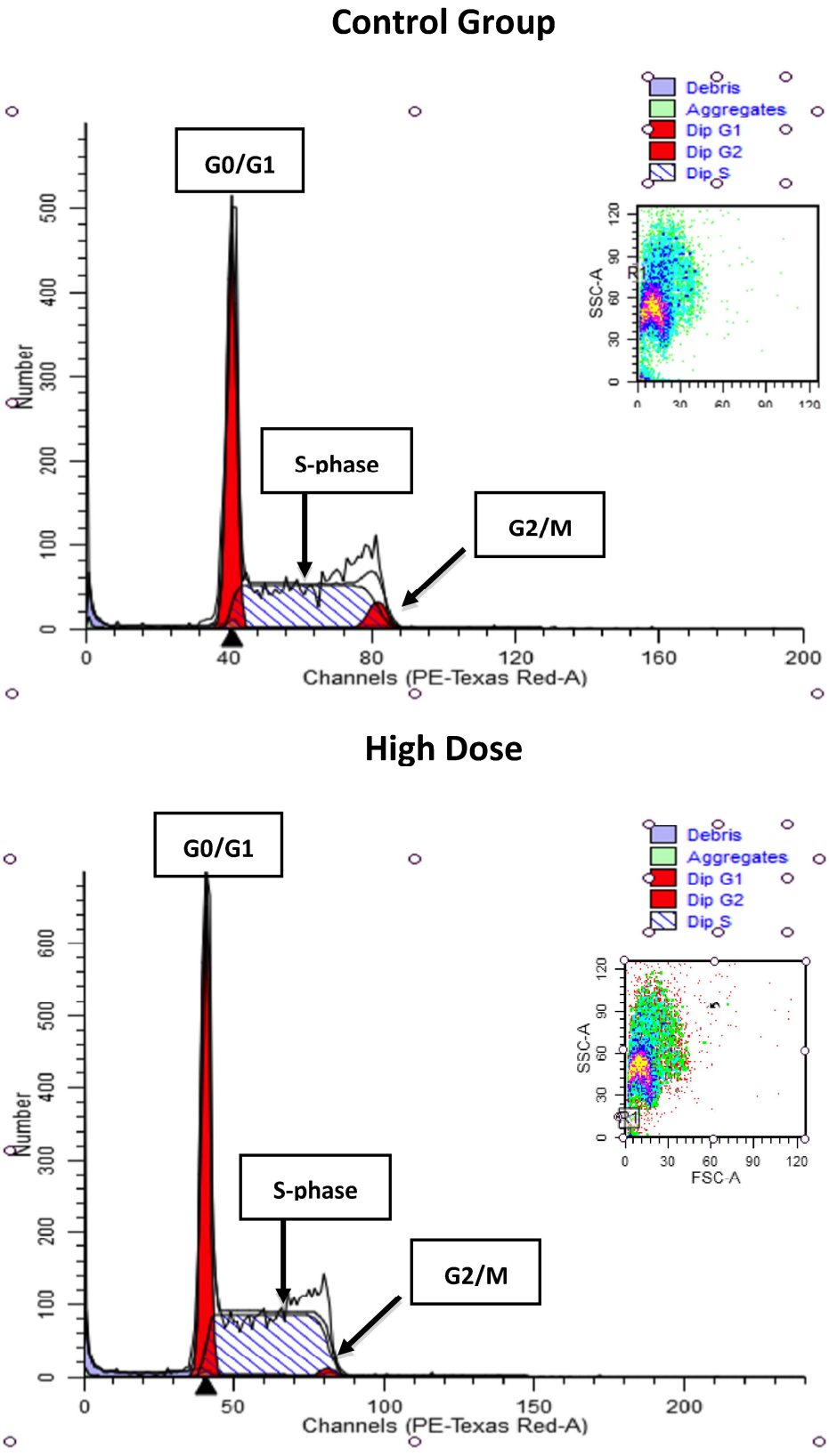

Figure 8: Cell Cycle Analysis Histograms

2.7 Immunocytochemistry

2.7.1 Double antibody (myogenin, PCNA) staining method

Cells were seeded at 40 000 per well and treated for either 24 or 48 hours with varying doses of IL-6. 4% (v/v) Paraformaldehyde [$(H.CHO)_n$, Hopkin & Williams Ltd, # 11945B86224] was added to fix cells to the coverslips. Coverslips were removed from wells and transferred to microscope slides. Slides were washed with PBS for 5 minutes and washing steps were performed after the addition of each new reagent. Ice-cold methanol was added to the slides and left on ice for 30 minutes. 0.25% (v/v) Triton X-100 was added to slides and incubated for 15 minutes at room temperature to perforate cell membranes. 20% (v/v) Goat Serum (PAA, # B15-035) was added to slides and incubated for 30 minutes at room temperature to block non-specific binding. Primary antibody #1, myogenin (Dako,Glostrup, Denmark, Ref : M3559, Lot 10012968) was added to the slides and incubated overnight at 4°C. Secondary antibody #1, Alexa Fluor 488 (Invitrogen, # A11029) was added to slides and incubated for 60 minutes at room temperature. Primary antibody #2, PCNA (Santa Cruz, sc-7907, # G0910) was added to the slides and incubated for 4 hours at room temperature. Secondary Antibody #2, Alexa Fluor 594 (Invitrogen, # A11012) was added to slides and incubated for 60 minutes at room temperature. Nuclear stain (Bis Benzimide H33422 trihydrochloride, # B2261) was added to slides and incubated for 15 minutes at room temperature. Coverslips were then transferred to new frosted slides and mounted with fluorescent mounting medium (Dako, # S5023). Slides were stored at -20°C until visualized by fluorescence microscopy (Olympus IX81 fitted with CellR® software) within a maximum of 7 days.

2.7.2 Mitochondrial and antibody (pSTAT3) staining method

Cells were seeded at 40 000 per well the day preceding IL-6 treatment. Medium supplemented with MitoTracker® Red CMX Ros (Mr = 531.52, #M7512) was added to cells where it is oxidized and sequestered by the mitochondria to create the active signal. Cells were treated with IL-6 for 5, 10, 15 and 30 minutes. 4% (v/v) Paraformaldehyde [$(H.CHO)_n$, Hopkin & Williams Ltd, # 11945B86224] was added to fix cells to the coverslips. Coverslips were removed from wells and transferred to microscope slides. Slides were washed with PBS for 5 minutes between each incubation step with each new reagent. Ice-cold methanol was added to the slides and left on ice for 30 minutes. 0.25% (v/v) Triton X-100 was added to slides and incubated for 15 minutes at room temperature to perforate cell membranes. 5% (v/v) Donkey Serum (Jackson Immun Research, # 017-000-121) was added to slides and

incubated for 30 minutes at room temperature to block non-specific binding. Phosphorylated-STAT3 Tyr705 (Cell Signalling, Danvers, MA, USA, Lot 6, # 9131S) primary antibody was added to the slides and incubated for 2 hours at room temperature. Secondary antibody, Donkey Anti-Rabbit IgG FITC (Santa Cruz, # sc-2090) was added to slides and incubated for 60 minutes at room temperature. Nuclear stain (Bis Benzimide H33422 trihydrochloride, # B2261) was added to slides and incubated for 15 minutes at room temperature. Coverslips were then transferred to new frosted slides and mounted with fluorescent mounting medium (Dako, # S5023). Slides were stored at -20°C until visualized by fluorescence microscopy (Olympus IX81 fitted with CellR® software) with a maximum storage time of 7 days.

Table 6: Immunocytochemistry Primary Antibody Specifications and Dilutions

1 °Antibody	Manufacturer	Description	Dilution
myogenin	DAKO	Mouse Monoclonal	1:100
PCNA	Santa Cruz	Rabbit Polyclonal	1:100
pSTAT3	Cell Signaling	Rabbit Polyclonal	1:100
DAPI (20 mg/ml)	Sigma	BisBenzimide	1:8000 (2.5 µg/ml)

Table 7: Immunocytochemistry Secondary Antibody Specifications and Dilutions

2°Antibody	Manufacturer	Description	Dilution
Alexa Fluor 594	Invitrogen	Goat Anti-rabbit IgG	1:500
Alex Fluor 488	Invitrogen	Goat Anti-mouse IgG	1:500
Anti-Rabbit	Santa Cruz	Donkey FITC conjugated	1:250

2.8 Statistical analysis

Analyses were performed with Graphpad Prism 4.0. One-way Anova was the statistical test used with Dunnetts post hoc test. Values are expressed as mean ± standard error of the mean (SEM). Statistical significance was accepted when $p < 0.05$.

3.Results

3.1 Cell cycle

Flow Cytometric Analysis evaluates a number of parameters, including the size and granularity of a cell. The fluorescence emitted by the intercalated DNA stain is assessed and the quantification of the fluorescent signal can be utilized in the determination of cell cycle phases. The cell cycle phases in question are G0/G1, S and G2/M. The G0/G1 phase is usually described as a growth and differentiation phase. The S or Synthesis phase is associated with DNA replication and proliferation just before mitosis (G2/M phase) is set underway.

Satellite cells were exposed to varying concentrations of IL-6 and the treated cells were harvested for flow cytometric analysis 24 (Fig. 9A) and 48 (Fig. 9B) hours after IL-6 treatment. Each set of the experiment was repeated in triplicate.

The data presented in Figure 5 shows the percentage of cells in each cell cycle phase and the statistical analysis determined whether treatment significantly changed the percentage of cells in a specific phase compared to the same phase in Control. After 24 hours of IL-6 treatment a change in cell cycle distribution was evident (Fig. 9A). The Medium (39.5±0.37) as well as the Low doses (38.7±0.31) of IL-6 significantly decreased ($p<0.05$) the percentage of cells in the G0/G1 phase when compared to the Control group (41.4±0.18). This was not accompanied by a significant increase in percentage of cells in the S-phase in both groups. Only the Low dose (58.7±0.67) significantly increased ($p<0.05$) the percentage of cells in the S-phase of the cell cycle when compared to the Control group (53.7±1.75).

At 48 (Fig. 9B) hours of IL-6 treatment the phase shift differed to that seen at 24 hours. At this time point it was found that the High (57.8 ± 0.61), Medium (57.5 ± 0.55) and Low (58.3 ± 0.12) treatments significantly decreased ($p<0.05$) the percentage of cells in the G0/G1 phase when compared to the Control group (60.85±0.34). The High (38.9 ± 0.79), Medium (39.1 ± 0.54) and Low (39.4 ± 0.14) doses also significantly increased ($p<0.05$) the percentage of cells in the S-phase of the cell cycle.

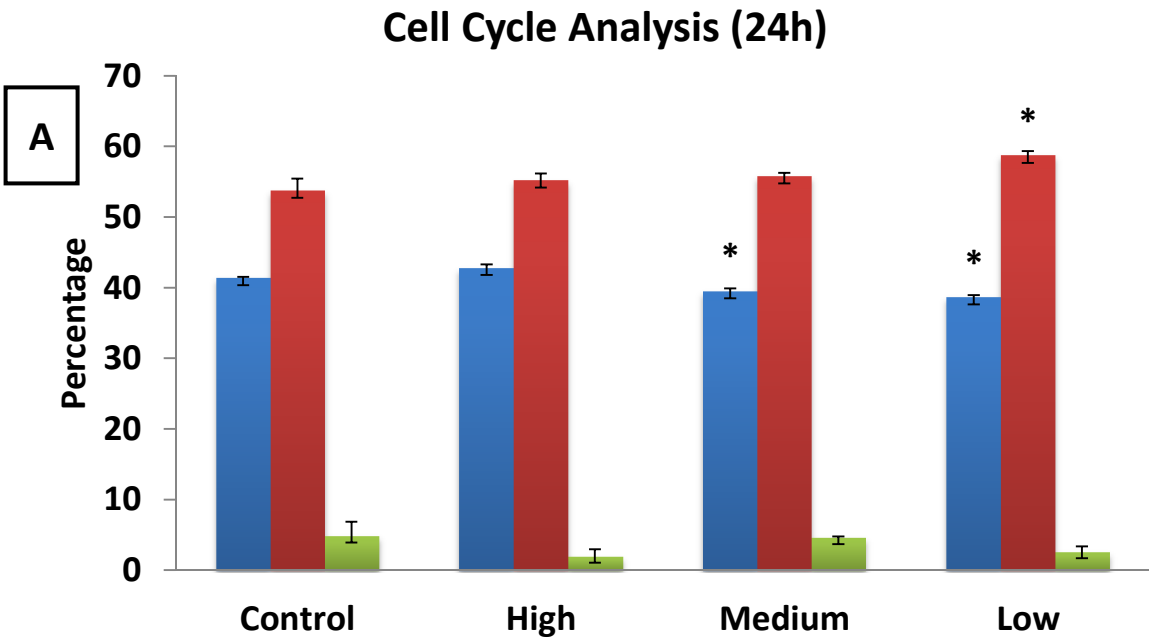

G0/G1	41.35±0.18	42.79±0.52	39.52±0.37*	38.65±0.31*
S	53.72±1.75	55.17±1.02	55.78±0.47	58.68±0.67*
G2/M	4.93±1.92	2.04±0.92	4.70±0.09	2.68±0.69

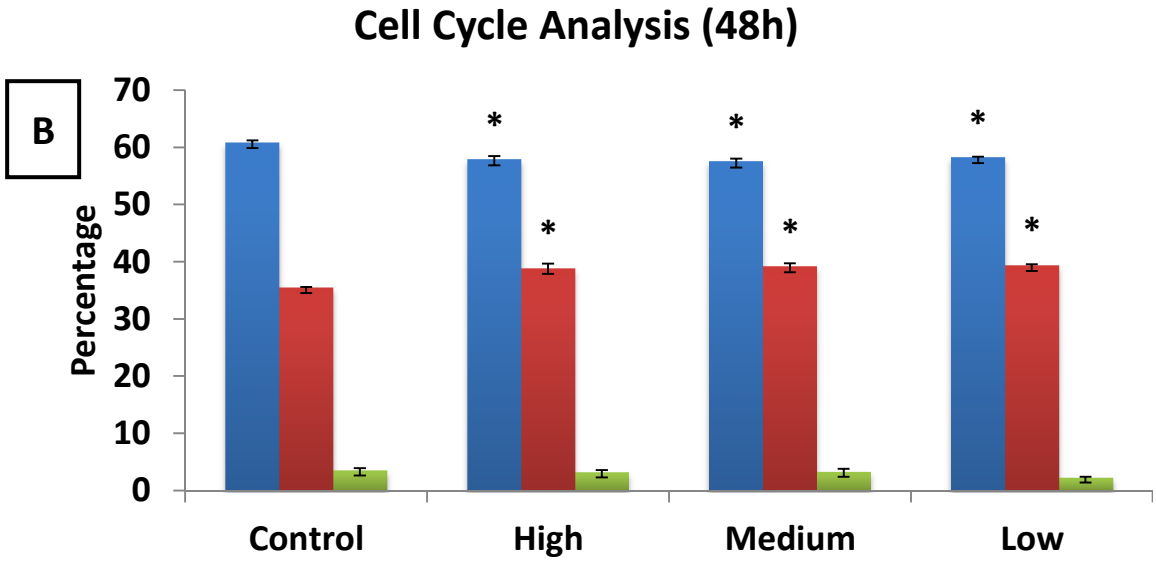

G0/G1	60.85±0.34	57.84±0.61*	57.46±0.55*	58.25±0.13*
S	35.53±0.06	38.86±0.79*	39.17±0.54*	39.39±0.14*
G2/M	3.62±0.28	3.3±0.26	3.37±0.41	2.36±0.01

Figure 9: Cell cycle fractions at 24 (A) and 48 hours (B) of IL-6 treatment. (n=3, Mean±SEM, $p<0.05$, *vs control)

3.2 Myogenic regulatory factors

Myogenic regulatory factors (MRFs) are in part responsible for the progression of satellite cells through the cell cycle. Their expression patterns in particular are altered as the cells progress through the cell cycle. MyoD is a regulatory protein associated with the late phases of proliferation as well as early phase differentiation (G0/G1 phase). Myogenin signals the exit of cells from the cell cycle and is associated with terminal differentiation (G0/G1). PCNA (proliferating cell nuclear antigen) is expressed by cells in the proliferation phase i.e. when they are actively dividing in the S-phase.

The expression of MRFs was semi-quantitively assessed at 24 (Fig. 10) as well as 48 (Fig. 11) hours of IL-6 treatment.

At 24 hours the expression of MyoD was unaffected by IL-6 treatments but PCNA expression was significantly increased by the Medium and Low doses when compared to the Control group. Myogenin expression was miniscule as a result of cells being cultured in Proliferation Medium and terminal differentiation at 24 hours is highly unlikely (no protein could be quantified).

Myogenin expression was significantly increased after 48 hours of High dose IL-6 treatment. MyoD promotes the expression of myogenin thus the pattern of MyoD expression was similar, although not statistically significant. After 48 hours of Medium and Low dose treatment the expression of PCNA was highly elevated on average 8-fold when compared to the Control group, although the fold-increase varied between the 3 different experiments. The Low dose seems to decrease the expression of both MyoD and myogenin 48 after 48 hours of IL-6 treatment, but not to a statistically significant effect.

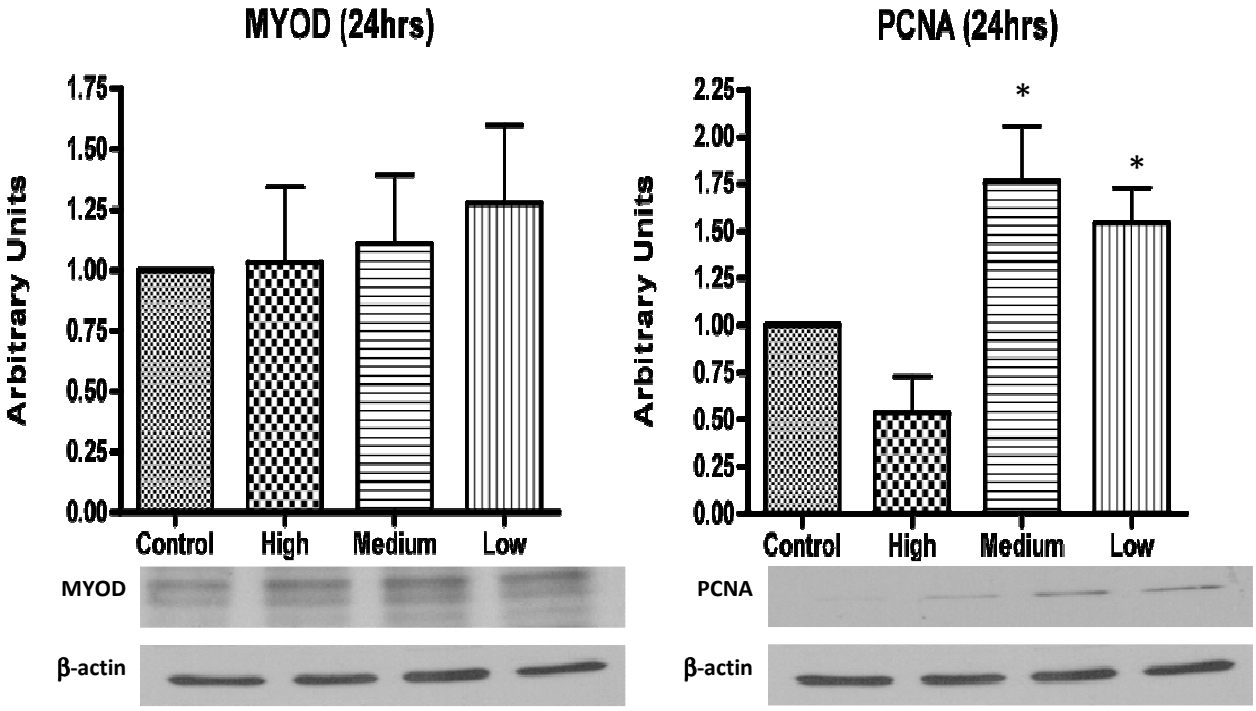

Figure 10: Protein expression levels of MyoD and PCNA, 24 hours after IL-6 treatment. (n=3, Mean±SEM, $p<0.05$, *vs control)

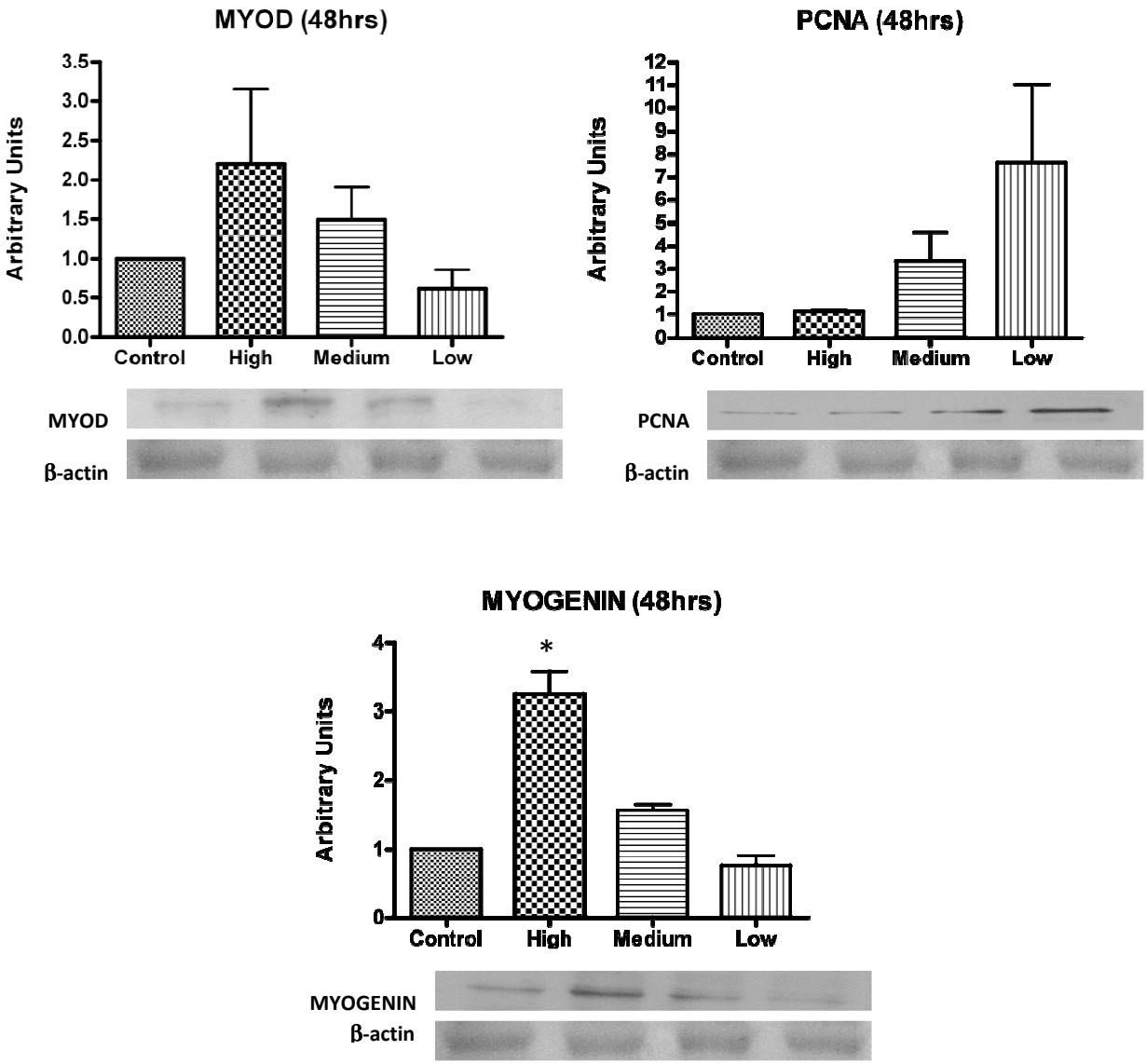

Figure 11: Protein expression levels of MyoD, PCNA and Myogenin, 48 hours after IL-6 treatment. (n=3, Mean±SEM, p<0.05,*vs control)

3.3 Visualization of myogenin and PCNA

By performing immunocytochemistry it is possible to qualitatively evaluate the levels of MRF expression as well the relative position of these regulatory factors within the cell. The signal strength between groups could be accurately compared as a result of constant intensity and exposure time settings between groups.

In the following figures, myogenin (green) and PCNA (red) are first presented individually in order that the intensity of staining can be more easily seen. The merged images resulted in an orange colour when myogenin and PCNA were expressed in the same cell. The nuclear region (blue) confirms the presence and also the size of the nucleus and allows for the determination of single cells, clustered cells and dividing cells. It is also possible to visualize the extent of the PCNA expression. Arrows provided to indicate the same group of cells in each image.

When evaluating the expression of the MRFs at 24 hours it mirrors the results seen when the protein was semi-quantified. The Medium (Fig. 14A) and Low (Fig. 15A) doses clearly increased the expression of PCNA when compared to the Control group (Fig. 12A). Interestingly the High (Fig. 13A) dose seems to have decreased the expression of PCNA at 24 hours, which was only seen as a trend with protein quantification.

At 48 hours the images resemble that of the western blotting. When compared to the Control group (Fig. 16A) and High (Fig. 17A) dose, the Medium (Fig. 18A) and Low (Fig. 19A) dose distinctly increased PCNA expression within the cells. The myogenin expression in the High (Fig. 17B) group also appears to be higher than the myogenin expression in the Medium (Fig. 18B) and Low (Fig. 19B) doses.

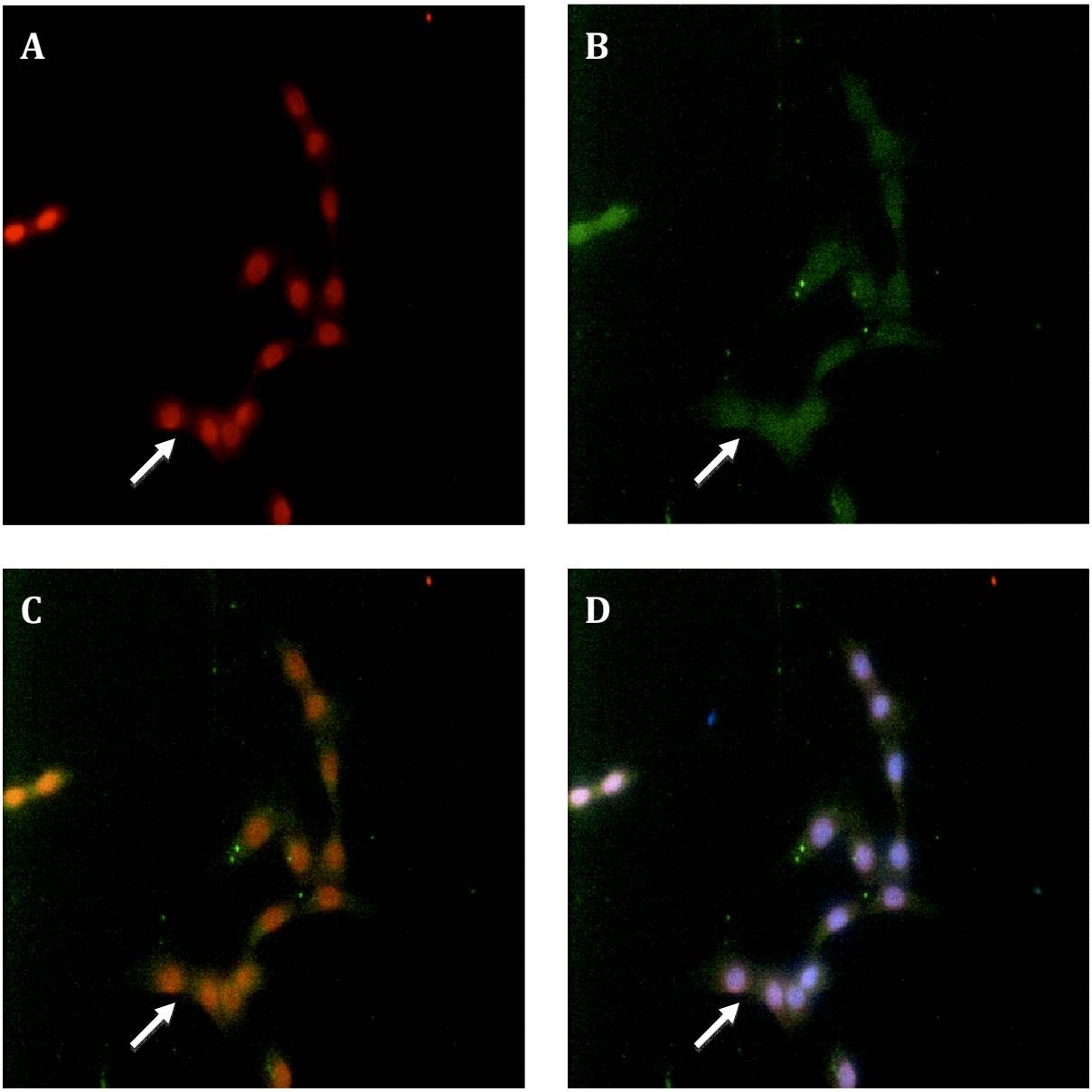

Figure 12: Immunocytochemical Analysis of Control group visualizing the expression of PCNA (A), Myogenin (B), PCNA & Myogenin (C) and PCNA, Myogenin and DAPI (D) at 24 hours. Arrows provided to indicate the same group of cells in each image.

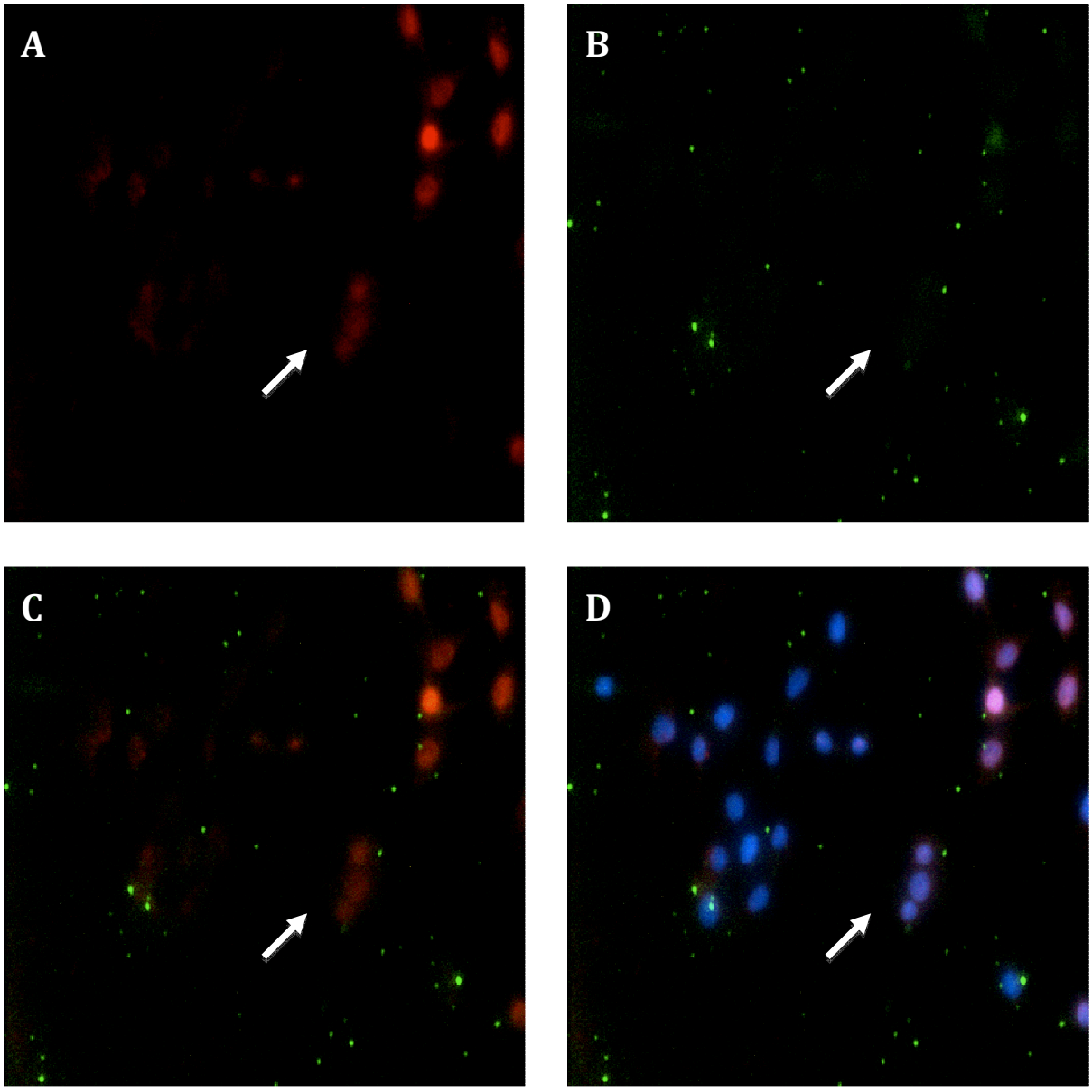

Figure 13: Immunocytochemical Analysis of High IL-6 treatment group visualizing the expression of PCNA (A), Myogenin (B), PCNA & Myogenin (C) and PCNA, Myogenin and DAPI (D) at 24 hours.

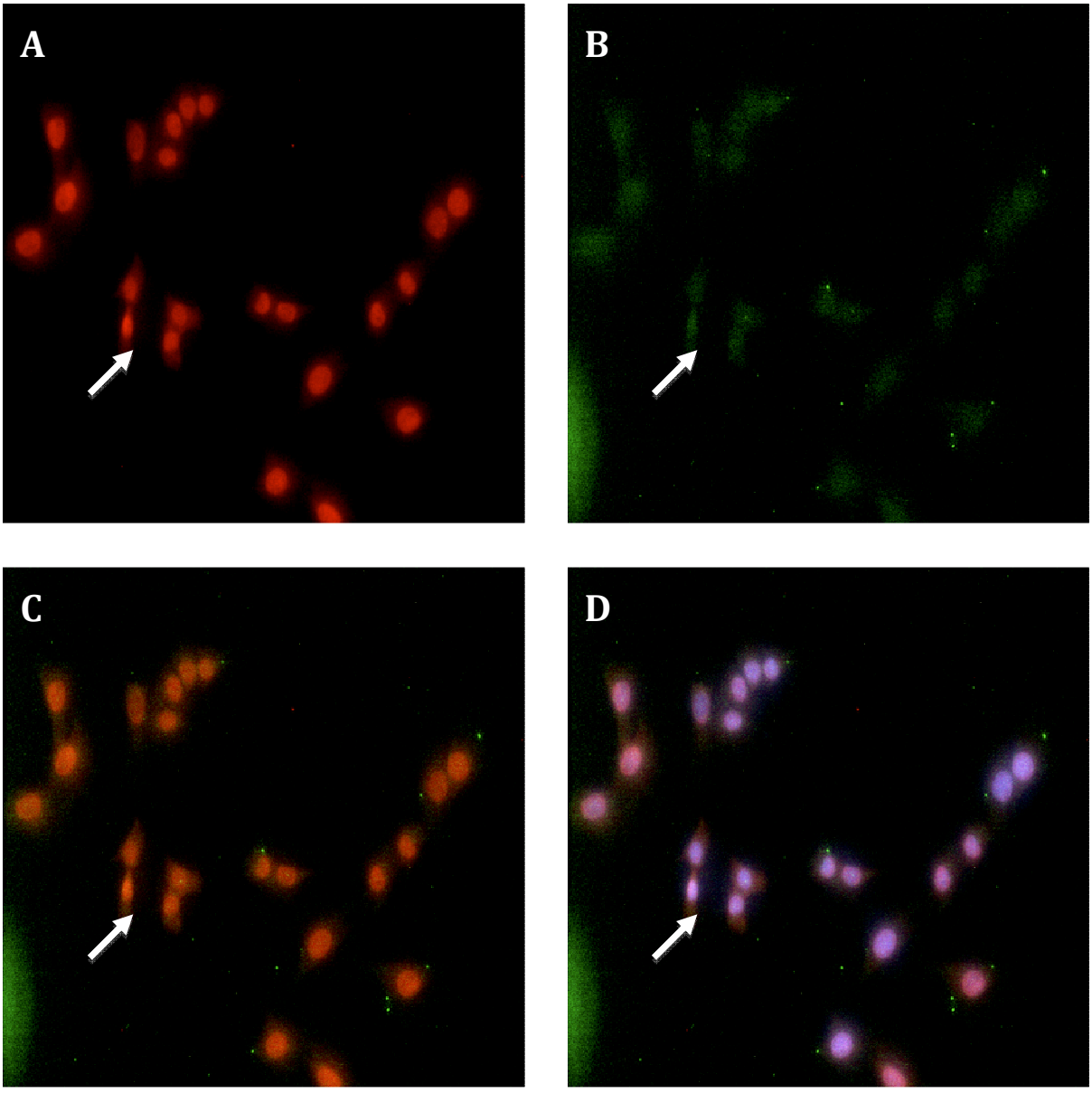

Figure 14: Immunocytochemical Analysis of Medium IL-6 treatment group visualizing the expression of PCNA (A), Myogenin (B), PCNA & Myogenin (C) and PCNA, Myogenin and DAPI (D) at 24 hours.

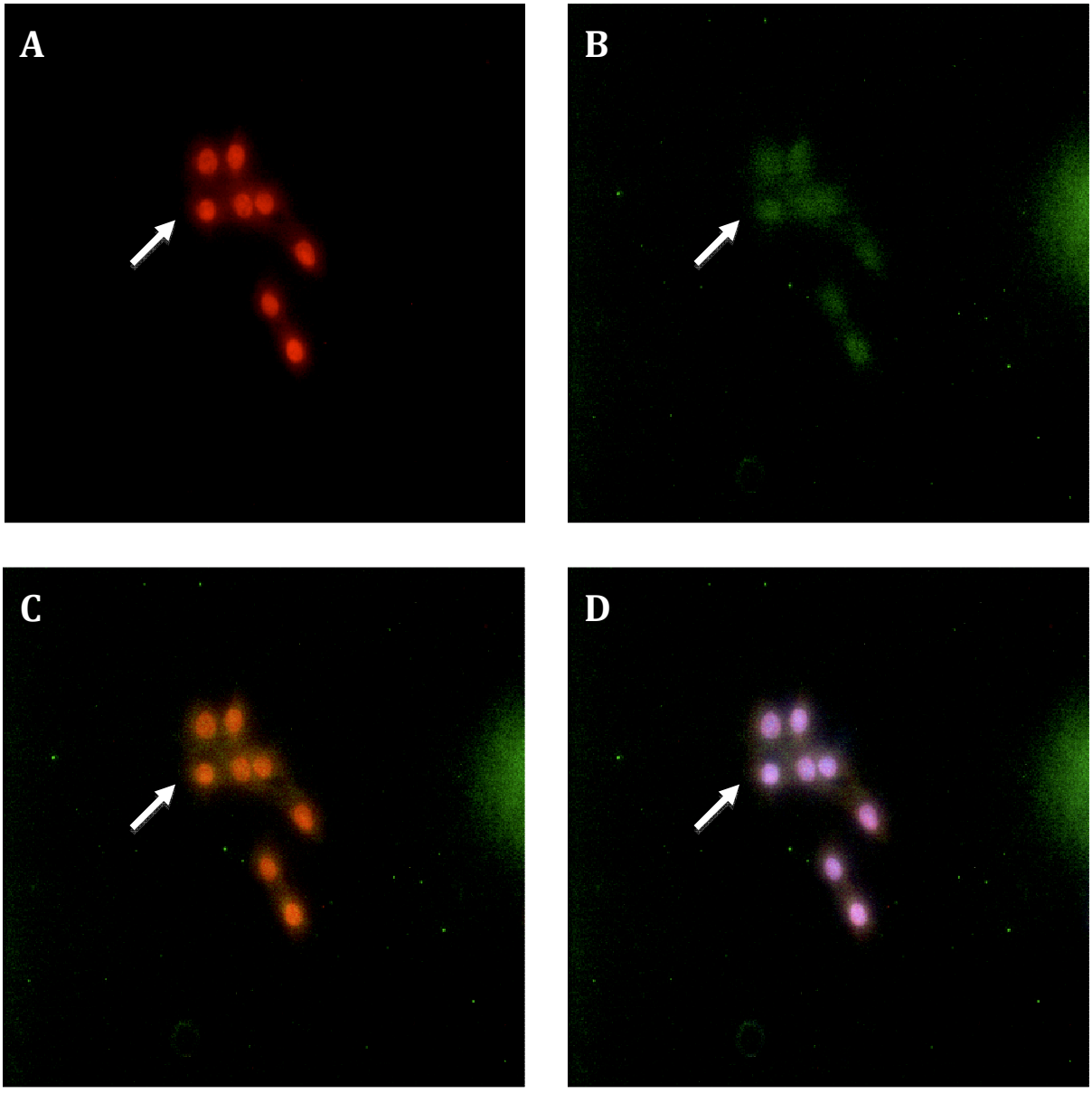

Figure 15: Immunocytochemical Analysis of Low IL-6 treatment group visualizing the expression of PCNA (A), Myogenin (B), PCNA & Myogenin (C) and PCNA, Myogenin and DAPI (D) at 24 hours.

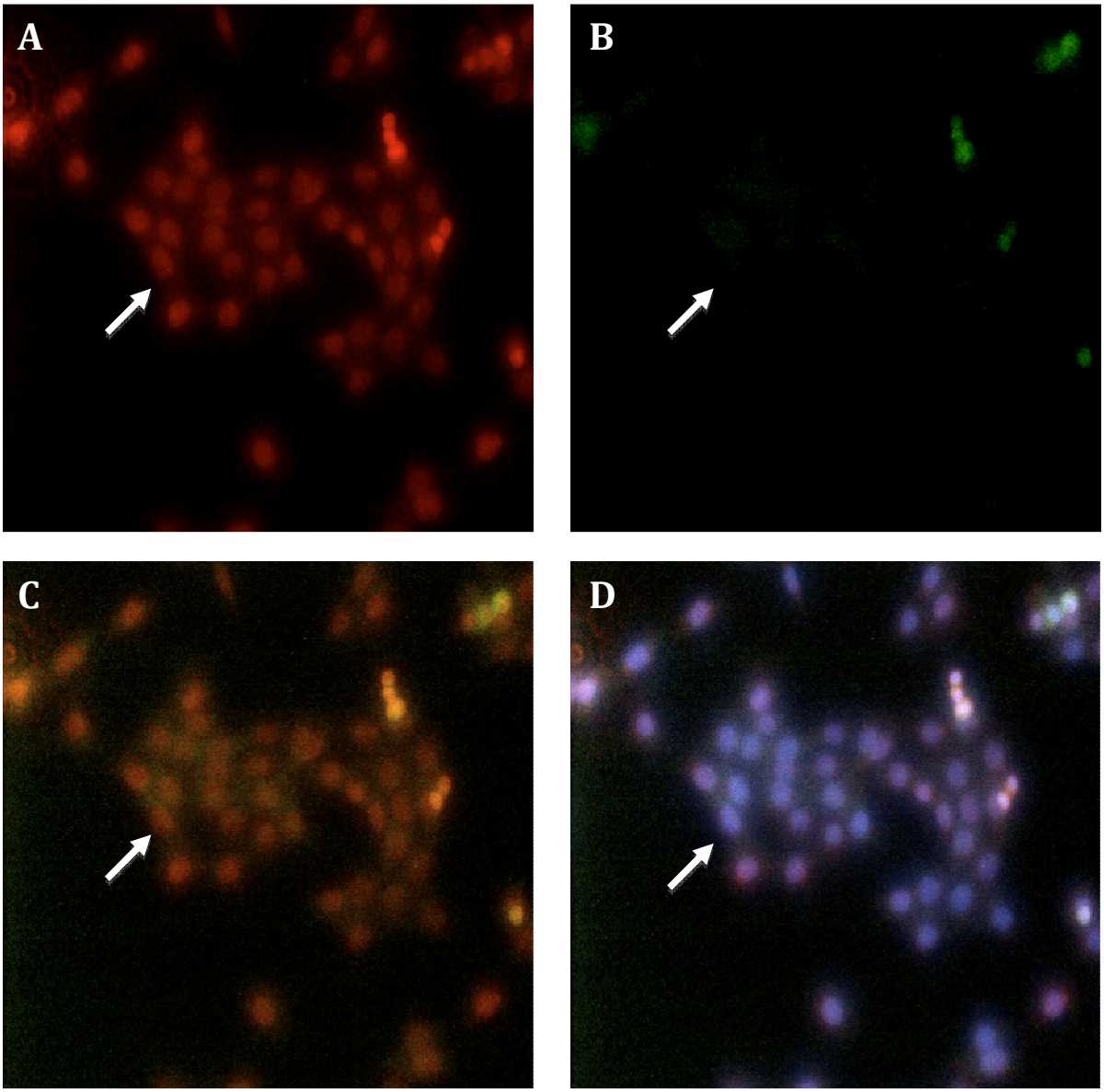

Figure 16: Immunocytochemical Analysis of Control group visualizing the expression of PCNA (A), Myogenin (B), PCNA & Myogenin (C) and PCNA, Myogenin and DAPI (D) at 48 hours.

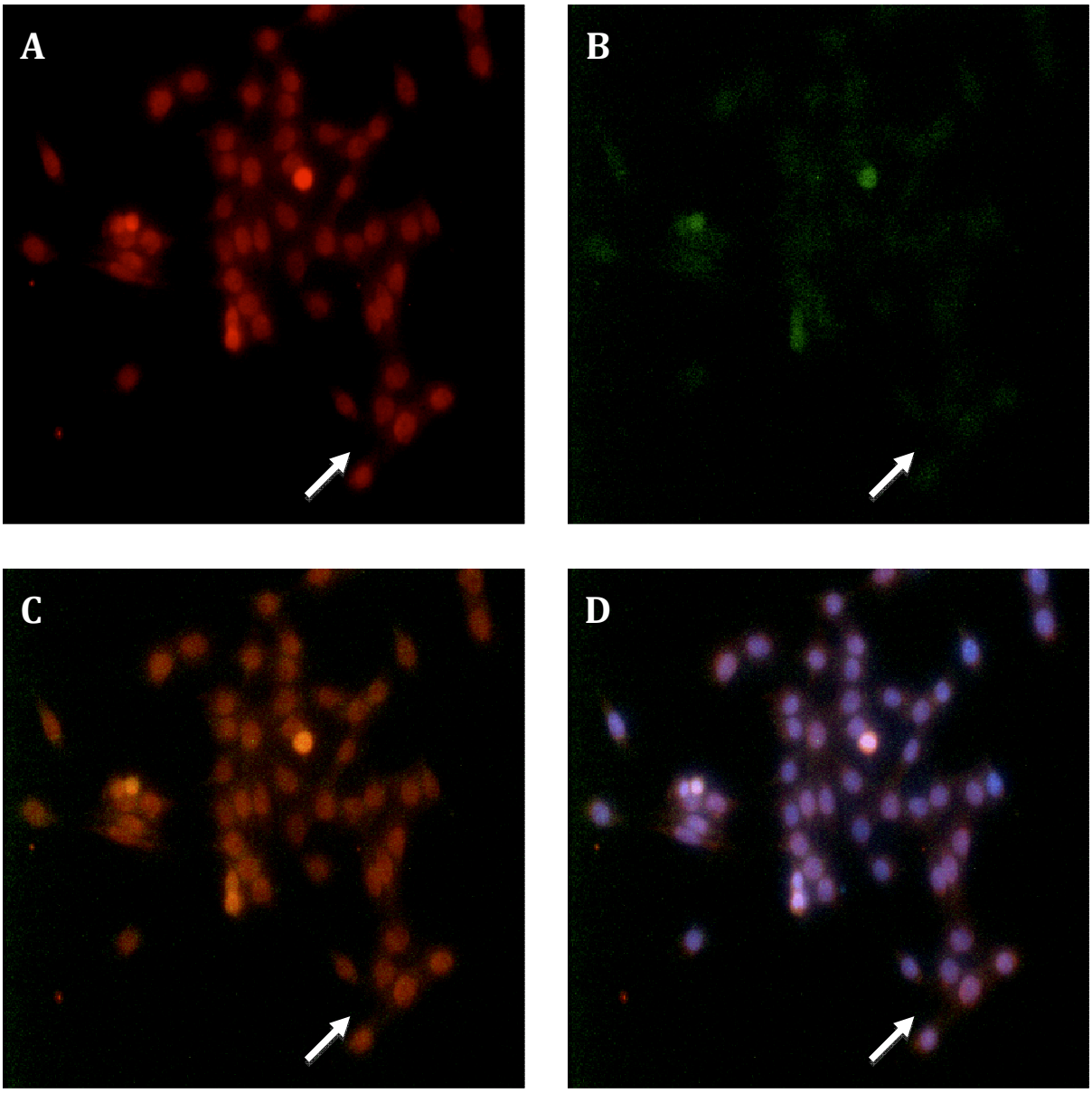

Figure 17: Immunocytochemical Analysis of High IL-6 treatment group visualizing the expression of PCNA (A), Myogenin (B), PCNA & Myogenin (C) and PCNA, Myogenin and DAPI (D) at 48 hours.

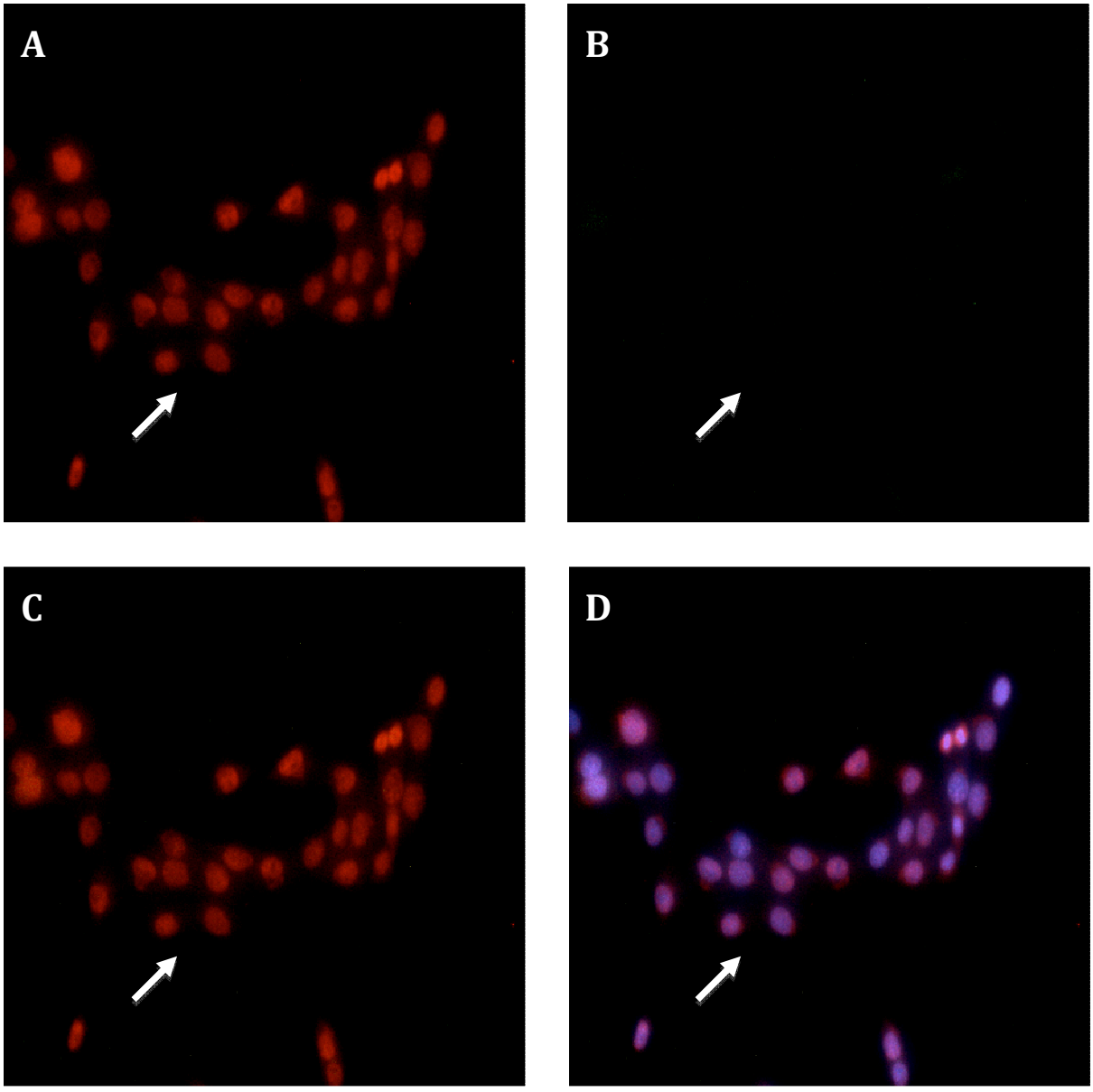

Figure 18: Immunocytochemical Analysis of Medium IL-6 treatment group visualizing the expression of PCNA (A), Myogenin (B), PCNA & Myogenin (C) and PCNA, Myogenin and DAPI (D) at 48 hours.

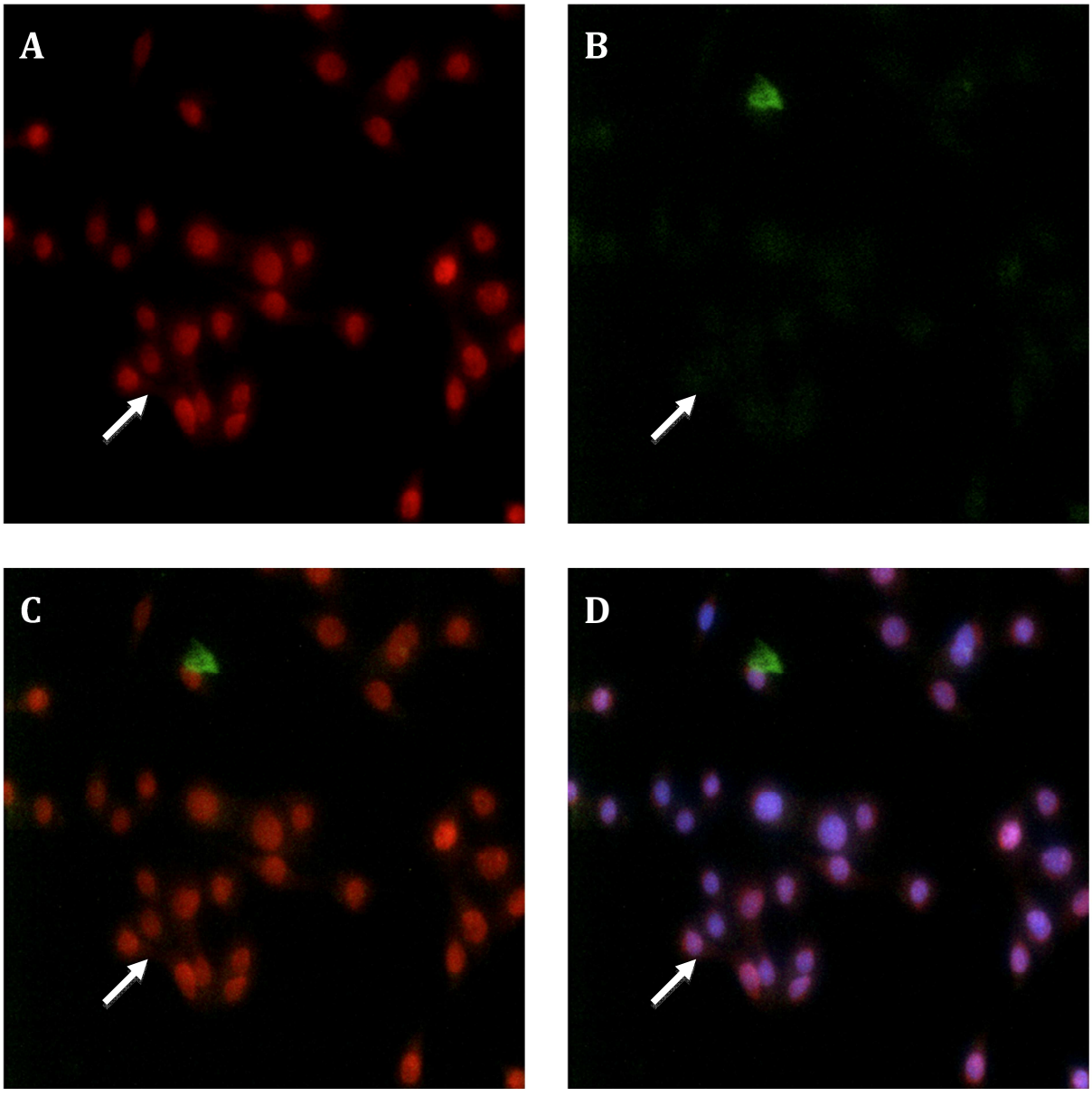

Figure 19: Immunocytochemical Analysis of Low IL-6 treatment group visualizing the expression of PCNA (A), Myogenin (B), PCNA & Myogenin (C) and PCNA, Myogenin and DAPI (D) at 48 hours.

3.4 Signalling downstream of IL-6

IL-6 signals through its receptor consisting of two gp130 subunits. The gp130 subunits attract the JAK kinases. The JAK molecule activates resident STAT3 molecules within the cell by phosphorylation of the STAT3 signal transducer. When the phosphorylated STAT3 (pSTAT3) is formed, the molecule translocates to the nucleus where it interacts with a wide range of gene sequences. This process occurs very rapidly thus immunocytochemical analysis had to be done at 5, 10, 15 and 30 minute intervals.

Mitochondria (red) as well as pSTAT3 (green) expression were visualized. The mitochondria were stained in order to assess whether activated STAT3 has any targets other than the DNA in the nucleus of the cell. In the following images each stain is represented in a separate image and a merged image (yellow) shows the expression of both these molecules within the same cell. The nuclear region (blue) confirms the presence and also the size of the nucleus and allows for the determination of single cells, clustered cells and dividing cells. It is also possible to visualize the expression of pSTAT3 within the nucleus. Arrows provided to indicate the same group of cells in each image.

After 5 minutes of IL-6 administration it is visually clear that the incidence of pSTAT3 is higher in all treatment groups (Fig. 21-23B) when compared to the Control group (Fig. 20B). pSTAT3 levels decreased in the Medium (Fig. 26B) and Low (Fig. 27B) groups 10 minutes after IL-6 exposure whereas pSTAT3 levels in the High (Fig. 25B) group remained elevated when compared to the Control (Fig. 24B) group. As time progressed the levels of pSTAT3 in the treatment groups decreased and returned to levels seen in the Control group. When pSTAT3 expression is highest at 5 minutes, the majority of the pSTAT3 is seen in the cytoplasm with a lesser extent seen in the nucleus of the IL-6 treated cells. When observing the distribution of pSTAT3 at the 30 minute interval, it appears that the pSTAT3 is concentrated around the nucleus with the possibility of pSTAT3 nuclear translocation.

Interestingly the activated STAT3 distribution seems to be closely related to the mitochondrial distribution. There seems to be co-localization between the pSTAT3 and the mitochondria and this is evident in the treatment groups at 5 and 10 minutes.

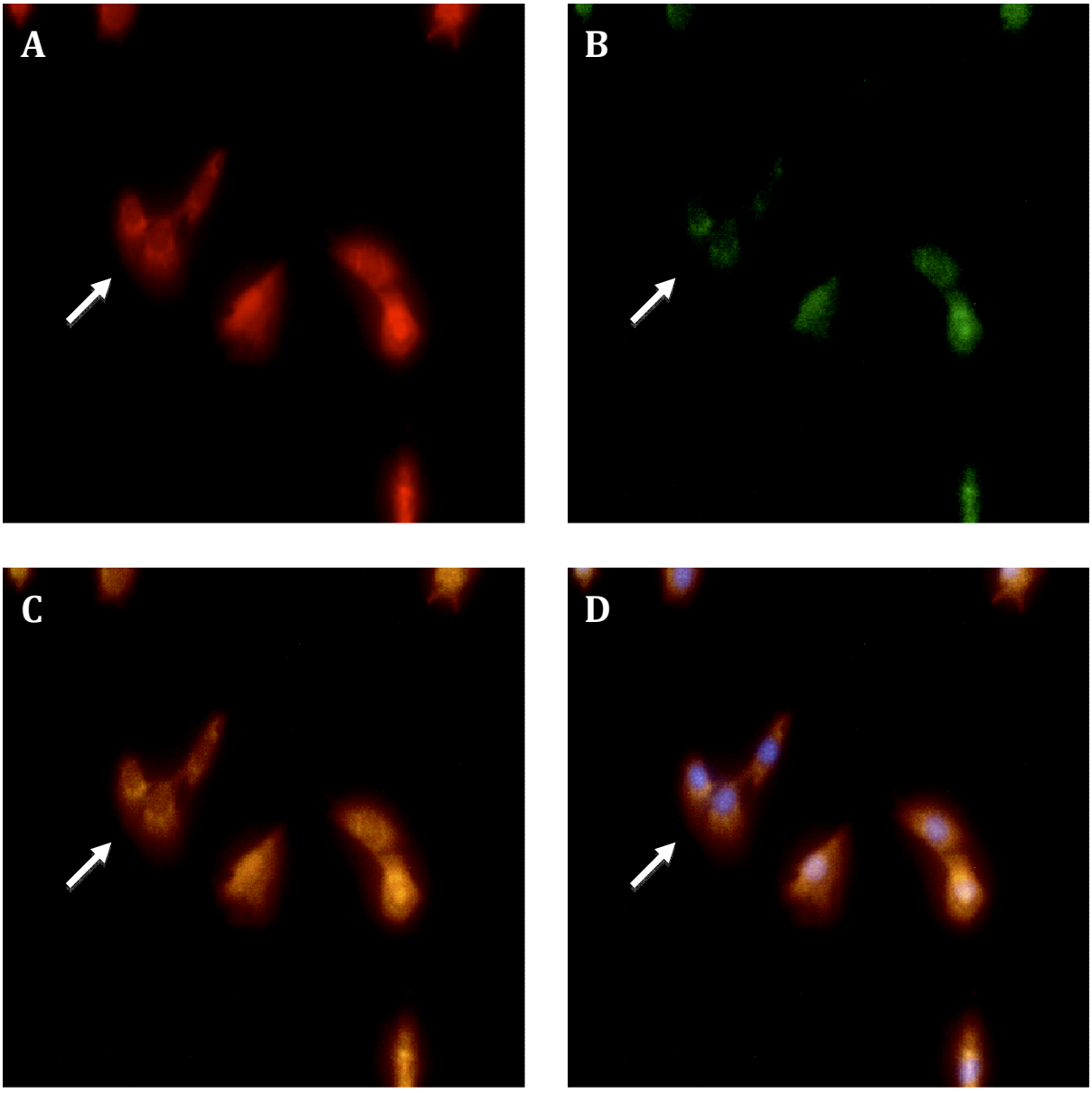

Figure 20: Immunocytochemical Analysis of Control group visualizing the Mitochondria (A), pSTAT3 (B), Mitochondria & pSTAT3 (C) and Mitochondria, pSTAT3 and DAPI (D) at 5 minutes. Arrows provided to indicate the same group of cells in each image.

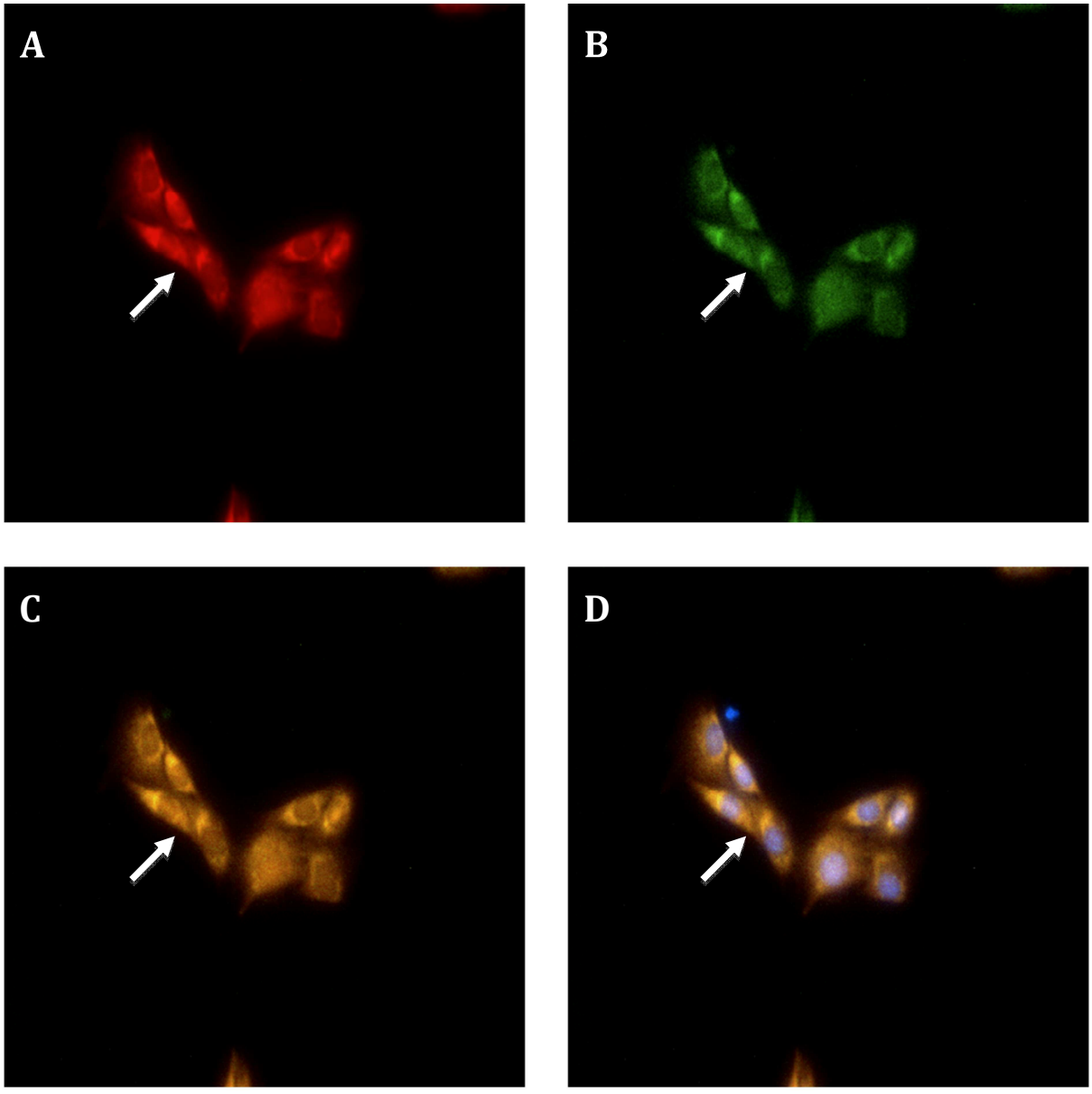

Figure 21: Immunocytochemical Analysis of High IL-6 treatment group visualizing the Mitochondria (A), pSTAT3 (B), Mitochondria & pSTAT3 (C) and Mitochondria, pSTAT3 and DAPI (D) at 5 minutes.

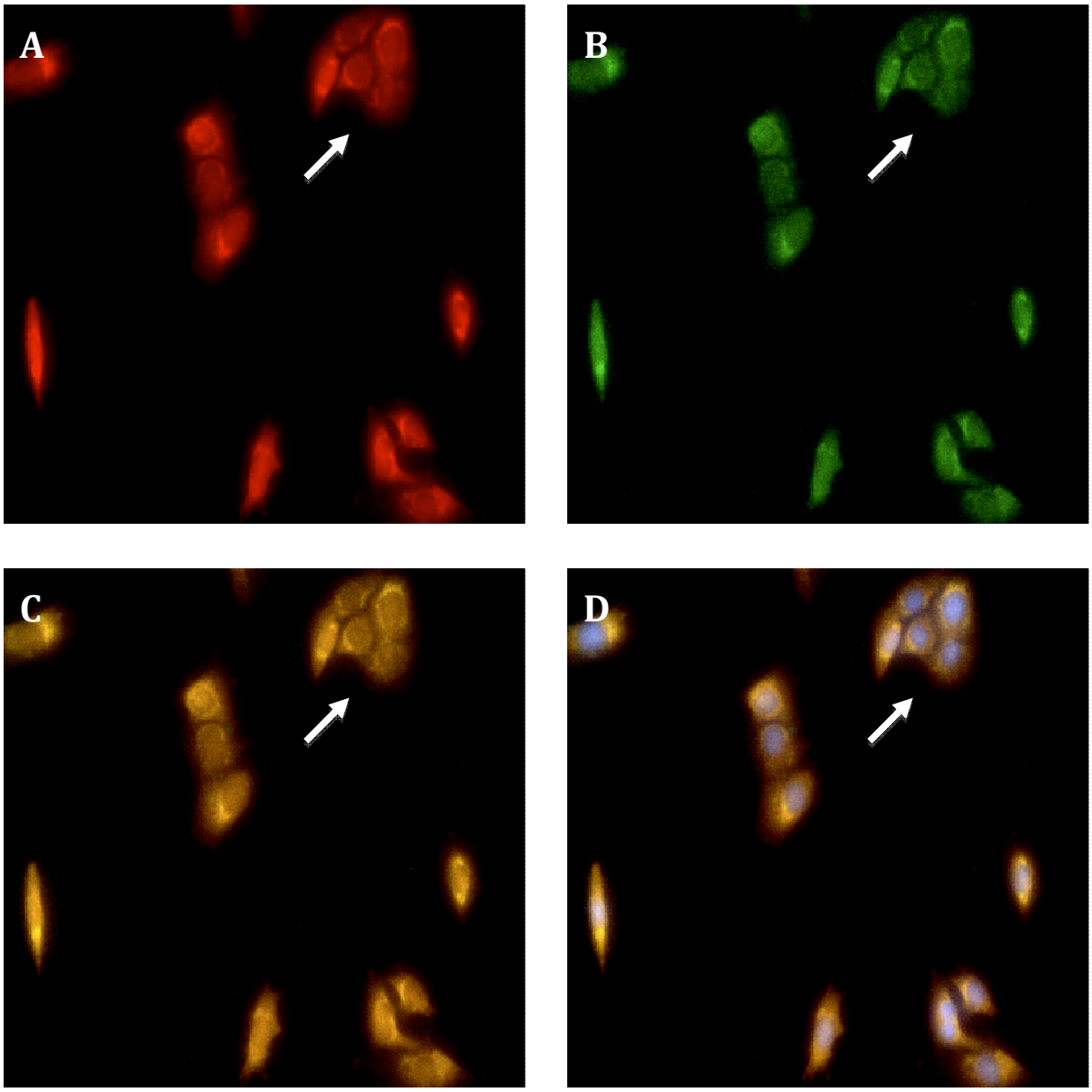

Figure 22: Immunocytochemical Analysis of Medium IL-6 treatment group visualizing the Mitochondria (A), pSTAT3 (B), Mitochondria & pSTAT3 (C) and Mitochondria, pSTAT3 and DAPI (D) at 5 minutes.

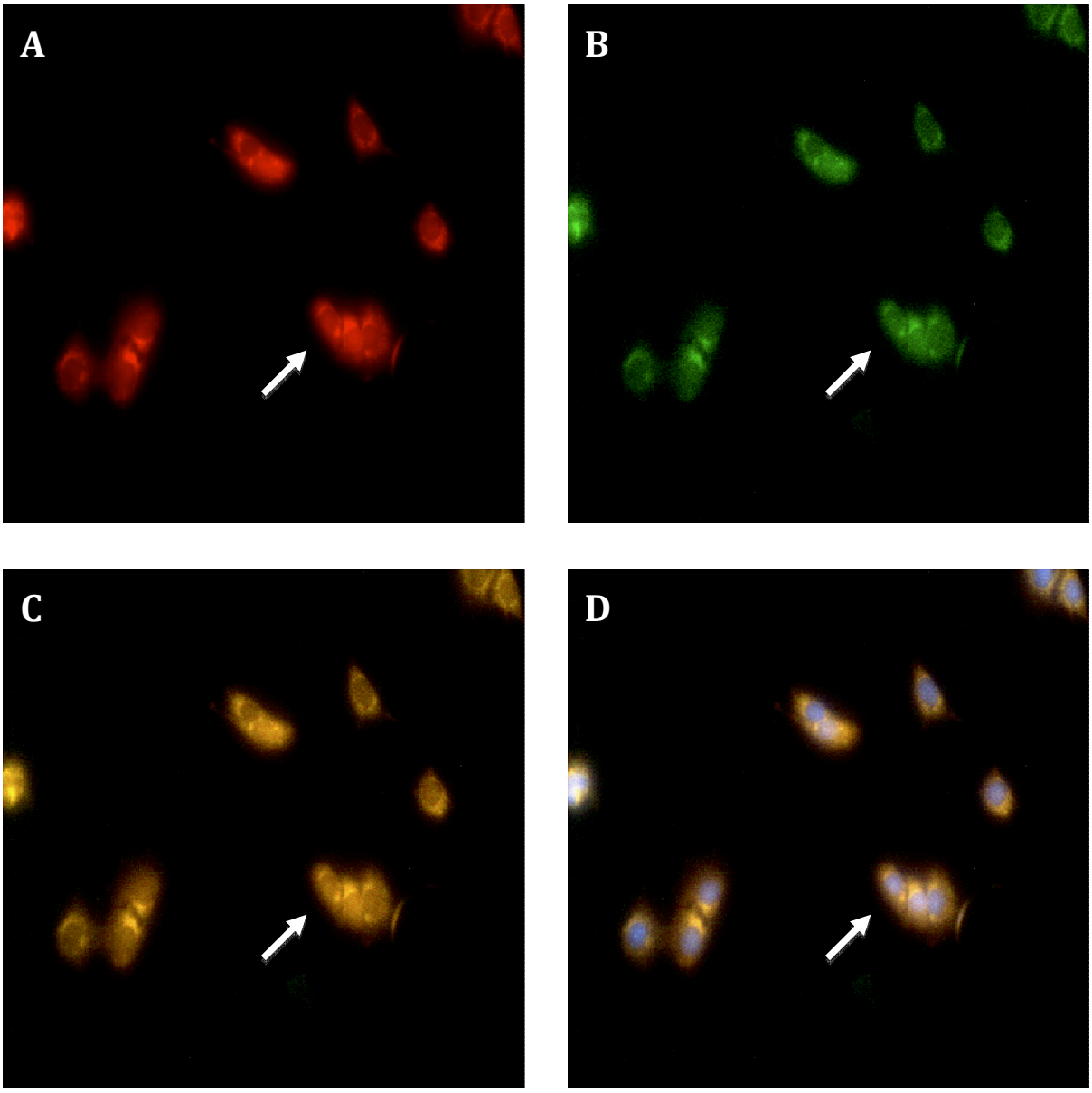

Figure 23: Immunocytochemical Analysis of Low IL-6 treatment group visualizing the Mitochondria (A), pSTAT3 (B), Mitochondria & pSTAT3 (C) and Mitochondria, pSTAT3 and DAPI (D) at 5 minutes.

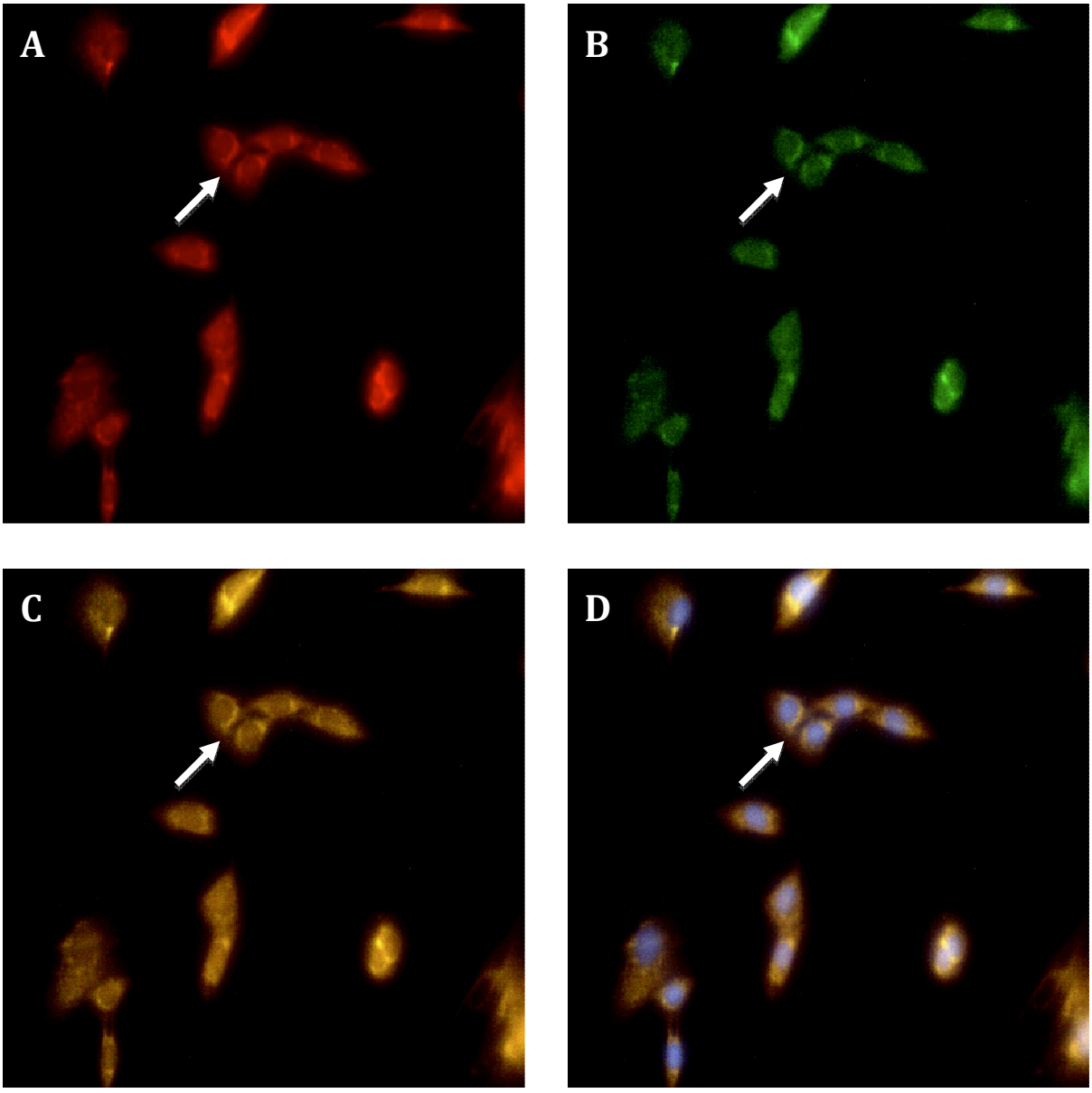

Figure 24: Immunocytochemical Analysis of Control group visualizing the Mitochondria (A), pSTAT3 (B), Mitochondria & pSTAT3 (C) and Mitochondria, pSTAT3 and DAPI (D) at 10 minutes.

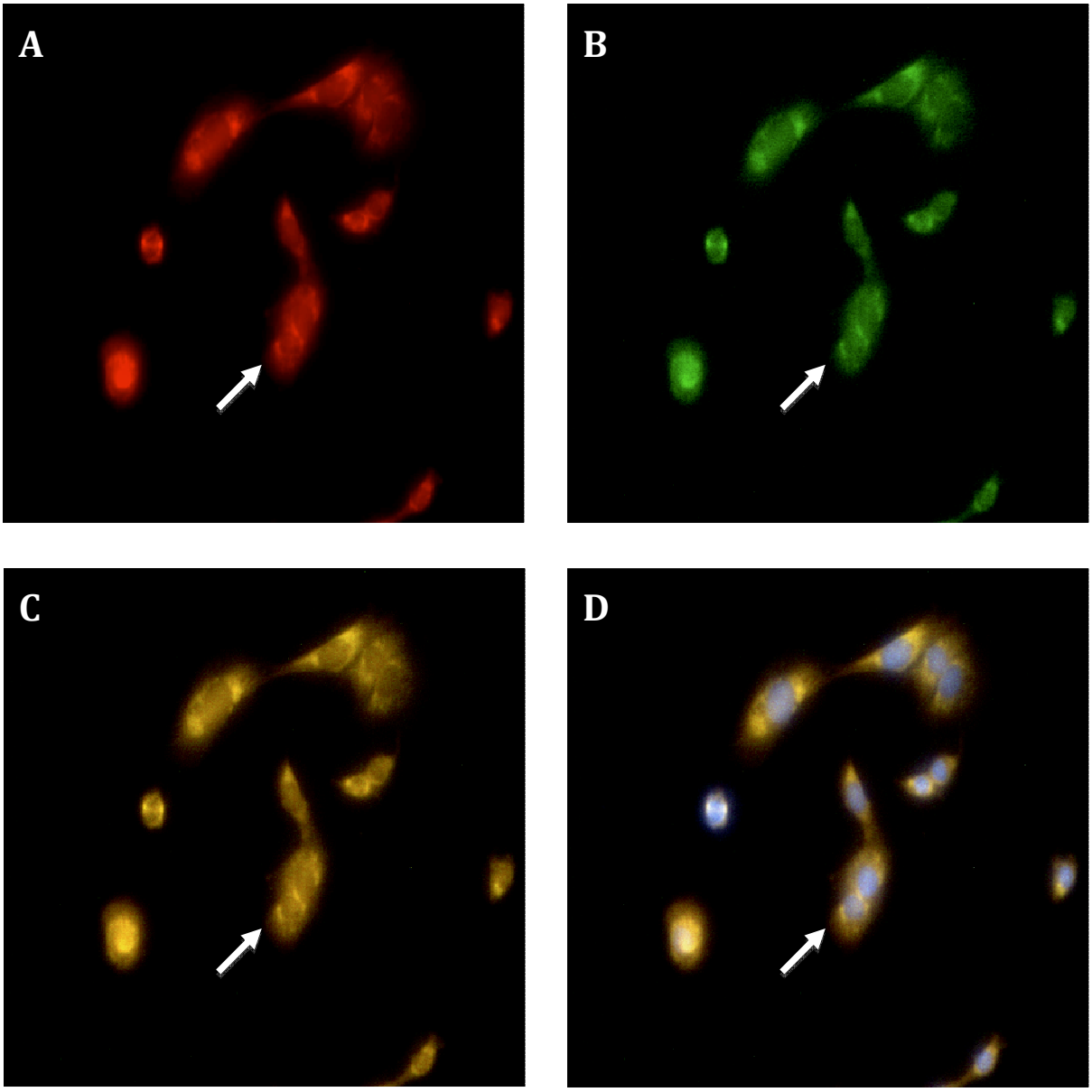

Figure 25: Immunocytochemical Analysis of High IL-6 treatment group visualizing the Mitochondria (A), pSTAT3 (B), Mitochondria & pSTAT3 (C) and Mitochondria, pSTAT3 and DAPI (D) at 10 minutes.

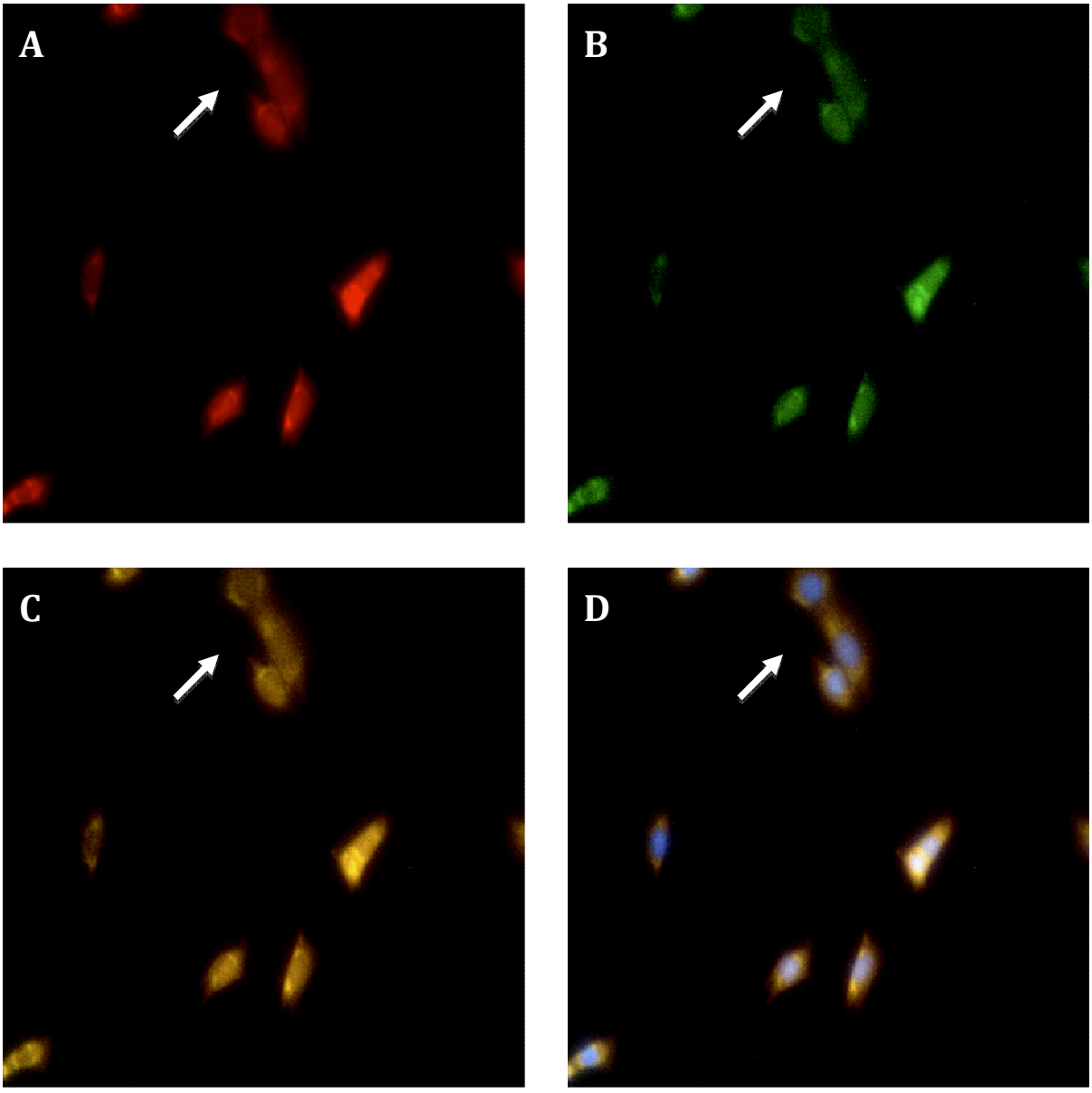

Figure 26: Immunocytochemical Analysis of Medium IL-6 treatment group visualizing the Mitochondria (A), pSTAT3 (B), Mitochondria & pSTAT3 (C) and Mitochondria, pSTAT3 and DAPI (D) at 10 minutes.

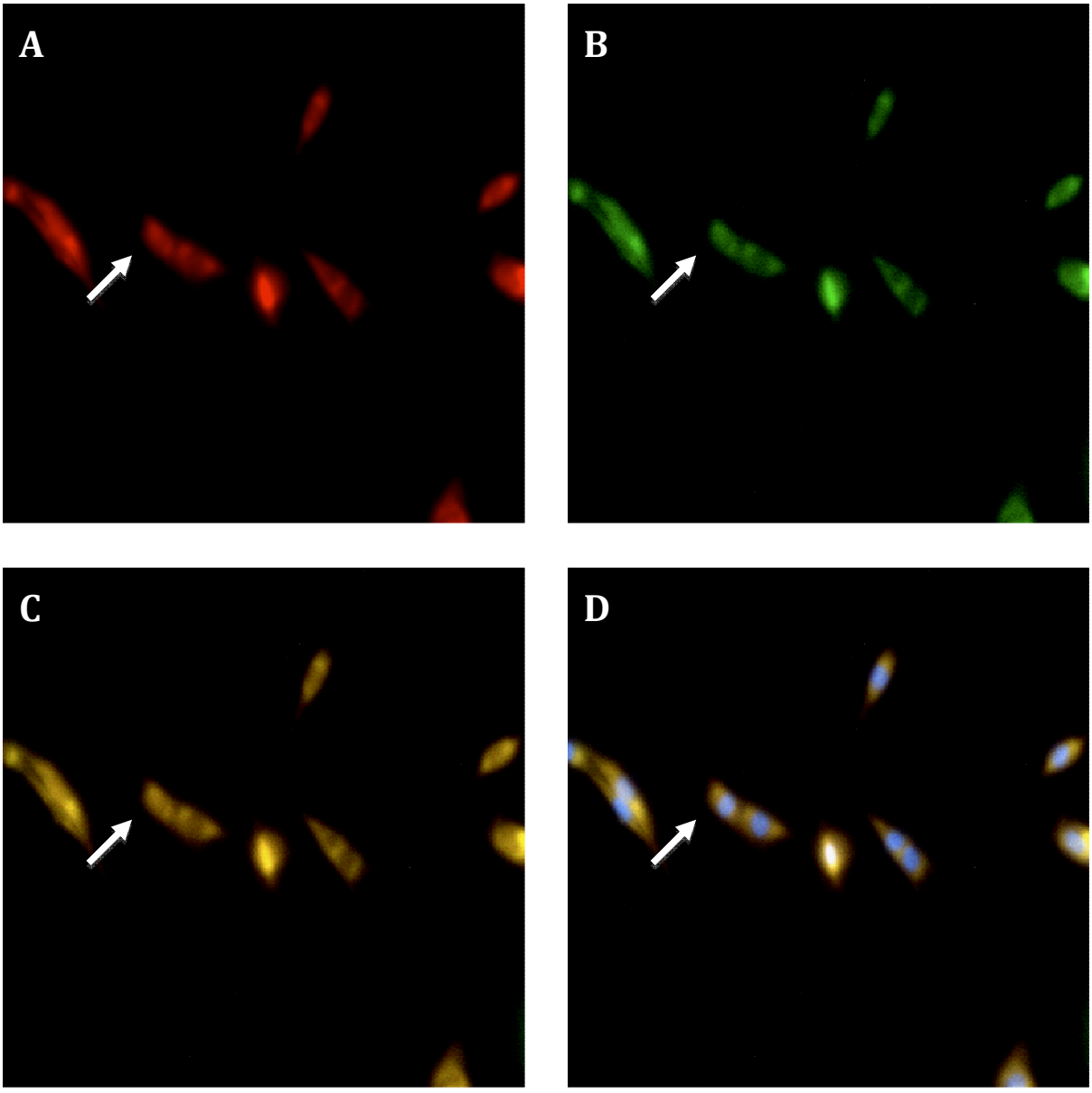

Figure 27: Immunocytochemical Analysis of Low IL-6 treatment group visualizing the Mitochondria (A), pSTAT3 (B), Mitochondria & pSTAT3 (C) and Mitochondria, pSTAT3 and DAPI (D) at 10 minutes.

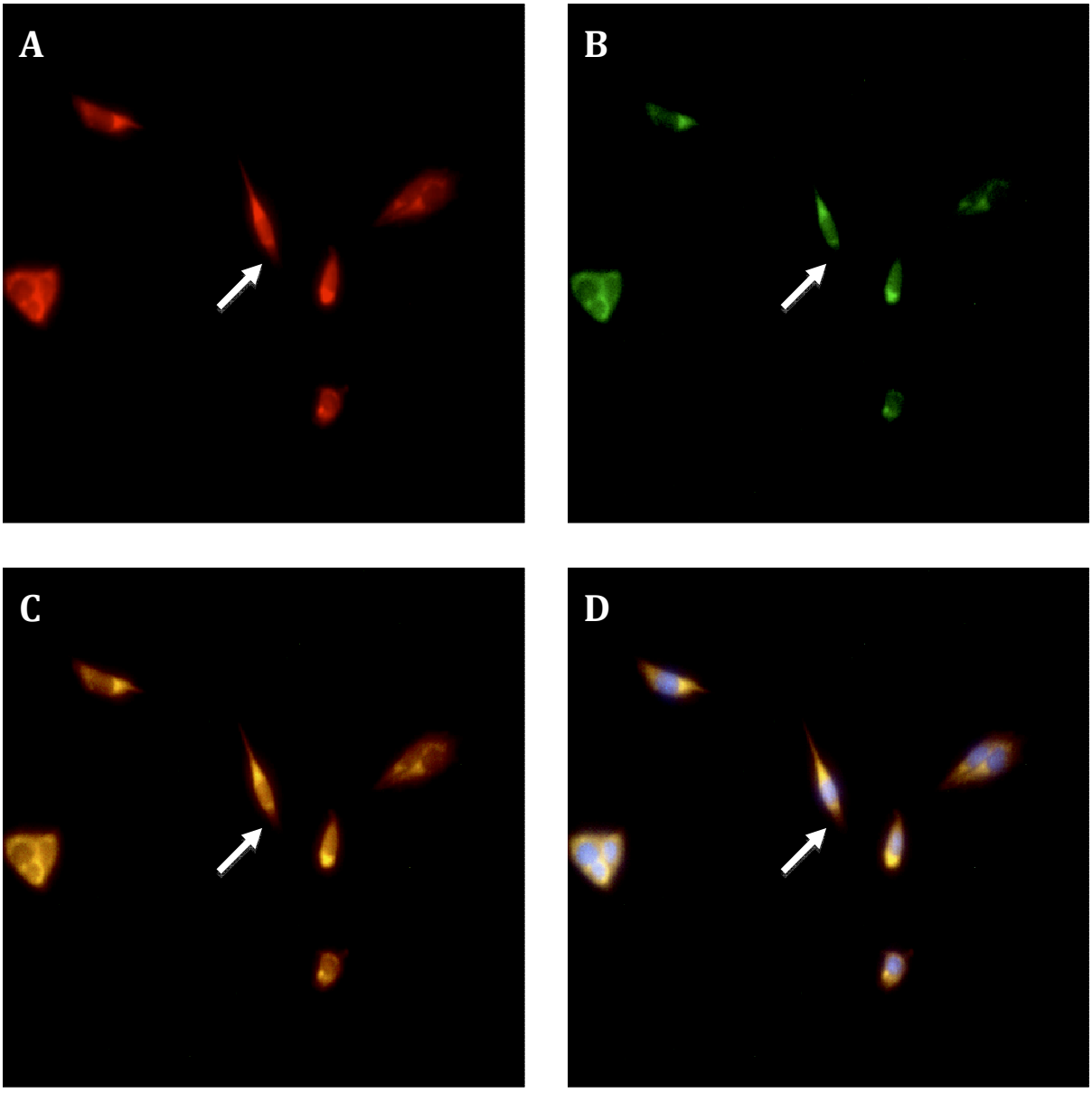

Figure 28: Immunocytochemical Analysis of Control group visualizing the Mitochondria (A), pSTAT3 (B), Mitochondria & pSTAT3 (C) and Mitochondria, pSTAT3 and DAPI (D) at 15 minutes.

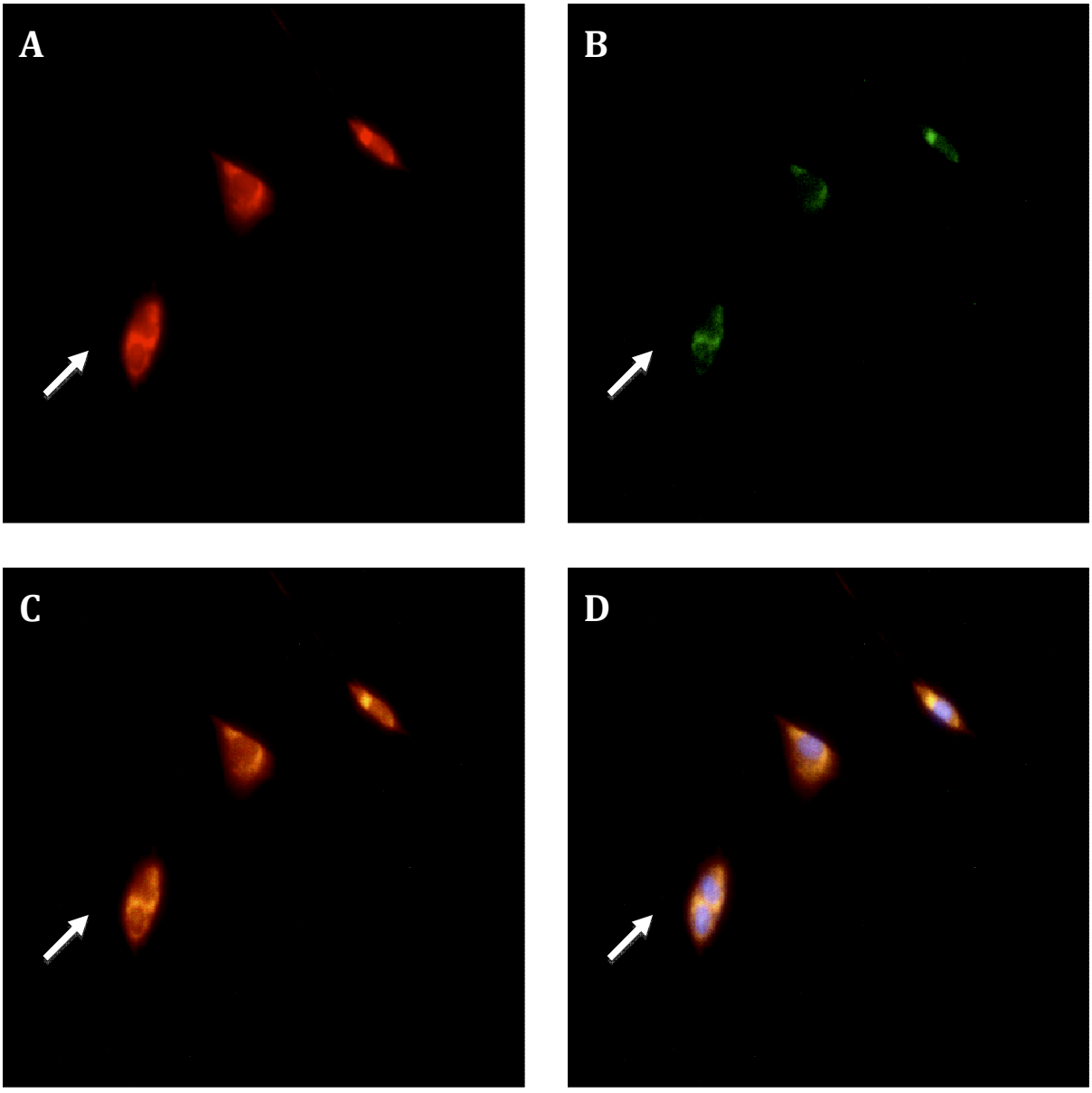

Figure 29: Immunocytochemical Analysis of High IL-6 treatment group visualizing the Mitochondria (A), pSTAT3 (B), Mitochondria & pSTAT3 (C) and Mitochondria, pSTAT3 and DAPI (D) at 15 minutes.

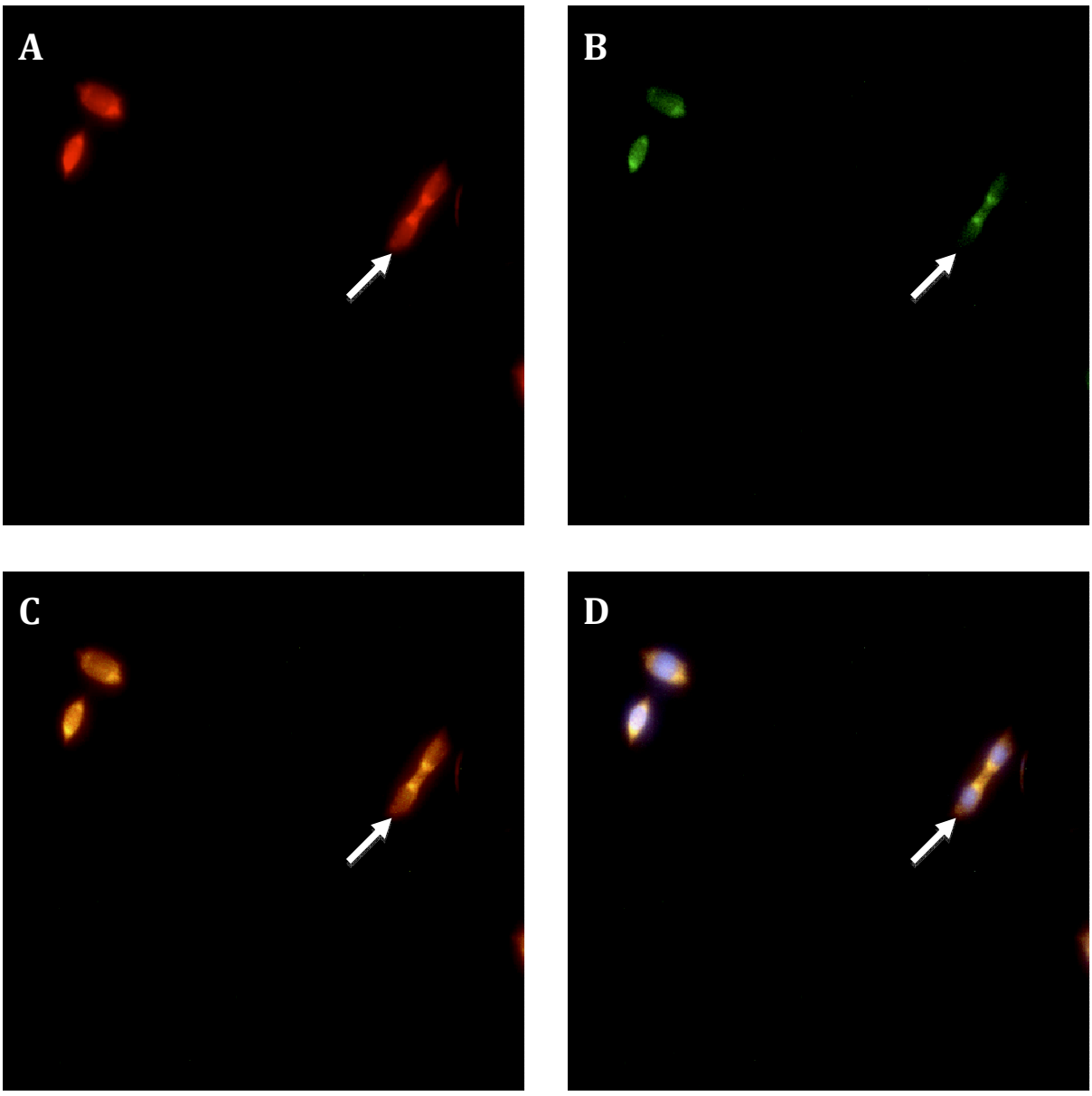

Figure 30: Immunocytochemical Analysis of Medium IL-6 treatment group visualizing the Mitochondria (A), pSTAT3 (B), Mitochondria & pSTAT3 (C) and Mitochondria, pSTAT3 and DAPI (D) at 15 minutes.

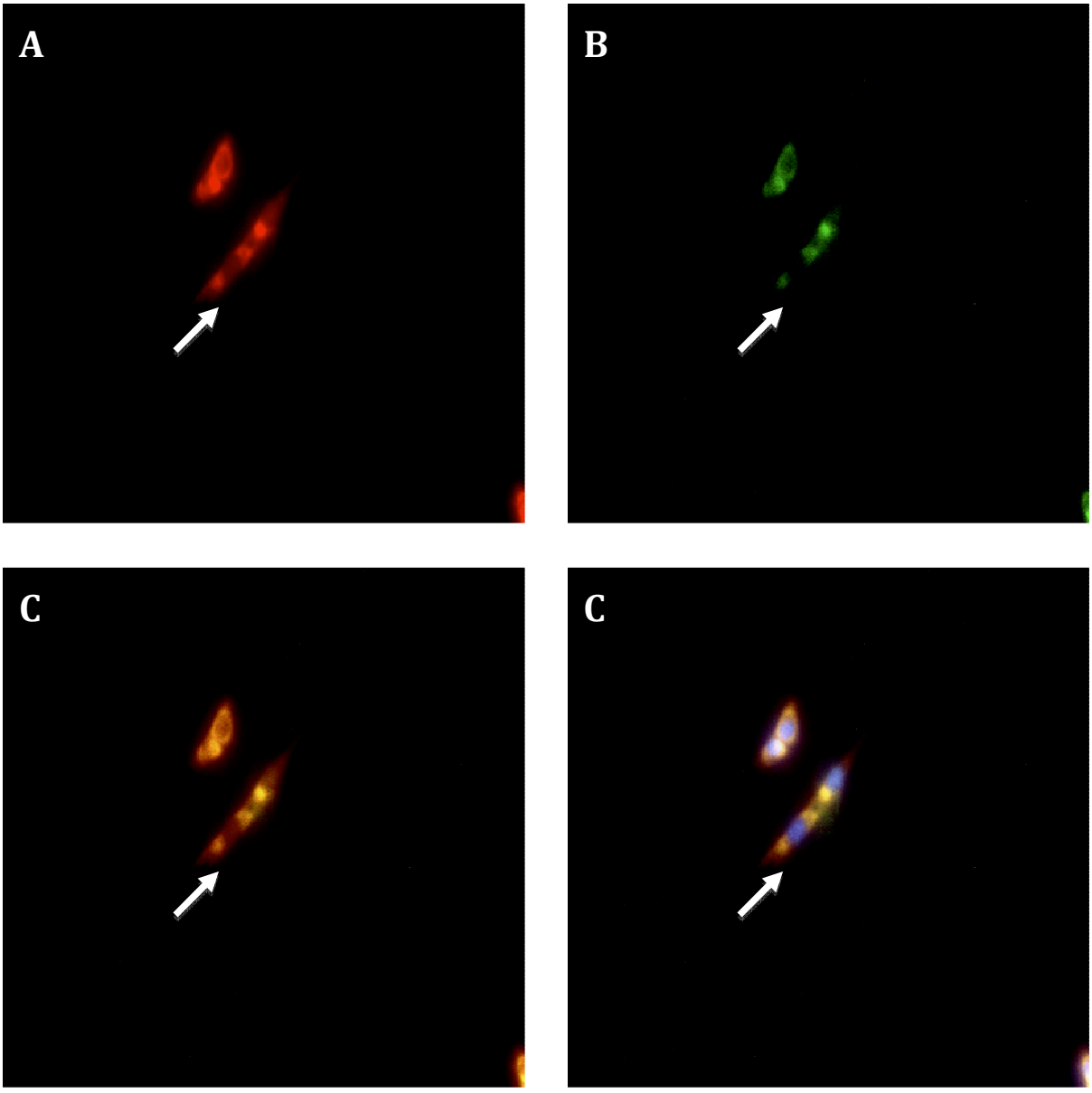

Figure 31: Immunocytochemical Analysis of Low IL-6 treatment group visualizing the Mitochondria (A), pSTAT3 (B), Mitochondria & pSTAT3 (C) and Mitochondria, pSTAT3 and DAPI (D) at 15 minutes.

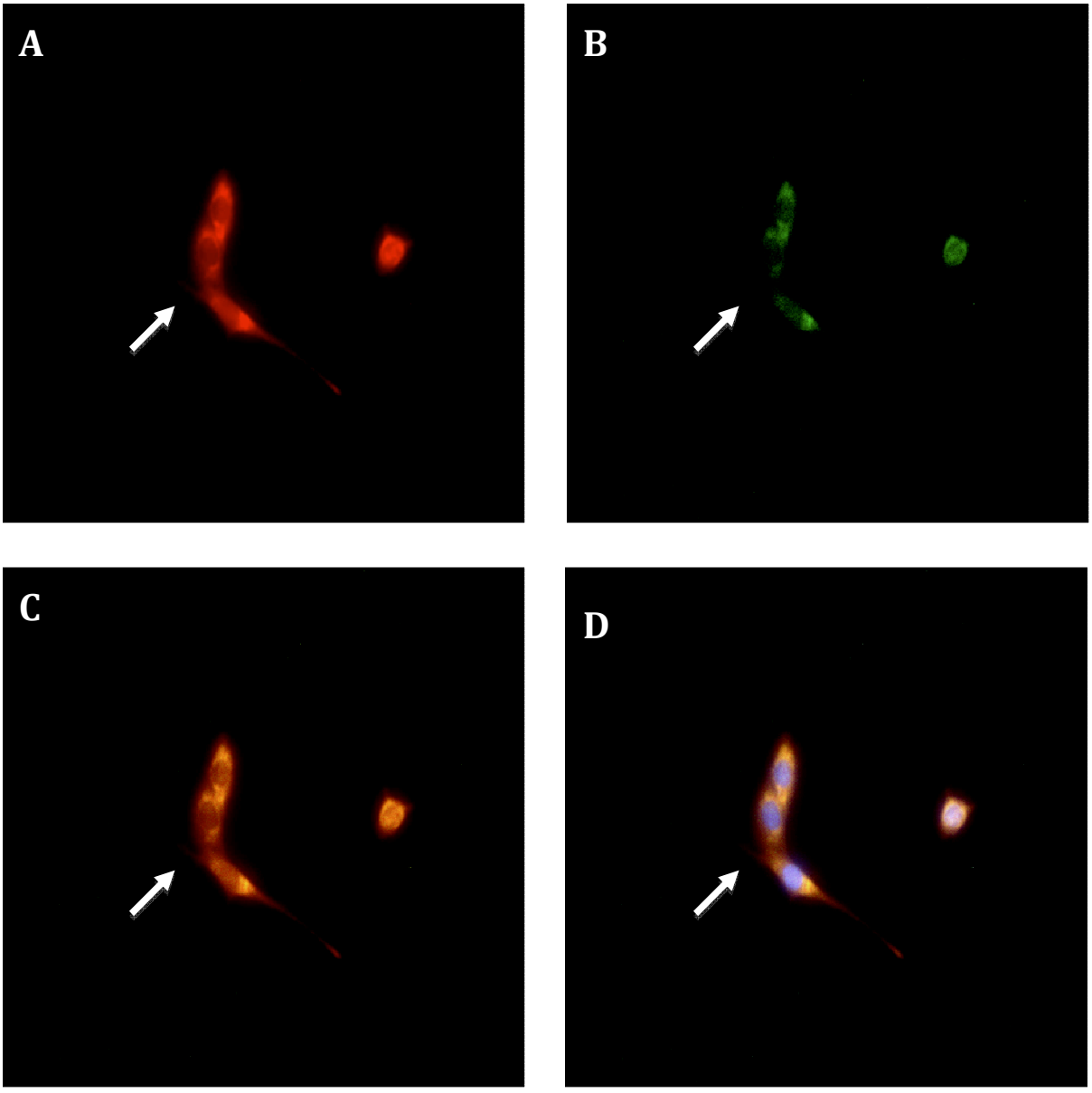

Figure 32: Immunocytochemical Analysis of Control group visualizing the Mitochondria (A), pSTAT3 (B), Mitochondria & pSTAT3 (C) and Mitochondria, pSTAT3 and DAPI (D) at 30 minutes.

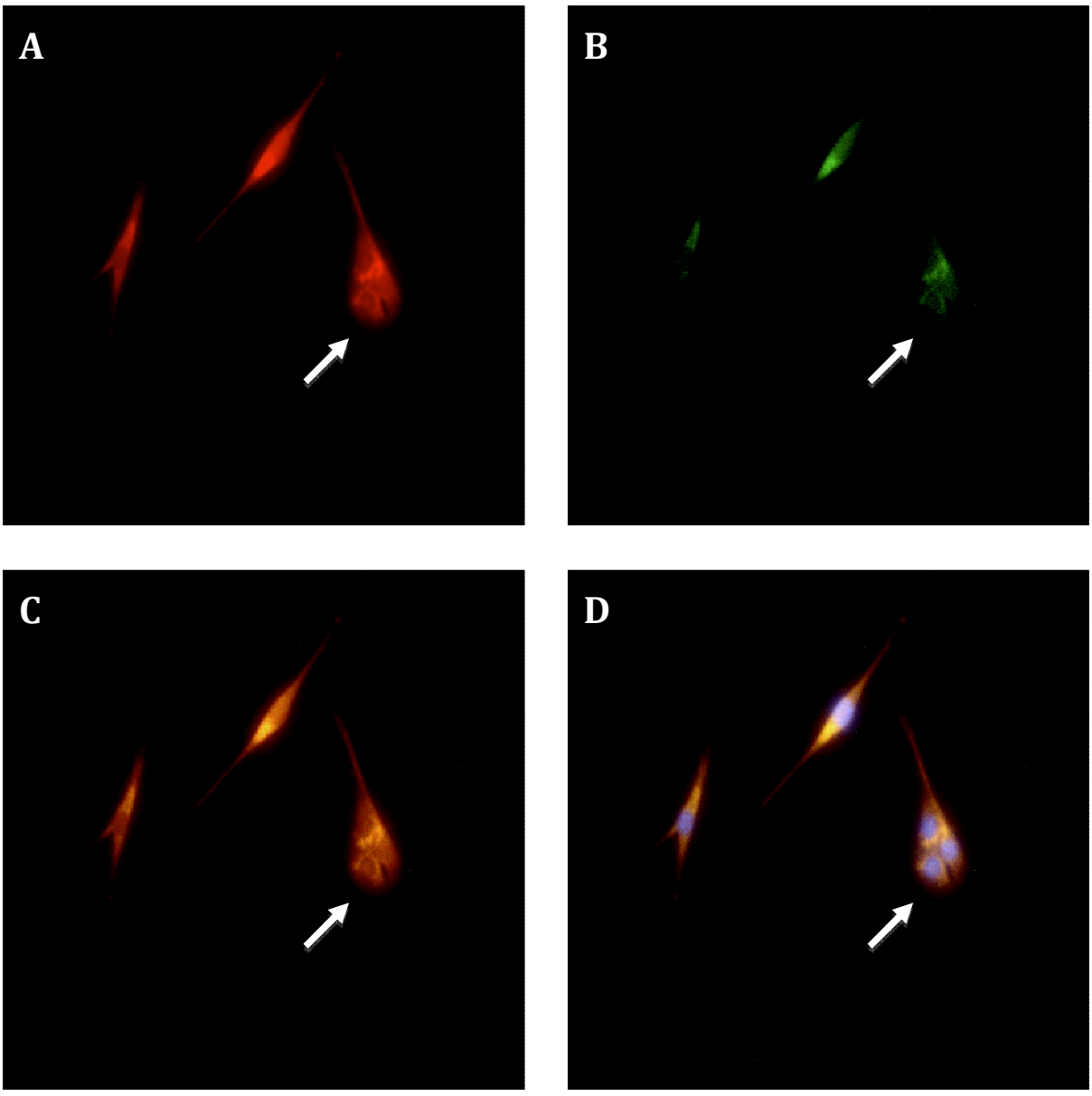

Figure 33: Immunocytochemical Analysis of High IL-6 treatment group visualizing the Mitochondria (A), pSTAT3 (B), Mitochondria & pSTAT3 (C) and Mitochondria, pSTAT3 and DAPI (D) at 30 minutes.

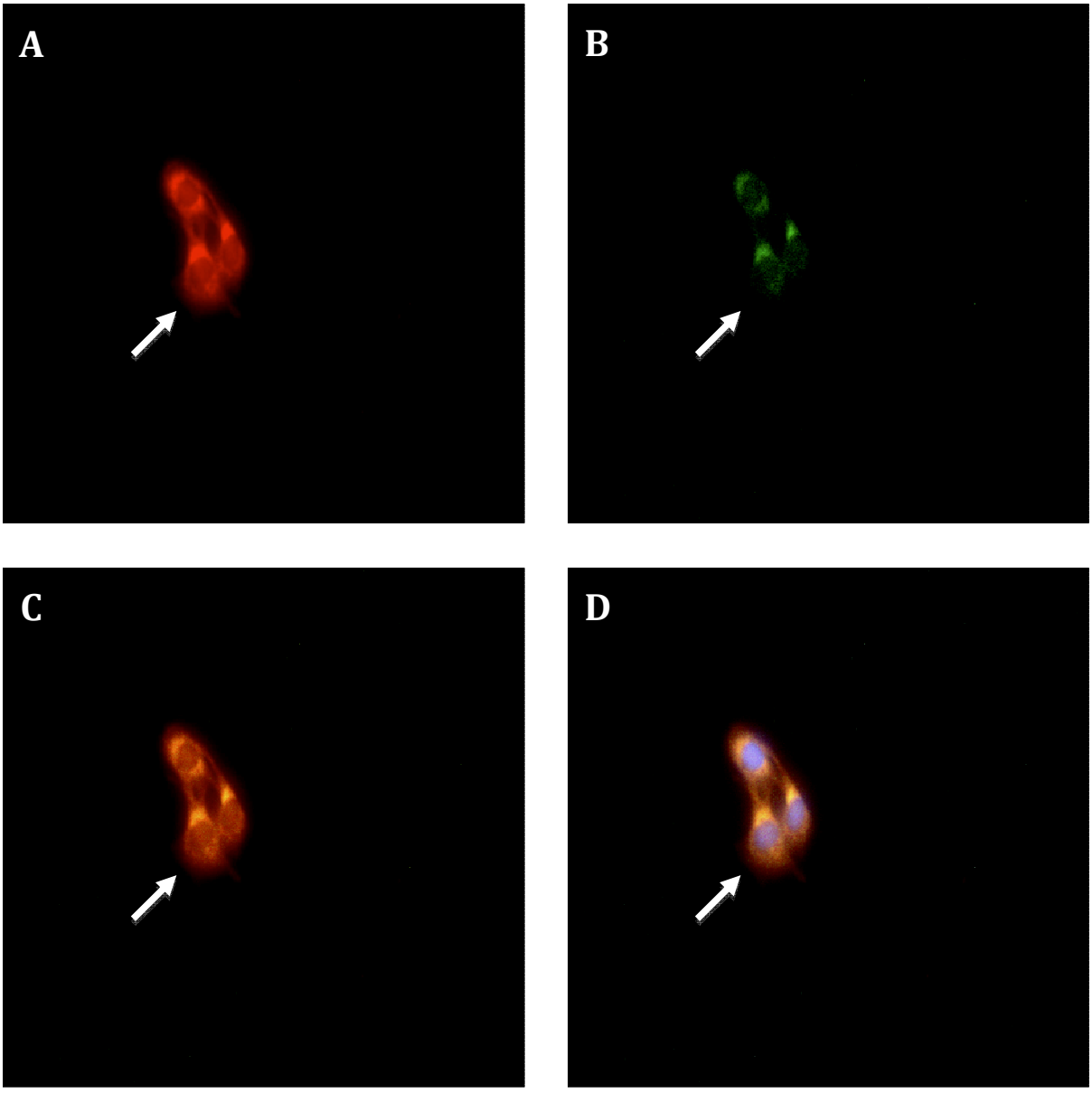

Figure 34: Immunocytochemical Analysis of Medium IL-6 treatment group visualizing the Mitochondria (A), pSTAT3 (B), Mitochondria & pSTAT3 (C) and Mitochondria, pSTAT3 and DAPI (D) at 30 minutes.

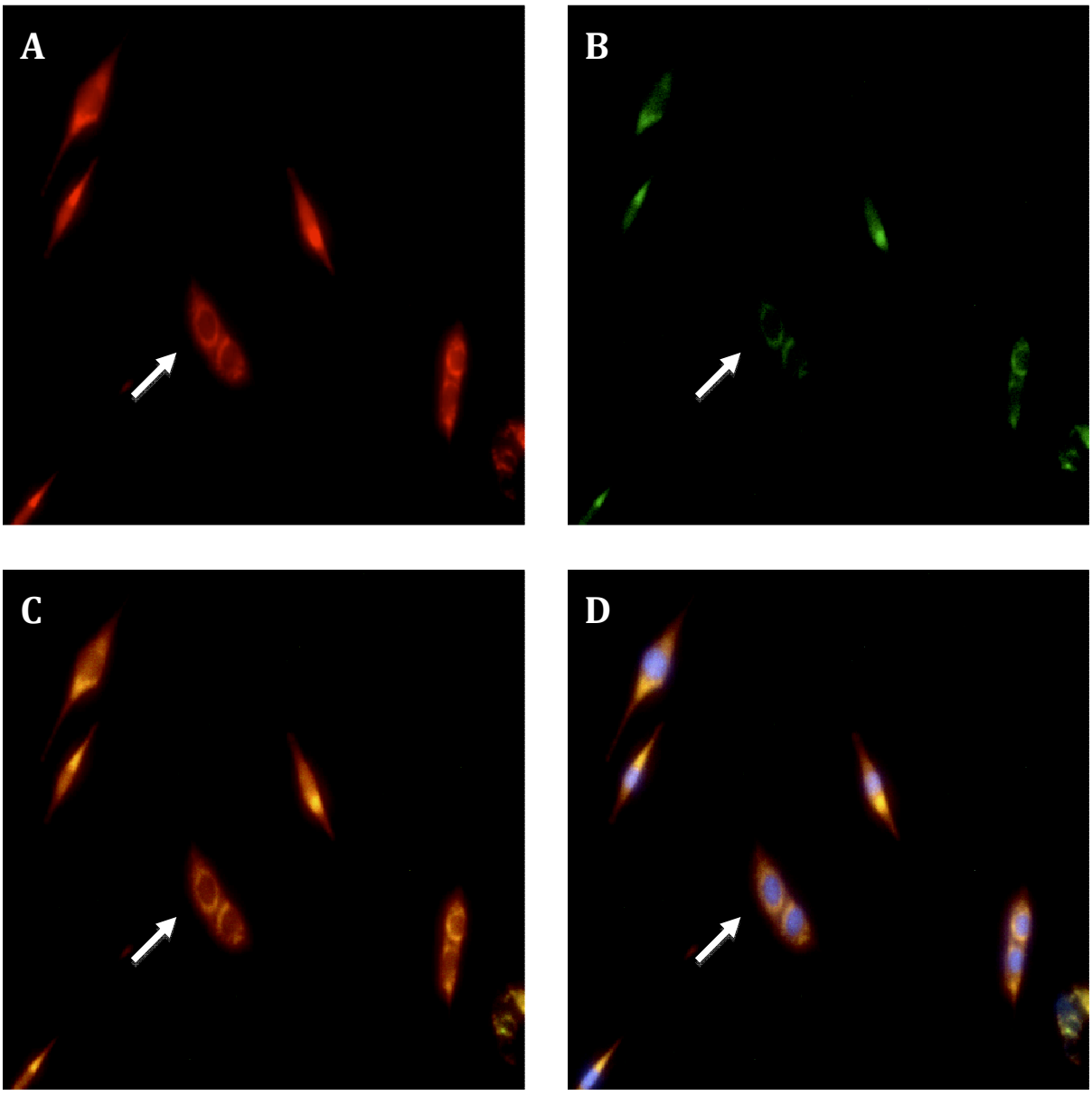

Figure 35: Immunocytochemical Analysis of Low IL-6 treatment group visualizing the Mitochondria (A), pSTAT3 (B), Mitochondria & pSTAT3 (C) and Mitochondria, pSTAT3 and DAPI (D) at 30 minutes.

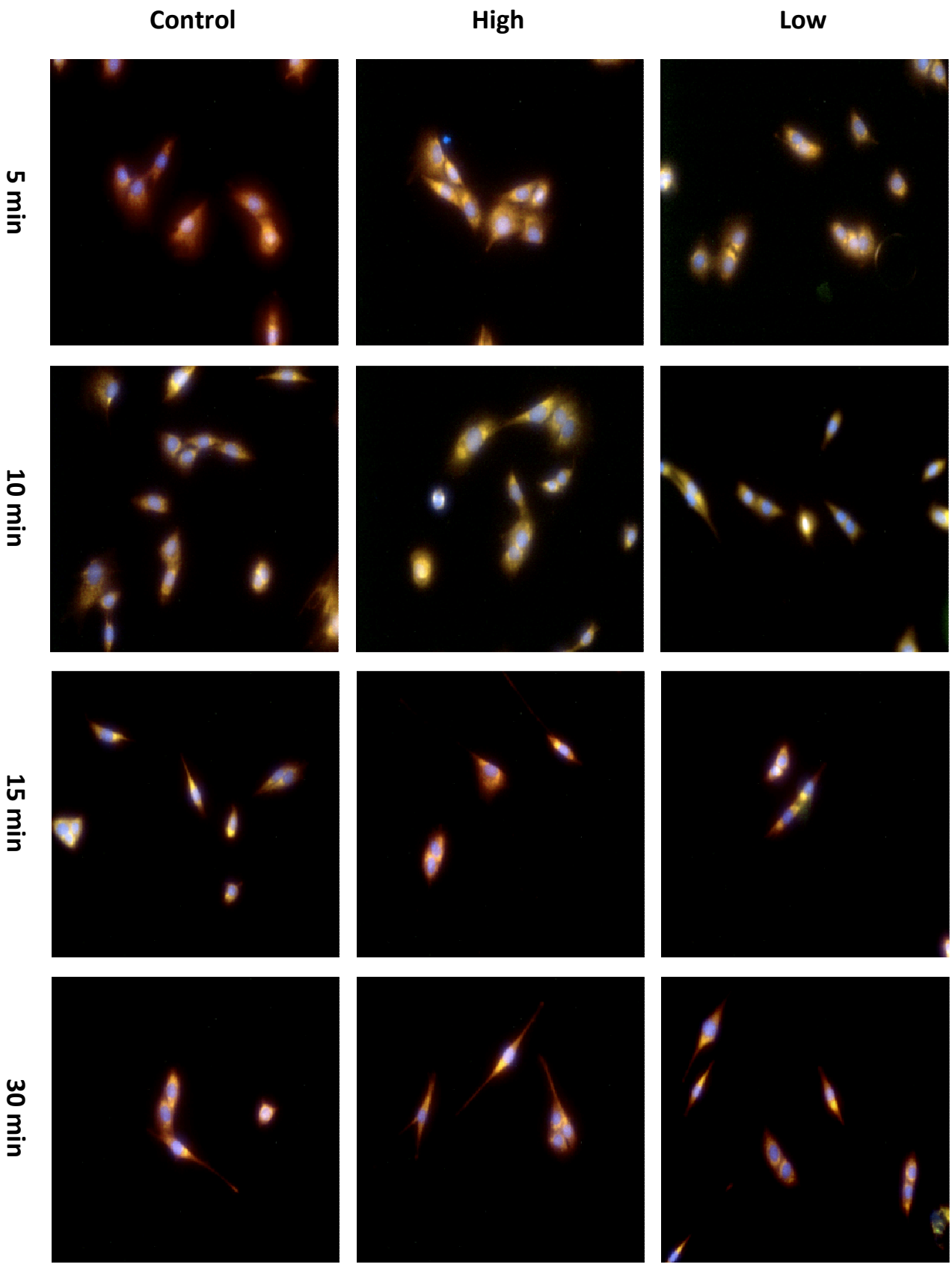

Figure 35E: Immunocytochemical Analysis of Control group as well as High and Low IL-6 treatment group visualizing the Mitochondria (red), pSTAT3 (green) and the nucleus DAPI (D) at 5, 10, 15 and 30 minutes.

3.5 Protein analysis of IL-6 signalling

In order to confirm the qualitative assessment of the images, protein levels of pSTAT3 as well as the total levels of STAT3 (tSTAT3) were determined. tSTAT3 was quantified to confidently state that it was the levels of pSTAT3 that changed and not only the total amount of STAT3 that fluctuated. In order to assess whether loading inequalities occurred the levels of β-actin were blotted and remained unchanged between all groups.

These results (Fig. 36) correlated with the results seen by means of Immunocytochemistry. The High and Low doses elevated levels of pSTAT3 5 minutes after IL-6 exposure but without statistical significance. The SEM of the two doses was too variable thus significance could not be found. Both decreased by 10 minutes although the High dose remained elevated above control, whereas the Low dose decreased to levels found in the Control group. The proceeding time points analysed showed that the levels of pSTAT3 in both the treatment groups significantly decreased ($p<0.05$) to levels below the Control, 15 minutes after IL-6 administration. Both treatment groups returned to Control levels 30 minutes after IL-6 administration. Total STAT3 (Fig. 37) levels remained unchanged throughout the treatment time period so it can be said with confidence that the fluctuations seen in STAT3 levels are those of pSTAT3.

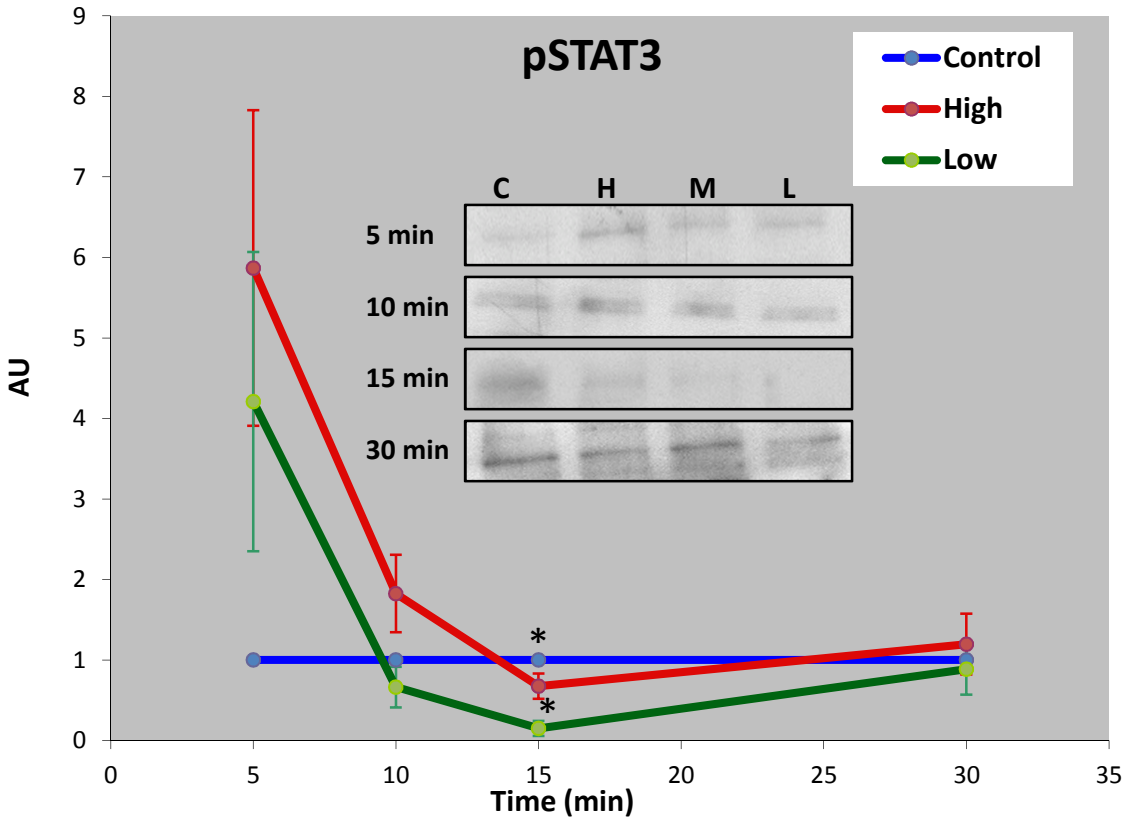

Figure 36: Representation of phosphorylated STAT3 expression after IL-6 treatment. (n=3, Mean±SEM)

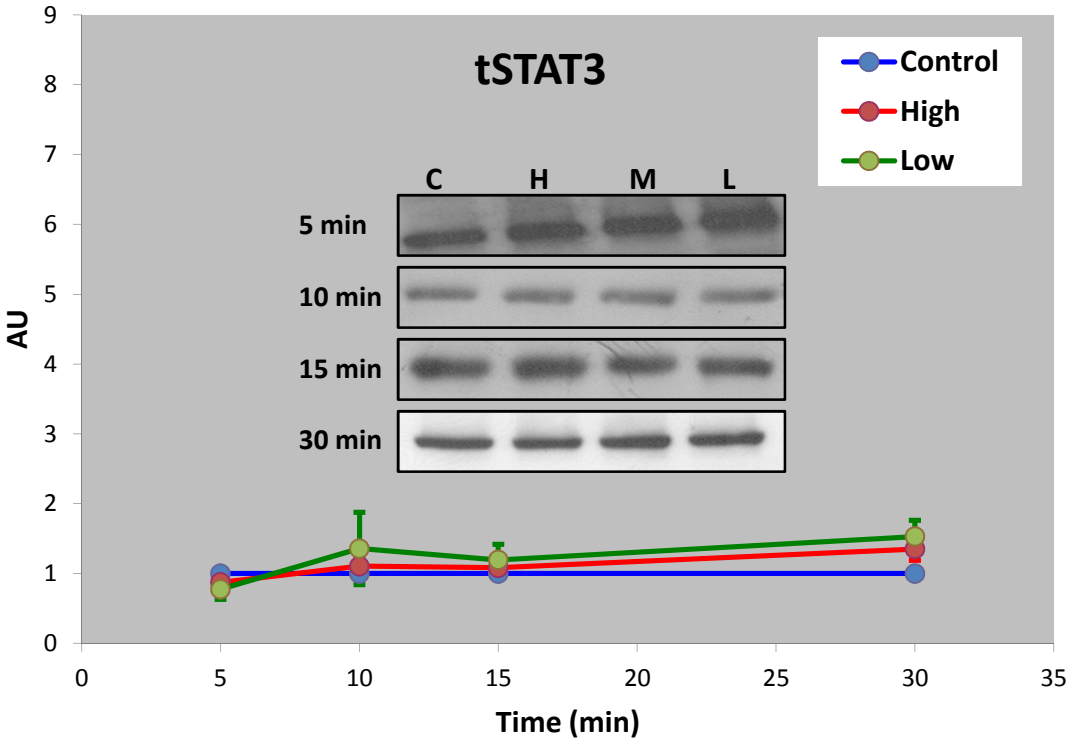

Figure 37: Representation of total STAT3 expression after IL-6 treatment. (n=3,Mean±SEM)

4. Discussion

IL-6 has been implicated in various processes occurring in skeletal muscle. It is an established fact that IL-6 levels dramatically increase in individuals exposed to strenuous exercise (Febbraio and Pedersen 2002). The origin of elevated IL-6 levels was thought to be as a result of the immune response seen following strenuous exercise (Nieman, Nehlsen-Cannarella et al. 1998) but it has been shown that it is the muscle cells that are producing the majority of this exercise-related IL-6 (Moldoveanu, Shephard et al. 2000). Injury of the skeletal muscle has also been known to increase interstitial levels of IL-6 as a result satellite cell IL-6 excretion as well as immune cell infiltration (Faunce, Gregory et al. 1998; Farnebo, Lars-Erik et al. 2009). The production of acute-phase response proteins is also under the control of IL-6 and these are thought to facilitate muscle repair (Karlsson, Yarmush et al. 1998).

It is possible that the IL-6 accumulation during exercise and injury could have a possible mitogenic property. An increase in IL-6 during exercise could lead to the activation and proliferation of satellite cells in order to increase muscle mass as well as the satellite cell pool. During injury the integrity of the muscle fibres are compromised and need to be repaired. Resident increased levels of IL-6 could be responsible for the differentiation of satellite cells in order to create new myofibres to repair the affected area.

Previous studies assessed the effect of IL-6 on the skeletal muscle cell cycle. The results obtained from these studies are quite contradictory and IL-6 was implicated in both the proliferation and differentiation of skeletal myoblasts. Thus the exact effect of IL-6 on the skeletal muscle cell cycle is still unknown. The discrepancies can wholly be attributed to a lack of assessment of IL-6 effects at varying, physiologically relevant doses as well as the real time analysis of IL-6 signaling through its receptor.

The aim of this thesis was therefore to provide a comprehensive assessment of the effects of IL-6 at varying, physiologically relevant doses on proliferating myoblasts. The doses utilized in this study (10 ng/ml, 100 pg/ml and 10 pg/ml) are all encountered under different physiological conditions. IL-6 concentration in skeletal muscle at rest has been found to range between 1 and 8 pg/ml (Gray, Clifford et al. 2009; Robson-Ansley, Cockburn et al. 2010), which corresponds to the Low dose of 10 pg/ml, utilized in this study. The levels of IL-6 after strenuous exercise have been known to reach 120 pg/ml (Gray, Clifford et al. 2009; Robson-

Ansley, Cockburn et al. 2010) thus the Medium dose of 100 pg/ml in this study remains relevant. When sepsis occurs in skeletal muscle the levels of IL-6 skyrocket into ranges of 2 to 200 ng/ml (Damas, Ledoux et al. 1992) and the High dose of 10 ng/ml takes this diseased state into account. All these IL-6 concentrations observed were measured in the plasma, however this may underestimate the actual interstitial levels in the muscle (Levitt 2003).

Model of satellite cell proliferation

One of the main aims of the study was to effectively establish a proliferating satellite cell model. It may seem that this would be a simple matter of following normal culture methods for myoblasts, but when cultured satellite cells are allowed to become over confluent or when the cells are in close relation to each other, cellular fusion and the expression of pro-differentiation proteins occurs. Satellite cell confluency was closely monitored in order to maintain sufficient spacing between growing myoblasts. In order to achieve this aim, satellite cells were cultured in a 10% (v/v) Fetal Calf Serum medium, which simulates a niche conducive to proliferation and the cells were split into a low seeding density of 1600 cells/cm^2.

This aim was achieved and is evident when observing the Control group in the cellular model. Superficial observation of cells in the Control group (Fig. 12, 16) showed sufficient spacing and the cells maintained a cellular structure typical of a proliferating cell. Analysis of cell cycle phases also proves the success in the maintenance of a proliferating cell model. The majority of cells in the Control group are within the S-phase of the cell cycle 24 hours after seeding (Fig. 9A), pointing towards proliferation. The maintenance of proliferation is also evident when investigating the expression of the terminal differentiation marker, myogenin. This marker was completely absent and was undetectable 24 hours after seeding. The pro-proliferation marker, PCNA, showed an elevated trend (Fig. 10). As time progresses the cells actively divide, increasing their number and decreasing the space between neighboring cells as a result of growth factors in the media (McFarland, Pesall et al. 1993; Velleman, Zhang et al. 2010). An expected, minor increase in differentiation is inevitable and can be observed by an increase in cells in the G0/G1 phase and a decrease in the number of cells in the S-phase of the cell cycle 48 hours after seeding (Fig. 9B). The progression of cells to the G0/G1 phase of the cell cycle and the subsequent arrest of cells in the G0/G1 phase has been utilized as a marker of differentiation (Wirt, Adler et al. 2010) as well as the assessment of markers associated with differentiation (Ferri, Barbieri et al. 2009) and these were the methods used in this study. Satellite cells grown in proliferation medium are continuously activated and do

not enter quiescence as a result of growth factors in the proliferation medium promoting proliferation thus no cells will be found in the G0 phase of the cell cycle and the cells are classified in the G0/G1 phase because of their continuous activation. The expression of myogenin is also relatively low in the Control group 48 hours after seeding, suggesting the maintenance of a proliferating cellular model.

This evidence suggests that a proliferating cellular model was successfully obtained and this subsequently allowed us to investigate the effect of IL-6 doses on this model.

Effect of IL-6 doses on satellite cell cycle progression

In order to properly classify IL-6 as a mitogen of the satellite cell cycle, the progression of IL-6 treated cells through the cell cycle was assessed. The majority of cells were found to be located in the S-phase of the cell cycle in all groups 24 hours after IL-6 administration (Fig. 9A). This shows that proliferation is actively occurring in all the treatment groups. The Medium and Low doses showed a significant decrease in the G0/G1 phase of the cell cycle when compared to the Control Group. These data suggest that these doses are responsible for the progression of cells from the differentiation phase (G0/G1) to other phases leading to an anti-differentiation effect. The fact that the Low dose also showed a significant increase in the percentage of cells in the S-phase of the cell cycle makes it possible to conclude definitively that the Low dose is initiating proliferation as well as retarding differentiation after 24 hours of IL-6 dosage. The concentration of IL-6 in the Medium and Low doses mimic that of muscle cells at rest. It is possible that this dose could be responsible for cellular remodeling as well as the replenishment of the cellular pool.

The profiles of the cell cycle in all the groups seem to reverse 48 hours after treatment. The majority of cells are now in the G0/G1 phase and not in the S-phase of the cell cycle. This is not due to the administration of IL-6 as the Control group displays the same reversal. This occurrence is expected as a result of time progression and the proximity of cells to each other as growth occurs. It is well known that when myoblasts are cultured for long periods of time, fusion occurs and differentiation is clearly underway with the appearance of myotubes (Trotter and Nameroff 1976). However, in all the treatment groups there is a significant decrease in the proportion of cells in the G0/G1 phase when compared to the Control group. This suggests that all the doses of IL-6 have an anti-differentiation effect and this is cemented by the significantly higher proportion of cells in proliferation (S) phase of the cell cycle 48 hours after IL-6 treatment with all the doses.

The results found here are in agreement with previous studies where IL-6 dosage (10 ng/ml) significantly increased myoblast numbers (Wang, Wu et al. 2008) as well as shifting a greater portion of cells into the S-phase of the cell cycle when IL-6 was administered in conjunction with TNF-α (Al-Shanti, Saini et al. 2008). These studies only assessed the effect of IL-6 at a single dose and the doses used did not cover the broad range of IL-6 concentrations found in vivo.

In order for IL-6 to act as a mitogen of the cell cycle it needs to regulate the expression of proteins associated with cell cycle progression.

Effect of IL-6 doses on myogenic regulatory factor expression

Myogenic regulatory factors (MRF) play a pivotal role in the determination of satellite cell fate in relation to the cell cycle fate. MyoD is an MRF that is associated with the late proliferation/early differentiation phase of the cell cycle and it is also responsible for the expression of the terminal differentiation marker myogenin (Charge and Rudnicki 2004). On the other end of the scale is the proliferation marker, proliferating cell nuclear antigen (PCNA) (Schafer 1998), a marker of satellite cell proliferation. The effective quantification of these markers gives crucial insight into the stage that the activated satellite cells are in and thus these markers were studied in the IL-6 treated cells.

After 24 hours of IL-6 treatment the expression of MyoD remained unaffected in all the groups (Fig. 10) compared to the control group at this time point. The expression of myogenin was absent at the 24 hour time point and this was expected as a result of the proliferating cell model and terminal differentiation would be unlikely at this time point. The expression of PCNA was significantly increased in the C2C12 cells exposed to the Medium as well as the Low doses (Fig. 10). This suggests that at least at some concentrations, IL-6 may directly stimulate increased expression of the proliferation marker PCNA. This occurrence has been seen in a similar model where a crush injury in rats lead to an increase in the LIF-associated protein, PCNA. IL-6 and LIF belong to the same super-family of cytokines and they both relay their signal in a similar manner and it is well known that muscle injury stimulates the release of IL-6 (Faunce, Gregory et al. 1998).

After 48 hours of IL-6 treatment (Fig. 11) a difference was seen in MRF expression between the treatment groups. The High dose showed no change in the expression of PCNA when

compared to the Control group at this time point. The High dose had a tendency toward higher expression of MyoD whilst significantly increasing the expression of myogenin. These changes suggest that a High dose of IL-6 will facilitate the differentiation of skeletal muscle satellite cells. The confluency of cultured cells was strictly monitored and maintained by low seeding density. This is evident from images obtained at the 24 (Fig. 12-15) and 48 hour (Fig. 16-19) time points. An elevated level of MyoD and myogenin was seen in the Medium and Low dose group as well. This increase in differentiation can be attributed to the High dose of IL-6 and not the over confluency of cells.

The Low dose seemed to have the opposite effect of that seen in the High dose. The Low dose showed a marked increase in the expression of PCNA when compared to the Control group. It also appeared as if the Low dose showed a decrease in the expression of MyoD as well as myogenin, however none of these reached statistical significance, most likely due to the number of wells analysed. It thus appears that the Low dose favors the expression of the proliferation marker PCNA as well as negatively effecting the expression of the pro-differentiation markers. This evidence is consistent with the description of IL-6 behaving as a mitogen, but the current study proves that such statements should be qualified by making reference to dose.

Immunocytochemistry was also utilized to visually assess the expression of MRFs as well as their relative position within the cell. PCNA was exclusively found to be within the nucleus of the cells and this was to be expected as PCNA is a nuclear antigen and the nucleus is its main site of action. Myogenin was found to be in the nucleus of the cell. Myogenin is responsible for the expression of M-cadherin, which is responsible for terminal myogenic differentiation as well as myoblast fusion (Hsiao and Chen 2010).

The High dose of IL-6 showed a decrease in the expression of PCNA 24 hours after treatment (Fig. 13A) but also interestingly showed a decrease in the expression of myogenin (Fig. 13B), which was unexpected. The Medium (Fig. 14A) as well as the Low (Fig. 15A) doses showed a marked increase in the expression of PCNA after 24 hours. The levels of myogenin in the Medium (Fig. 14B) and Low (Fig. 15B) doses were comparable to that of the Control group, thus there were no visual differences at 24 hours.

Qualitatively a decrease in the expression of PCNA could also be seen in the High dose group 48 hours after treatment (Fig. 17A) when compared to the Control (Fig. 16A) group and this was accompanied by an increase in the expression of myogenin (Fig. 17B). An increased PCNA

expression was evident in the Medium (Fig. 18A) and Low (Fig. 19A) doses when compared to the Control group (Fig. 16A). The Medium (Fig. 18B) and Low (Fig. 19B) groups also showed an evident decrease in the expression of myogenin when compared to the Control (Fig. 16B) group.

PCNA and myogenin seem to be on different sides of the spectrum of IL-6 dose-response. From observations it appears that the High dose facilitates differentiation and retards proliferation by means of a decrease in PCNA expression and an increase in myogenin expression, except at the 24 hour time point where the High dose decreases myogenin expression. This could be as a result of differentiation taking an extended time period to initiate and thus the effects can only be seen at the 48 hour time point. The medium and Low doses seem to facilitate proliferation and retard differentiation and this could be accomplished by an increase in PCNA expression and a decrease in the expression of myogenin. It is possible that PCNA acts alongside Pax3 and Pax7 in order to facilitate proliferation as a result of IL-6 dosage (Collins, Gnocchi et al. 2009).

The question then arises as to how the IL-6 signal is relayed from its receptor to the nucleus where the expression of these MRFs is regulated?

IL-6 signaling through its receptor

IL-6 successfully relays its signaling through a number of STAT-mediated mechanisms. The cytokine binds to its receptor consisting of two gp130 subunits (Heinrich, Behrmann et al. 1998). The JAK kinases associate with the gp130 receptors and these are responsible for the activation of the Signal Transducer and Activator of Transcription (STAT) 3. As described in the Introduction, activation of resident STAT3 is accomplished by its phosphorylation and this is mediated by the JAK kinases. The phosphorylated STAT3 (pSTAT3) dimerizes and translocates to the nucleus and is responsible for the activation or suppression of gene transcription (Wen, Zhong et al. 1995). All these signaling mechanisms act in unison to sufficiently relay IL-6 signaling from the cell membrane to the nucleus. This process occurs very rapidly (Trenerry, Carey et al. 2007), thus pSTAT3 signaling was assessed at 5, 10, 15 and 30 minutes post IL-6 addition.

Protein expression of pSTAT3 as well as the total levels of signal transducers and activators of transcription 3 (tSTAT3) were examined. The assessment of tSTAT3 has been done in order to assess whether fluctuations in STAT3 levels were as a result of pSTAT3 level alterations or whether the changes seen were simply due to changing tSTAT3 levels.

A certain amount of pSTAT3 is always present within the cell regardless of IL-6 administration. This is evident by inspection of the Control groups where a pSTAT3 presence is seen within the cytoplasm although these cells were not treated with IL-6. Other studies have also shown this in their control samples (Takahashi, Abe et al. 2005).

Within the first 5 minutes after treatment the pSTAT3 levels were elevated in all three treatment groups regardless of dose (Fig. 21B, 22B, 23B). This is to be expected as it is well known that IL-6 is an initiator of STAT3 phosphorylation (Horvath 2004). At this time point the majority of pSTAT3 was found within the cytoplasm of the cell, but a noticeable amount of pSTAT3 could be seen in the nucleus of the treated cells (Fig. 21D, 22D, 23D).

After 10 minutes of IL-6 administration a pattern seems to develop. The levels of pSTAT3 in the High (Fig. 25B) group remained elevated indicating a prolonged IL-6 signaling effect, although the pSTAT3 levels in the Medium (Fig. 26B) and Low (Fig. 27B) groups returned to levels seen in the Control (Fig. 24B) group. It is known that the strength of signaling pathway activation is known to play a key role in the cellular responses as well as the duration of the signal. In PC12 cells a transient activation of the ERK 1/2 cascade induces proliferation, whereas the sustained activation of the same MAPK pathway induces differentiation (Marshall 1995; Takahashi, Abe et al. 2005). The p38 MAPK activation is also responsible for the phosphorylation of substrates just as JAK is responsible for the phosphorylation of STAT3.

However, since the action of STAT3 is to initiate transcription, which is then followed by translation, the actual effect of pSTAT3 lasts significantly longer than the short intracellular signaling period. It is possible that the second application of IL-6 in the High dose group at the 24 hour time point was responsible for another sustained activation of pSTAT3 and this duration of the pSTAT3 would lead to an opposing differentiation action as is seen in the MAPK pathway (Park, Kim et al. 1999; Puri, Wu et al. 2000; Mace, Miaczynska et al. 2005).

At the 15 minute time interval further changes are apparent. All three treatment groups' (Fig. 29B, 30B, 31B) pSTAT3 decreased to levels just below that seen in the Control (Fig. 28B). The reason for this could be as a result of a negative feedback loop, where pSTAT3 levels were abolished to levels below the Control group in order to reinstate homeostasis of pSTAT3. There are two mechanisms by which this downregulation of STAT3 can occur. The SOCS3 is responsible for the suppression of JAK/STAT signaling by the inactivation of the JAK molecule, which would lead to the inactivation of STAT3 and decreased levels of pSTAT3 (Krebs and Hilton 2001; Lang, Pauleau et al. 2003). The signaling molecule, Wnt5a, is also responsible for

the regulation STAT3 activation and a decrease in this signaling molecule could be responsible for the decrease in pSTAT3 levels (Hao, Li et al. 2006; Dissanayake, Olkhanud et al. 2008).

The 30 minute time interval seems to signal the return of pSTAT3 back to levels associated with the Control group (Fig. 32B). The pSTAT3 in all three treatment groups (Fig. 33B, 34B, 35B) were restored to levels seen in the absence of IL-6. The majority of the pSTAT3 is concentrated around the nucleus at this time point and this suggests that nuclear translocation of pSTAT3 is possible and this translocation could be responsible for effects seen in cell cycle progression and MRF expression (Fig. 33D, 34D, 35D).

Interestingly at the height of pSTAT3 levels, there seems to be an association between the activated STAT3 and another organelle other than the nucleus. This can be seen in all the treatment groups at the 5 (Fig. 21C, 22C, 23C) and 10 minute (Fig. 25C, 26C, 27C) intervals with a possible co-localization between pSTAT3 and the mitochondria. In recent years it has been found that STAT3 might play a role in the function of oxidative phosphorylation within the mitochondria (Reich 2009). STAT3 has been found in the mitochondria of cultured cells as well as primary cultures and the knockdown of STAT3 resulted in dysfunction of the electron transport chain (ETC and) STAT3 modifed by serine phosphorylation may also be responsible for the augmentation of oxidative phosphorylation in mitochondria (Reich 2009; Wegrzyn, Potla et al. 2009). Studies performed focused on the interaction between STAT3 and mitochondria in tumors (Gao, Li et al. 2010) or within a cardiac model (Boengler, Hilfiker-Kleiner et al. 2010). No data is available showing this interaction within a skeletal muscle context and the discovery of this association is novel and could play a pivotal role in mitochondrial biogenesis as well as metabolism. Further study is required to investigate the role of IL-6 in this very recently discovered interaction between STAT3 and mitochondria.

Protein expression levels seem to correlate with the changes detected by means of immunocytochemistry (Fig. 36, 37). Protein analysis of pSTAT3 is advantageous as protein levels can be measured semi-quantitively whereas with immunocytochemistry the assessment is qualitative although it does provide insight into the movement of STAT from the cytoplasm to the nucleus.

The visualization of STAT3 has not been extensively performed and to our knowledge this is the first study where the expression of STAT3 has been visualized in a C2C12 model as well as the real time visual analysis of STAT3 phosphorylation.

The complete picture of IL-6 satellite cell regulation

We hypothesize that it is this sustained elevation in the High group, which is responsible for the differentiation seen within this group. It is possible that it is the increased dose of IL-6 that is responsible for the increase in differentiation, but previous studies have suggested that the duration of the signal could also be responsible for opposing effects (Marshall 1995; Takahashi, Abe et al. 2005) and this could be possible as another High dose of IL-6 was administered at the 24 hour time point, which could increase the duration of pSTAT3 signaling leading to the activation of a differentiation program (Park, Kim et al. 1999; Puri, Wu et al. 2000; Mace, Miaczynska et al. 2005).

STAT3 is well known as an activator of transcription, but it can also act as part of a cytoplasmic signaling protein response to a stressor. With elevated levels of pSTAT3 in the High group it is highly likely that other signaling pathways are activated.

The NFκB signaling pathways have been implicated in proliferation as well as the differentiation of human embryonic stem cells (hESC). It has been suggested that the canonical NFκB pathway regulates differentiation and the non-canonical NFκB pathway is responsible for the maintenance of proliferation within hESC (Yang, Atkinson et al. 2010). An interaction between STAT3 and NFκB has been shown (Yu, Zhang et al. 2002) and this interaction could occur with either of the two opposing pathways for NFκB signaling. Activated STAT3 has been shown to interact with Nanog and these bind to NFκB and this complex inhibits the pro-differentiation transcriptional activity of NFκB within mouse embryonic stem cells (Torres and Watt 2008). However, there is an alternate interaction between STAT3 and NFκB.

MyoD is pivotal in the regulation of cell cycle fate. STAT3 can inhibit the transcriptional activity of MyoD by direct interaction (Kataoka, Matsumura et al. 2003) and MyoD in turn can inhibit the activity of STAT3 by direct interaction and this association can lead to an increase in differentiation within muscle stem cells (Yang, Xu et al. 2009). MyoD and STAT3 activities are vital in the determination of myoblast cell cycle fate.

STAT3 phosphorylation is downstream of either JAK2 or the JAK1 receptor. The JAK2/STAT2/STAT3 signaling pathway has been implicated in the differentiation within myoblasts (Wang, Wang et al. 2008) and the effect of STAT3 on proliferation of myoblasts is thought to occur through the JAK1/STAT1/STAT3 pathway (Sun, Ma et al. 2007). It is possible that IL-6 administration would activate either or both of these pathways to regulate proliferation and differentiation. This could possibly be attributed to receptor affinity. It is

possible that a high affinity IL-6 receptor exists which could be responsible for proliferation signaling through the JAK1/STAT1/STAT3 pathway in the presence of Low concentrations of IL-6. Differentiation could also be initiated by a low affinity IL-6 receptor that can activate the JAK2/STAT2/STAT3 signaling pathway in the presence of High concentrations of IL-6. Another possibility could be the presence of multiple binding sites on the IL-6 receptor, which could be responsible for alterations in downstream signaling.

What is evident from this study is that a High dose of IL-6 increases the expression of the pro-differentiation proteins, MyoD and myogenin, 48 hours after treatment. The Low and Medium doses of IL-6increased the expression of the proliferation marker, PCNA, 24 and 48 hours after treatment.

It appears as if the Medium and Low doses increased the percentage of cells in the proliferation (S) phase of the cell cycle, 24 and 48 hours after treatment, whereas the High dose only increased the proliferation phase after 48 hours of treatment. The cell cycle data combined with protein expression data suggest that the Low and Medium doses effectively initiate proliferation. The High dose group is within the proliferation phase of the cell cycle, but the cells have an increased expression of differentiation proteins, which could suggest that these cells are tending towards differentiation.

From the data acquired we have proven our hypothesis that varying doses of IL-6 have a diverse effect on the cell cycle progression of skeletal muscle satellite cells.

Limitations to the study

The satellite cells used in this study were not synchronized to a specific phase of the cell cycle and a clearer picture of cell cycle progression could be achieved if this was done. This is a limitation in the field as it is currently impossible to separate living cells into their respective phases of the cell cycle by flow cytometry. The only method of separation that exists requires fixing and consequently kills the cells. Other methods of cell cycle synchronization that have been attempted have relied on the principle of an outside intervention to synchronize the cells prior to the intervention of interest. These include the inhibition of DNA synthesis by thymidine, but the effect of this is variable. Another method of cell synchronization is by centrifugal separation, but this method requires a specific centrifuge and rotor.

Protein expression levels were only analyzed in whole cell lysates and the isolation of mitochondrial fractions could have been useful in characterizing the association between STAT3 and the mitochondria. An option for the analysis of these mitochondrial proteins would

co-immunoprecipitation in order to assess interactions between STAT3 and mitochondrial complexes.

The assessment of various JAK signaling pathways as well as different STAT signaling could have been useful in characterizing the signaling pathways of different concentrations of IL-6. This could have been accomplished by protein analysis through western blotting or through the inhibition of a specific JAK molecule to assess the exact effect of the inhibited JAK molecule.

Both phosphorylation patterns of STAT3 (Tyrosine and Serine) could have been assessed and a clearer picture could have been obtained. Other studies performed showed that Serine phosphorylated STAT3 is responsible for a mitochondrial association (Reich 2009; Wegrzyn, Potla et al. 2009) and this characterization could show how pSTAT3 affects the mitochondria.

Images obtained by means of Immunocytochemistry show crystallization of the specific antibodies and further troubleshooting is needed.

The majority of analysis performed had a sample size of 3. A larger sample size could have yielded statistical significance in certain areas.

The study was performed on the C2C12 immortal cell line and the use of primary cultures could have been more applicable.

Future studies

A primary culture will be utilized to determine if the effect of the cytokine is similar in cells exposed to an internal environment first and not immortalized. The long-term effects of IL-6 will be studied in experiments with a longer time span to assess whether the IL-6 doses' effects are short term or adaptive. If they are a short-term response, the cells would return to a state seen before the addition of IL-6. However, if the response is adaptive, I hypothesize that terminal differentiation could be seen in groups treated with High doses of IL-6.

The expression of the JAK1 and JAK2 molecules will be assessed to determine if this expression differs when comparing proliferation versus differentiating C2C12 cells. The signaling mechanism of STAT3 in both proliferation as well as differentiation will be studied as well as the effect of the STAT3 phosphorylation site (Tyrosine and Serine) on its action.

Since IL-6 is a pro-inflammatory cytokine, the signaling through the NFκB signalling pathways will be studied to assess the interaction between STAT3 and NFκB within a skeletal muscle

niche. The interaction between STAT3 and the mitochondria will be further studied to properly characterize this association and to determine whether this could be part of the inflammatory response, or if there are also possible metabolic effects of different IL-6 doses.

5. Conclusion

Interleukin-6 is implicated in immunity, inflammation, exercise as well as muscle repair processes. The exact effect IL-6 on skeletal muscle satellite cells is not clear and the results from different studies are contradictory. However, the concentrations of IL-6 administered differ between studies performed with the majority only assessing the effect of one concentration of IL-6 on satellite cells. Here, we provide a comprehensive characterization of the dose-dependent effects of supplemented IL-6 on satellite cell proliferation and differentiation. This research sheds light on the exact effect that varying, physiologically relevant doses of IL-6 have on the progression of satellite cells through the cell cycle. The percentage of cells in each phase of the cell cycle after IL-6 supplementation will give insight into the state of satellite cells under various physiological conditions, including diseased states such as sepsis.

This thesis demonstrates that: IL-6 supplementation has varying effects at different concentrations. High (10 ng/ml) doses of IL-6 promoted the expression of markers of differentiation and this was accompanied by prolonged activation of STAT3. Medium (100 pg/ml) and Low (10 pg/ml) doses of IL-6 enhanced proliferation by increasing the expression of proliferation markers as well as the progression of cells into the proliferation (S) phase of the cell cycle. There is an association between activated STAT3 and the mitochondria after IL-6 supplementation.

6. Appendices

6.1 Preparation of rhIL-6

High concentration (10 ng/ml): Dilute stock solution 1:1000

1µl Stock (10 µg/ml) rhIL-6 was added to 999µl PM

Medium concentration (100 pg/ml): Dilute High concentration 1:100

10µl High concentrated rhIL-6 medium was added to 990µl PM

Low concentration (10 pg/ml): Dilute Medium concentration 1:10

100µl Medium concentrated rhIL-6 medium was added to 900µl PM

6.2 Cell culture

6.2.1 Materials

- Trypsin-EDTA solution (1X, Batch # 048K2421)
- Sterile Phosphate Buffered Saline (PBS) containing (per l distilled H_2O)
    - 8g NaCl (Merck, # MH6M561954, Mr = 40)
    - 0.2g KCl (Merck, # 1026446, Mr = 74.55)
    - 1.44g Na_2HPO_4 (# CAS 7558-80-7, Mr = 119.98)
    - 0.24g KH_2PO_4 (Merck, # 1022810, Mr = 136.09)
    - Autoclaved at 121°C
- RIPA-Buffer
    - Tris (hydroxymethyl) aminomethane ($NH_2C(CH_2OH)_3$, # 201-064-4, Mr = 121.14)
    - TRIS-HCL 1M (#T2913)
    - 1% (v/v) NP-40 (# NP40S)
    - Na-deoxycholate (# DA5670)
    - 0.25% w/v ethylenediaminetetraacetic acid (EDTA) ($C_{10}H_{14}N_2Na_2O_8 \cdot 2H_2O$, # 205-358-3, Mr = 372.24
    - Sodium fluoride (NaF) (# 231-667-8, Mr = 41.99)

    - 4 µg/ml SBTI (# T-9003)
    - Phenylmetyl sulfonyl fluoride (PMSF) ($C_7H_7FO_2S$, # 206-350-2, Mr = 174.19)
    - Benzamidine hydrochloride hydrate ($C_6H_5C(=NH)NH_2 \cdot HCl \cdot xH_2O$, # 216-795-4, Mr = 156.61)
    - 1 µg/ml Leupeptin hydrochloride ($C_{20}H_{38}N_6O_4 \cdot HCl$, # L9873, Mr = 463.01)
- Citrate buffer (200ml)
    - 250 mM Sucrose (UnivAR, $C_{12}H_{22}O_{11}$, # 588150, Mr = 342.30)
    - 40 mM Trisodium citrate (B&M Scientific, $Na_3C_6H_5O_7.2H_2O$, # LOB-0680 Mr = 294.10)
    - 0.5% (v/v) DMSO ($(CH_3)_2SO$, # D2650, Mr = 78.13)
    - pH adjusted to 7.60 pH with meter (Consort C830, Serial # 69519)
- Haemocytometer (MarienFeld, Germany, Neubauer Improved)
- 37°C Waterbath (Gefran 600)
- 70% (v/v) Ethyl Alcohol (Illovo, Batch # 203/8/63) (C_2H_5OH)
- 1,5 ml Eppendorf tubes
- Ice bucket
- Cell scraper
- Micropipettes (Quality Scientific Plastics, Petaluma, CA, USA, 100µl- 1000µl)
- T75 and T25 Flasks (Grenier bio-one CellStar ® Tissue culture flasks, Kremsmunster, Austria)
- 6-well plates (Grenier bio-one Cellstar ®, Kremsmunster, Austria, Batch # 657160)
- Incubator set at 37°C, 5% CO_2 (SL, Shel Lab CO_2 Incubator)
- Light Microscope (Olympus CKX41, Serial # 4F05829, Olympus Corporation, Tokyo, Japan
- Flow cabinet (LAB and AIR, Serial # 10051104-BII)
- Centrifuge (Digicen 20, Serial # 040377/05)
- Pipettes 1µl- 5ml (Nichiryo Nichipet)
- Aspirator (PIPETBOY *comfort* Serial # 400415, IBS Integra Biosciences)
- Sonicator (ViniSonic 300, Serial # V1256 200830)
- 15ml/ 50ml tubes (BD Falcon ™ polypropylene Conical tubes)
- Disposable gloves (HI-care Disposable Nitrile Examination Gloves)
- Vortex (Thermolyne, Serial # 3,850,580)
- Shaker Incubator (Orbital, M.R.C. LTD, Serial # 9401310056C)

6.2.2 Preparation of proliferation medium

To 500 ml of Dulbeccos Modified Eagle Medium (DMEM, Batch # 0.38K2345) the following was added:

- 1% (v/v) Penicillin/ Streptomycin (PenStrep, Highveld Biological (PTY) LTD, Johannesburg, South Africa, Batch # CN3286)
- 10% (v/v) Foetal Bovine Serum (FBS, GIBCO™, Paisley, Scotland, Batch # 41F5180F)
- 6.8% (v/v) L-Glutamine (20mM, Batch # 068K2352)

The resultant solution shall henceforth be referred to as Proliferation Medium (PM).

6.2.3 Cell passaging

- When the cells reached 70 % confluence they were passaged
- Old medium was discarded from T75 flasks
- Cells were rinsed with 5ml preheated, sterile PBS (37°C) to remove traces of old medium
- T75 flasks with PBS were agitated for 15 seconds
- PBS was decanted
- 4 ml of Trypsin-EDTA was added to the cells
- Cells were incubated in a heated shaker at 37°C for 5 minutes
- 8ml of preheated (37°C) PM was added to deactivate the Trypsin
- The total volume was transferred to a 15ml Falcon tube
- The Falcon tube was centrifuged for 3min at 325*g* at room temperature
- The supernatant was discarded and the cell pellet was re-suspended in 5ml of preheated PM

6.2.4 Cell counting

- The haemocytometer and the cover slip was cleaned with 70% ethanol
- The cover slip was slid onto the haemocytometer and fixed as a result of Newton's attraction affect
- 40µl of the re-suspended PM was pipetted under the cover slip
- Cells in centre square of the five squares were counted on both sides of the haemocytometer
- The average cells in both squares was found by dividing the total count by 2

- The average was multiplied by 10 000 to get the total amount of cells per 1 ml of suspension
- This number was multiplied by 5 as the cell pellet was re-suspended in 5 ml of DMEM
- This gives the total amount of cells in the T75 flask
- 40 000 cells were added to each plate of a six well plate along with 2 ml of PM
    - For immunocytochemistry a sterile coverslip was placed at the bottom of each well
- 500 000 cells were added to a T75 flask along with 13 ml of PM
- 100 000 cells were added to a T25 flask along with 8 ml of PM
- Cells were incubated in a humidified incubator at 37°C with 5% (v/v) CO_2

6.2.5 Cell harvesting for flow cytometric analysis

- Cells were harvested as described in the cell passaging protocol
- The pellets were resuspended in citrate buffer after centrifugation
    - 10^6 cells/400µl citrate buffer
- Cells were stored at - 80°C

6.2.6 Protein harvesting

- Old medium was decanted from the six well plates
- 2 ml of ice cold PBS was added to each well
- The plates were agitated for 15 seconds
- The PBS was decanted and the process was repeated
- 300µl of RIPA-buffer was added to cover each well and the plates placed on ice for 10 minutes
- The cells were removed from the surface of each well using a cell scraper cleaned with 70% (v/v) Ethanol
- For each sample group, the cells of three wells were combined to maximize protein concentrations
- Eppendorf tubes were labelled and the cell suspension containing the RIPA-buffer was pipetted into the Eppendorf tubes and were kept on ice at all times
- The head of the sonicator was washed with dH_2O before and after the sonication
- The sonicator was set at its lowest setting

- The sonicator was activated and the head was moved up and down 5 times until foam developed
- The foam was allowed to settle by placing the samples on ice for 10 minutes
- The cells were then centrifuged for 10 minutes at 18000*g* at 4°C
- After centrifugation the supernatant was decanted into new Eppendorf tubes
- The sample was then split into Eppendorf tubes with 150 µl of sample in each
- The samples were stored at -80°C until further experiments were carried out

6.3 Bradford protein quantification

6.3.1 Bradford reagents

- 500mg Coomassie Brilliant Blue G was added into 250ml of 95% (v/v) Ethanol and the solution was vortexed. 500ml Phosphoric acid was added and the mixture stirred. The solution was then filled up to a total volume of 1L with distilled water (dH_2O). The solution was double filtered and stored at 4°C.

6.3.2 Standard curve

- Bovine Serum Albumin (BSA) stock solution of 200 µg/ml was prepared
  100µl BSA (1 mg/ml) was added to 400µl dH_2O and aliquoted into a 1.5 ml Eppendorf tube

Table 8: Bradford standard curve dilutions

Protein Concentration (µg/ml)	200 µg/ml BSA	Distilled H_2O	Bradford Reagent
20	100µl	0µl	900µl
16	80µl	20µl	900µl
12	60µl	40µl	900µl
8	40µl	60µl	900µl
4	20µl	80µl	900µl
2	10µl	90µl	900µl
0 (Blank)	0µl	100µl	900µl

- The samples were vortexed and incubated at room temperature for 5 minutes
- The absorbance was read spectrophotometrically at 595nm
- The Absorbance readings were then utilized to plot a standard curve

6.3.3 Lysate protein quantification

- Lysates were removed from -80°C and left at room temperature to defrost
- 5µl of each sample was pipetted into separate, marked Eppendorf tubes
    - Each sample was read in triplicate
- 95µl dH2O and 900µl Bradford reagent was added into each tube
- Tubes were vortexed and incubated at room temperature for 10 minutes
- The samples were read at 595nm by the spectrophotometer
- The Absorbance readings were then compared to the standard curve in order to determine protein concentrations
- If the readings were out of range of the standard curve, the samples were diluted 5X or 10X by the addition of RIPA buffer

6.3.4 Sample preparation

- A specific volume of the sample was pipetted into marked Eppendorf tubes in order to contain a total 20 mg
- Loading buffer was prepared by adding 850 µl sample buffer to 150 µl mercaptoethanol
- A pin size hole was punched in the lid of the Eppendorf tubes
- The samples were frozen at -80°C

6.4 Western blotting

6.4.1 Materials

- 0.45 µm PVDF membrane (Pall Corporation, # T010981)
- Extra thick blotting paper (BIO RAD Protean XL size, # 1703969)
- Protein marker (peQGold Protein Marker IV, peQLab, # 48770)
- Temperature controlled centrifuge (ALC Multispeed Refrigerated Centrifuge PK121R, Serial # 30103759)
- 1x Phosphate buffer saline (PBS)
- Pipette tips (Quality Scientific Plastics, 20-1000 µl)
- Pipettes (Nichiryo Nichipet, 10-5000 µl)
- Pasteur pipettes
- BIO RAD PowerPac Basic™ (Serial # 041BR19278)
    - Short plates
    - Space plates
    - Casting frame
    - Gray casting stand basket
    - Gel combs
- Glass beakers
- Tupperware containers
- 5oml tubes (BD Falcon ™ polypropylene Conical tubes)
- BIO RAD Trans - Blot® SD Semi-dry transfer cell, Serial # 221BR30734)
- pH meter (Consort C830, Serial # 69519)
- pH standards (IUPAC Standard, Radiometer Analytical)
    - pH 10.012 (Batch # C01125)
    - pH 7.000 (Batch # C01327)

- The Belly Dancer (Stoval Life Science Corporation, Breensboro, NC, USA, Patent # 4,702,610
- Stirrer (Stuart heat stir CB162, Serial # R000100176)
- Magnetic stirrers
- Agitator (Dynal Sample Mixer, Serial # 01/0803WH)
- Amersham™ Hyperfilm™ ECL (GE Healthcare LTD, Buckinghamshire, HP84SP, UK)
- Scotch tape
- Scissors
- Transparent film
- Hypercassette™ (Amersham Biosciences UK Limited, England, Batch # 0803)
- Test tube
- Tinfoil
- Scanner (hp scanjet 3500c, Serial #Q2800A)
- Spectrophotometer (Cary 50 Conc UV visible spectrophotometer, Vorna Valley, RSA, Serial # EL00034073)
- Densitometry software (ImageJ 1.43µ, Wayne Rasband, National Institutes of Health, USA)
- -80°C Freezer (Snijders Scientific Holland)
- Scale (Shimudzu AW220, Serial # D43231014)
- 2-Mercaptoethanol (Batch # 09524MH)
- N,N,N`,N` - Tetramethylethylen - diamine ($C_6H_{16}N_2$, TEMED, Batch # 125K0718))
- 40 % Bis Acrylamide (37.5:1) (Merck, # UN3426)
- Methanol (uniLAB Merck, Mr = 74.12, Batch # 1026522)
- isoButanol ($C_4H_{10}O$, Batch # 72480)
- Glycine (BDH, Mr = 75.07,NH_2CH_2COOH)
- Hydrochloric acid (Merck, Mr = 36.46)
- Sodium Hydroxide (Merck, Mr = 40, Batch # MH6M561954)
- Sodium chloride (Merck, # 1035968, Mr = 58.44)
- Tween® 20 (uniLAB®, # 1031255)
- 6-Aminohexanoic acid (# 025K00421)
- Tris base (Trishydroxymethylaminomethane, Trizma® base, ($C_4H_{11}NO_3$), Mr = 121.14, # 13729845010824)
- Rabbit primary antibodies
    - Phosphorylated-STAT3 (Cell Signalling, Danvers, MA, USA, Lot 6, # 9131S)

    - STAT3 (Cell Signalling, Danvers, MA, USA, Lot 3, # 9132)
- Mouse Monoclonal antibodies
    - MyOD (Dako, Glostrup, Denmark, Ref: M3512, Lot 00002861)
    - myogenin (F5D) (Santa Cruz, # G0510)
    - PCNA (Santa Cruz, sc-7907, # G0910)
- Anti-Rabbit Donkey IgG Horseradish Peroxidase linked secondary antibodies (GE Healthcare UK Limited, # 362613)
- Anti-mouse Peroxidase labelled antibodies (GE Healthcare UK Limited, Ref: NIF825, # 358607)
- Amersham™ ECL™ Western Blotting Detection Reagent (GE Healthcare, Buckinghamshire, UK, # 56, Pack: W364982)
- 10% Ammonium persulfate APS ($(NH_4)_2S_2O_8$, Merck, # 1030115, Mr = 228,20)
- 10x Tris buffered Saline (TBS)
    - 24.2g Tris base and 80g NaCl into 5L of dH_2O
    - pH 7.6
- 1% TBS-Tween
    - 100ml of 10x TBS
    - 900ml distilled water (dH_2O)
    - 1ml Tween 20
- 10x Running buffer
    - Tris-base
    - SDS
- Blocking buffer
    - 5g non-fat milk powder (Country Pasture) to 100ml TBS-Tween
- 100mM Tris
    - 6.057g Tris (Trizma® base, ($C_4H_{11}NO_3$), Mr = 121.14, # 13729845010824)
    - Tris base was added to 500ml dH_2O
    - pH 6.7
- Tris-HCl pH 6.8
- Tris-HCl pH 8.8
- 10% Sodium dodecyl sulfate (SDS) ($C_{12}H_{25}SO_4Na$, # 016K0149)
- Tris/Glycine Buffer
    - 100 ml Tris/Glycine Buffer 10X (BIO RAD, # 161-0071)
    - 200 ml Methanol

- 700 ml dH_2O

- 0.2 M NaOH solution (Merck, # MH6M561954, Mr = 40.00)
- Blocking Buffer
  - 5 g of milk powder to 100 ml TBS-Tween
- X-Ray Developer (Axim Africa X-Ray Industrial and Medical (Pty) Ltd, Batch # FDC-DEVRU0010BB)
- X-Ray Fixer (Axim Africa X-Ray Industrial and Medical (Pty) Ltd, Batch # FFC-FIXRUHS10BB)

Table 9: Volumes of reagents for preparation of 10% loading gel

Reagent	Volume for 2 gels (µl)	Volume for 4 gels (µl)
dH_2O	3850	7700
1.5M Tris-HCl, pH 8.8	2500	5000
10% SDS stock	100	200
40% Acrylamide	2500	5000
10% APS	50	100
TEMED	5	10

Table 10: Volumes of reagents for preparation of 4% stacking gel

Reagent	Volume for 2 gels (µl)	Volume for 4 gels (µl)
dH_2O	3050	6100
1.5M Tris-HCl, pH 6.8	1250	2500
10% SDS stock	50	100
40% Acrylamide	500	1000
10% APS	50	100
TEMED	10	20

6.4.2 Gel preparation

- 0.75 mm space plates and short plates were cleaned with dH_2O and methanol
- The plates were placed on each other and slid into the casting frame on a level surface
- The casting frame was clamped in the pressure cams of the gray casting stand gasket
- dH_2O was added between the glass plates to check for any leakage
- The dH_2O was then decanted from the plates
- 10% Loading gel reagents were added into a 15ml beaker
- APS was added pen ultimately and the mixture was stirred
- TEMED was added last and the mixture was quickly stirred and added between the two glass plates by means of a Pasteur pipette before the gel set
- The loading gel was added to fill the glass plates to ¾
- A thin layer of isoButanol was added to remove excess bubbles
- The loading gel was left for one hour to set
- After an hour the layer of 1-isobutanol was washed away with dH_2O
- 4% Stacking gel reagents were added into 15ml beaker
- APS was added pen ultimately and the mixture was stirred
- TEMED was added last and the mixture was quickly stirred and added between the two glass plates by means of a Pasteur pipette before the gel set
- Combs were gently pushed between the plates to prevent bubble formation
- The stacking gel was left for 30 minutes to set and the combs were removed gently
- The wells were washed with dH_2O to remove acrylamide residue from the wells

6.4.3 Gel electrophoresis

- Glass plates were removed from the assembly apparatus and placed in the BIO RAD Mini-Protean 3® Cell
- Running buffer was added to cover the wells in order to assess whether the mounting assembly was leaking
- Protein ladder and samples were loaded into the wells carefully to prevent sample from exiting its specific well

- The mounting assembly was placed in the cell container so that the positive and negative electrodes align properly
- The container was filled
- The lid was closed and the electrodes were attached to their specific locations
- The first run was set at a constant voltage of 100V and 400mA for 10 minutes to allow the samples to pass the loading gel
- The second run was set at constant amperes of 400mA and 200V and ran for 50 minutes
- After the samples were run the gels were quickly removed from the container to prohibit loss of proteins

6.4.4 Semi-dry transfer

- The semi-dry transfer cell's Anode plate was first cleaned with dH_2O to remove remnants of gels and Whatmann paper
- 2 Squares of Extra thick blotting paper and one PVDF membrane was cut for each membrane
- The squares were cut to resemble each other and to completely cover the gel
- Squares of Extra thick blotting paper were submersed in Bio Rad transfer buffer
- The PVDF membrane was activated by submersion in pure methanol
- One square of extra thick blotting paper was placed on the Anode plate
- The activated PVDF membrane was carefully placed on the blotting paper to prevent bubble formation
- The gel was then removed from between the glass plates and the stacking gel was scraped off to only leave the loading gel portion
- The gel was carefully placed on the PVDF membrane to prevent breakage and bubble formation
- Another square of extra thick blotting paper was placed on top of the gel
- The Cathode plate was placed on the assembly of papers and gel
- The Safety lid was closed properly
- The proteins on the gel were transferred to the membrane by running the apparatus at 15V and 0.5A for one hour

6.4.5 Membrane probing

- After the proteins were successfully transferred to the membrane, the membrane was removed from between the blotting paper squares
- The membrane was again submerged in pure methanol to fix transferred proteins to the membrane
- The membrane was washed for 5 minutes on the belly dancer with TBS-Tween buffer
- After each washing step the TBS-Tween was decanted and new TBS-Tween was added
- The washing step was repeated three times
- After the washing step the membrane was blocked with 50 ml non-fat milk for one hour at room temperature with constant agitation
- After the blocking step the excess milk was washed off the membrane with TBS-Tween
- The washing step was repeated three times on the belly dancer
- After the washing steps, the membrane was incubated with primary antibodies overnight (or 6-8 hours) at 4°C with constant agitation
- After the primary antibodies were allowed to bind, the membrane was washed on the belly dancer with TBS-Tween three times
- The membrane was incubated in the secondary antibody for 1 hour at room temperature with constant agitation
- The membrane was washed three times with TBS-Tween

6.4.6 Protein visualization

- After incubation with the secondary antibody the ECL detection reagents were warmed to room temperature
- For each membrane 0.5 ml of substrate 1 and 0.5 ml of substrate 2 was added to each other in 15 ml Falcon tube covered with Tinfoil
- The membranes were removed from the secondary antibody and the ECL substrates were administered to the area of the membrane where the protein of interest was located
- The ECL substrates were left on the membrane for 1 minute
- The membranes were transferred to a Hypercassette™ thoroughly cleaned with 70% (v/v) ethanol

- The membranes were gently placed in between two sheets of transparent film to prevent bubble formation
- The Hypercassette™, containing the membranes, was taken to the dark room
- The ECL hyperfilm was then taken out of its container and covering
- The film was cut in order to cover the area of interest on the membrane
- The film was placed on top of the membrane covered by the transparent film
- The Hypercassette™ was closed and the film was left on the membrane for 5 minutes
- After 5 minutes the film was removed from the Hypercassette™ and placed in the X-ray developer
- The film was left in the developer until bands could clearly be seen on the film
- The film was developed in order to show shades of grey and to prevent bleaching
- The film was removed from the developer and washed with copious amounts of water
- The film was placed in X-ray fixer
- The film could then be taken into a well light area
- The film was taken out of the fixer and washed with copious amounts of water
- If the bands were too dark or too light to clearly see the difference between them, the process was repeated but the film was left on for a longer or shorter period of time on the membrane

6.4.7 Membrane stripping

- Antibodies were stripped from the membrane if the proteins on the membrane were to be probed for another protein
- The membrane was washed twice with dH_2O for five minutes on the belly dancer
- The dH_2O was then decanted from the membrane and was placed in 0.2 M NaOH for five minutes on the belly dancer
- The NaOH was then decanted
- The membrane was again washed twice with dH_2O for five minutes on the belly dancer
- After the stripping process was completed, the membranes were stored in between two sheets of transparent film in an area away from other protein sources at 4ºC

6.4.8 Densitometric analysis

- Developed membranes were scanned digitally after development
- The film was scanned in 256 Gray scale
- The scanned image was imported into the ImageJ software
- The data was analyzed to determine the relative amounts of proteins in the samples

6.5 Flow cytometry

6.5.1 Materials

- Flow cytometer (BD FACSAria™ Cell Sorter, Serial # P9990037, BD Biosciences, San Jose, CA 95133 USA)
- Centrifuge (Digicen 20, Serial # 040377/05)
- 15 ml Falcon tubes
- Pipettes
- Pipette tips
- -20°C Fridge
- Mendelov protocol solutions
    - Stock Solution (2L)
        - 2000mg Trisodium citrate (3.4 mM)
        - 2000µl Nonidet P 40 (Shell, Carrington, England)(0.1% (v/v))
        - 1044mg Sperminetetrahydrochloride (S2876)(1.5 mM)
        - 121 mg Tris (hydroxymethyl)-aminomethane (0.5 mM)
        - pH 7.6
    - Solution A (Room temperature)
        - 15mg Trypsin (T0134)
        - 500ml Stock Solution
        - pH 7.6
    - Solution B (Room temperature)
        - 250mg Trypsin Inhibitor (T9253)
        - 50mg Ribonuclease A (R4875)
        - 500ml Stock Solution
        - pH 7.6
    - Solution C (Ice-cold, light protected)
        - 208mg Propidium Iodide (Calbiochem, San Diego, CA)
        - 580mg Spermine tetrahydrochloride

- 500 ml Stock Solution
- pH 7.6

6.5.2 Cell cycle analysis

- Cell samples were removed from the -80ºC freezer and allowed to thaw
    - 10^6 cells/400µl citrate buffer
- 40µl cell suspension was added to 360µl Solution A
- Solution was left at room temperature for 10 minutes with regular inversion
- 300µl Solution B was added
- Solution was left at room temperature for 10 minutes with regular inversion
- 300µl Solution C was added
- The solution was placed on ice for 15 minutes, wrapped in foil
- Cell cycle fraction were analysed by FACSaria™ Cell Sorter

6.6 Immunocytochemistry

6.6.1 Materials

- Fluorescence Microscope
- Black box
- Sterile coverslips
- Frosted Microscope Slides (Frosted StarSelect by Lasec)
- Eppendorf tubes
- Pipettes
- Pipette tips
- 4°C Fridge
- -20°C Freezer
- Prepared rhIL-6
- Polystyrene Ice holder
- 4% Paraformaldehyde at 37°C ($(H.CHO)_n$, Hopkin & Williams Ltd, # 11945B86224)
- Phosphate Buffer Saline (PBS) (1L)
- Methanol (Ice cold)
- 0.25% (v/v) Triton X-100 (BDH, # 1014224)
- Blocking Serum

    - 20% (v/v) Goat serum (PAA, # B15-035) in 80% (v/v) PBS
    - 5% (v/v) Donkey serum (Jackson Immun Research, # 017-000-121 in 95% (v/v) PBS
- Primary Antibodies
    - myogenin (Dako, Glostrup, Denmark, Ref : M3559, Lot 10012968)
    - PCNA (Santa Cruz, sc-7907, # G0910)
    - Phosphorylated-STAT3 (Cell Signalling, Danvers, MA, USA, Lot 6, # 9131S)
- Secondary Antibodies
    - Alexa Fluor 594 (Invitrogen, # A11012)
    - Alexa Fluor 488 (Invitrogen, # A11029)
    - Donkey Anti-Rabbit IgG FITC (Santa Cruz, # sc-2090)
- Mitochondrial stain
    - MitoTracker® Red CMX Ros (Mr = 531.52, #M7512)
        - 1mM Stock solution (50µg MitoTracker® in 94.1µl DMSO)
        - 250nMWorking solution (2,5µl stock solution in 10ml PM)
- Nuclear stain
    - DAPI (Bis Benzimide H33422 trihydrochloride, # B2261
- Fluorescent mounting medium (Dako, # S5023)

6.6.2 Double antibody (myogenin, PCNA) staining method

- Cells were seeded at 40 000 per well and treated for either 24 or 48 hours with varying doses of IL-6
- 6 well plates containing sterile coverslips were aspirated
- 4% (v/v) Paraformaldehyde was added to saturate coverslips and left for 15 minutes at room temperature
- Coverslips were removed from wells and transferred to microscope slides
- Slides were washed with PBS for 5 minutes
- Washing steps were repeated three times
- Ice-cold methanol was added to the slides
- Slides were left on ice for 30 minutes
- Slides were washed three times with PBS
- 0.25% (v/v) Triton X-100 was added to slides and incubated for 15 minutes at room temperature
- Slides were washed three times with PBS

- Slides were moved to light blocking black box
- Blocking serum (20% (v/v) Goat Serum) was added to slides and incubated for 30 minutes at room temperature
- Blocking serum was decanted off the slides
- Primary antibody #1 (myogenin) was added to the slides and incubated overnight at 4°C
- Slides were washed three times with PBS
- Secondary antibody #1 (Alexa Fluor 488) was added to slides and incubated for 60 minutes at room temperature
- Slides were washed three times with PBS
- Primary antibody #2 (PCNA) was added to the slides and incubated for 4 hours at room temperature
- Slides were washed three times with PBS
- Secondary Antibody #2 (Alexa Fluor 594) was added to slides and incubated for 60 minutes at room temperature
- Slides were washed three times with PBS
- Nuclear stain (DAPI) was added to slides and incubated for 15 minutes at room temperature
- Slides were washed three times with PBS
- Coverslips were transferred to new frosted slides and mounted with fluorescent mounting medium
- Slides were stored at -20°C until visualized by fluorescence microscopy

6.6.3 Mitochondrial and antibody (pSTAT3) staining method

- Cells were seeded at 40 000 per well the day preceding IL-6 treatment
- Medium supplemented with MitoTracker® Red CMX Ros was added to cells
- Cells were treated with IL-6 for 5, 10, 15 and 30 minutes
- 6 well plates containing sterile coverslips were aspirated
- 4% Paraformaldehyde was added to saturate coverslips and left for 15 minutes at room temperature
- Coverslips were removed from wells and transferred to microscope slides
- Slides were washed with PBS for 5 minutes
- Washing steps were repeated three times
- Ice-cold methanol was added to the slides

- Slides were left on ice for 30 minutes
- Slides were washed three times with PBS
- 0.25% (v/v) Triton X-100 was added to slides and incubated for 15 minutes at room temperature
- Slides were washed three times with PBS
- Slides were moved to light blocking black box
- Blocking serum (5% (v/v) Donkey Serum) was added to slides and incubated for 30 minutes at room temperature
- Blocking serum was decanted off the slides
- Primary antibody (pSTAT3) was added to the slides and incubated for 2 hours at room temperature
- Slides were washed three times with PBS
- Secondary antibody (Donkey Anti-Rabbit FITC) was added to slides and incubated for 60 minutes at room temperature
- Slides were washed three times with PBS
- Nuclear stain (DAPI) was added to slides and incubated for 15 minutes at room temperature
- Slides were washed three times with PBS
- Coverslips were transferred to new frosted slides and mounted with fluorescent mounting medium
- Slides were stored at -20°C until visualized by fluorescence microscopy

7. References

Al-Shanti, N., A. Saini, et al. (2008). "Beneficial synergistic interactions of TNF-alpha and IL-6 in C2 skeletal myoblasts--potential cross-talk with IGF system." Growth Factors **26**(2): 61-73.

Al-Shanti, N. and C. E. Stewart (2008). "PD98059 enhances C2 myoblast differentiation through p38 MAPK activation: a novel role for PD98059." J Endocrinol **198**(1): 243-252.

Alm, K. and S. Oredsson (2009). "Cells and polyamines do it cyclically." Essays Biochem **46**: 63-76.

Alvarez, B., L. S. Quinn, et al. (2002). "Tumor necrosis factor-alpha exerts interleukin-6-dependent and -independent effects on cultured skeletal muscle cells." Biochim Biophys Acta **1542**(1-3): 66-72.

Ancey, C., E. Menet, et al. (2003). "Human cardiomyocyte hypertrophy induced in vitro by gp130 stimulation." Cardiovasc Res **59**(1): 78-85.

Anderson, J. E. (2006). "The satellite cell as a companion in skeletal muscle plasticity: currency, conveyance, clue, connector and colander." J Exp Biol **209**(Pt 12): 2276-2292.

Asakura, A. (2003). "Stem cells in adult skeletal muscle." Trends Cardiovasc Med **13**(3): 123-128.

Asakura, A., P. Seale, et al. (2002). "Myogenic specification of side population cells in skeletal muscle." J Cell Biol **159**(1): 123-134.

Baeza-Raja, B. and P. Munoz-Canoves (2004). "p38 MAPK-induced nuclear factor-kappaB activity is required for skeletal muscle differentiation: role of interleukin-6." Mol Biol Cell **15**(4): 2013-2026.

Baron, F., S. Copizza, et al. (2004). "CD34+ cell dose predicts costs after autologous peripheral blood stem cell transplantation for breast cancer." Haematologica **89**(9): 1146-1148.

Beadling, C., D. Guschin, et al. (1994). "Activation of JAK kinases and STAT proteins by interleukin-2 and interferon alpha, but not the T cell antigen receptor, in human T lymphocytes." EMBO J **13**(23): 5605-5615.

Beauchamp, J. R., L. Heslop, et al. (2000). "Expression of CD34 and Myf5 defines the majority of quiescent adult skeletal muscle satellite cells." J Cell Biol **151**(6): 1221-1234.

Bockhold, K. J., J. D. Rosenblatt, et al. (1998). "Aging normal and dystrophic mouse muscle: analysis of myogenicity in cultures of living single fibers." Muscle Nerve **21**(2): 173-183.

Boengler, K., D. Hilfiker-Kleiner, et al. (2010). "Inhibition of permeability transition pore opening by mitochondrial STAT3 and its role in myocardial ischemia/reperfusion." Basic Res Cardiol **105**(6): 771-785.

Bradford, M. M. (1976). "A rapid and sensitive method for the quantitation of microgram quantities of protein utilizing the principle of protein-dye binding." Anal Biochem **72**: 248-254.

Bromberg, J. and J. E. Darnell, Jr. (2000). "The role of STATs in transcriptional control and their impact on cellular function." Oncogene **19**(21): 2468-2473.

Bromberg, J. F., M. H. Wrzeszczynska, et al. (1999). "Stat3 as an oncogene." Cell **98**(3): 295-303.

Broussard, S. R., R. H. McCusker, et al. (2003). "Cytokine-hormone interactions: tumor necrosis factor alpha impairs biologic activity and downstream activation signals of the insulin-like growth factor I receptor in myoblasts." Endocrinology **144**(7): 2988-2996.

Buckingham, M., L. Bajard, et al. (2003). "The formation of skeletal muscle: from somite to limb." J Anat **202**(1): 59-68.
Cantini, M., M. L. Massimino, et al. (1995). "Human satellite cell proliferation in vitro is regulated by autocrine secretion of IL-6 stimulated by a soluble factor(s) released by activated monocytes." Biochem Biophys Res Commun **216**(1): 49-53.
Cao, Y., Z. Zhao, et al. (2003). "Role of metalloprotease disintegrin ADAM12 in determination of quiescent reserve cells during myogenic differentiation in vitro." Mol Cell Biol **23**(19): 6725-6738.
Chakravarthy, M. V., T. W. Abraha, et al. (2000). "Insulin-like growth factor-I extends in vitro replicative life span of skeletal muscle satellite cells by enhancing G1/S cell cycle progression via the activation of phosphatidylinositol 3'-kinase/Akt signaling pathway." J Biol Chem **275**(46): 35942-35952.
Charge, S. B. and M. A. Rudnicki (2004). "Cellular and molecular regulation of muscle regeneration." Physiol Rev **84**(1): 209-238.
Chellappan, S. P., S. Hiebert, et al. (1991). "The E2F transcription factor is a cellular target for the RB protein." Cell **65**(6): 1053-1061.
Chin, Y. E., M. Kitagawa, et al. (1996). "Cell growth arrest and induction of cyclin-dependent kinase inhibitor p21 WAF1/CIP1 mediated by STAT1." Science **272**(5262): 719-722.
Collins, C. A., V. F. Gnocchi, et al. (2009). "Integrated functions of Pax3 and Pax7 in the regulation of proliferation, cell size and myogenic differentiation." PLoS One **4**(2): e4475.
Cooper, R. N., G. S. Butler-Browne, et al. (2006). "Human muscle stem cells." Curr Opin Pharmacol **6**(3): 295-300.
Cooper, W. G. and I. R. Konigsberg (1961). "Dynamics of myogenesis in vitro." Anat Rec **140**: 195-205.
Cornelison, D. D. and B. J. Wold (1997). "Single-cell analysis of regulatory gene expression in quiescent and activated mouse skeletal muscle satellite cells." Dev Biol **191**(2): 270-283.
Croker, B. A., D. L. Krebs, et al. (2003). "SOCS3 negatively regulates IL-6 signaling in vivo." Nat Immunol **4**(6): 540-545.
Dalpke, A. H., S. Opper, et al. (2001). "Suppressors of cytokine signaling (SOCS)-1 and SOCS-3 are induced by CpG-DNA and modulate cytokine responses in APCs." J Immunol **166**(12): 7082-7089.
Damas, P., D. Ledoux, et al. (1992). "Cytokine serum level during severe sepsis in human IL-6 as a marker of severity." Ann Surg **215**(4): 356-362.
Danial, N. N., A. Pernis, et al. (1995). "Jak-STAT signaling induced by the v-abl oncogene." Science **269**(5232): 1875-1877.
Datta, B., W. Min, et al. (1998). "Increase in p202 expression during skeletal muscle differentiation: inhibition of MyoD protein expression and activity by p202." Mol Cell Biol **18**(2): 1074-1083.
Dhawan, J. and T. A. Rando (2005). "Stem cells in postnatal myogenesis: molecular mechanisms of satellite cell quiescence, activation and replenishment." Trends Cell Biol **15**(12): 666-673.
Dissanayake, S. K., P. B. Olkhanud, et al. (2008). "Wnt5A regulates expression of tumor-associated antigens in melanoma via changes in signal transducers and activators of transcription 3 phosphorylation." Cancer Res **68**(24): 10205-10214.
Farnebo, S., K. Lars-Erik, et al. (2009). "Continuous assessment of concentrations of cytokines in experimental injuries of the extremity." Int J Clin Exp Med **2**(4): 354-362.
Faunce, D. E., M. S. Gregory, et al. (1998). "Acute ethanol exposure prior to thermal injury results in decreased T-cell responses mediated in part by increased production of IL-6." Shock **10**(2): 135-140.

Febbraio, M. A. and B. K. Pedersen (2002). "Muscle-derived interleukin-6: mechanisms for activation and possible biological roles." FASEB J **16**(11): 1335-1347.
Ferri, P., E. Barbieri, et al. (2009). "Expression and subcellular localization of myogenic regulatory factors during the differentiation of skeletal muscle C2C12 myoblasts." J Cell Biochem **108**(6): 1302-1317.
Fredj, S., J. Bescond, et al. (2005). "Role of interleukin-6 in cardiomyocyte/cardiac fibroblast interactions during myocyte hypertrophy and fibroblast proliferation." J Cell Physiol **204**(2): 428-436.
Fujio, Y., T. Matsuda, et al. (2004). "Signals through gp130 upregulate Wnt5a and contribute to cell adhesion in cardiac myocytes." FEBS Lett **573**(1-3): 202-206.
Gal-Levi, R., Y. Leshem, et al. (1998). "Hepatocyte growth factor plays a dual role in regulating skeletal muscle satellite cell proliferation and differentiation." Biochim Biophys Acta **1402**(1): 39-51.
Gallegly, J. C., N. A. Turesky, et al. (2004). "Satellite cell regulation of muscle mass is altered at old age." J Appl Physiol **97**(3): 1082-1090.
Gao, L., F. Li, et al. (2010). "Inhibition of STAT3 and ErbB2 suppresses tumor growth, enhances radiosensitivity, and induces mitochondria-dependent apoptosis in glioma cells." Int J Radiat Oncol Biol Phys **77**(4): 1223-1231.
Garcia, R. and R. Jove (1998). "Activation of STAT transcription factors in oncogenic tyrosine kinase signaling." J Biomed Sci **5**(2): 79-85.
Garry, D. J., Q. Yang, et al. (1997). "Persistent expression of MNF identifies myogenic stem cells in postnatal muscles." Dev Biol **188**(2): 280-294.
Gauglitz, G. G., J. Song, et al. (2008). "Characterization of the inflammatory response during acute and post-acute phases after severe burn." Shock **30**(5): 503-507.
Geiger, T., T. Andus, et al. (1988). "Induction of rat acute-phase proteins by interleukin 6 in vivo." Eur J Immunol **18**(5): 717-721.
Goldberg, A. L., J. D. Etlinger, et al. (1975). "Mechanism of work-induced hypertrophy of skeletal muscle." Med Sci Sports **7**(3): 185-198.
Goudenege, S., D. F. Pisani, et al. (2009). "Enhancement of myogenic and muscle repair capacities of human adipose-derived stem cells with forced expression of MyoD." Mol Ther **17**(6): 1064-1072.
Gray, S. R., M. Clifford, et al. (2009). "The response of circulating levels of the interleukin-6/interleukin-6 receptor complex to exercise in young men." Cytokine **47**(2): 98-102.
Hao, J., T. G. Li, et al. (2006). "WNT/beta-catenin pathway up-regulates Stat3 and converges on LIF to prevent differentiation of mouse embryonic stem cells." Dev Biol **290**(1): 81-91.
Hawke, T. J. and D. J. Garry (2001). "Myogenic satellite cells: physiology to molecular biology." J Appl Physiol **91**(2): 534-551.
Hayflick, L. and P. S. Moorhead (1961). "The serial cultivation of human diploid cell strains." Exp Cell Res **25**: 585-621.
Heinrich, P. C., I. Behrmann, et al. (2003). "Principles of interleukin (IL)-6-type cytokine signalling and its regulation." Biochem J **374**(Pt 1): 1-20.
Heinrich, P. C., I. Behrmann, et al. (1998). "Interleukin-6-type cytokine signalling through the gp130/Jak/STAT pathway." Biochem J **334 (Pt 2)**: 297-314.
Hirano, T., K. Ishihara, et al. (2000). "Roles of STAT3 in mediating the cell growth, differentiation and survival signals relayed through the IL-6 family of cytokine receptors." Oncogene **19**(21): 2548-2556.
Holterman, C. E. and M. A. Rudnicki (2005). "Molecular regulation of satellite cell function." Semin Cell Dev Biol **16**(4-5): 575-584.
Horvath, C. M. (2004). "The Jak-STAT pathway stimulated by interleukin 6." Sci STKE **2004**(260): tr9.

Hsiao, S. P. and S. L. Chen (2010). "Myogenic regulatory factors regulate M-cadherin expression by targeting its proximal promoter elements." Biochem J **428**(2): 223-233.
Irintchev, A., M. Zeschnigk, et al. (1994). "Expression pattern of M-cadherin in normal, denervated, and regenerating mouse muscles." Dev Dyn **199**(4): 326-337.
Ishido, M., K. Kami, et al. (2004). "Localization of MyoD, myogenin and cell cycle regulatory factors in hypertrophying rat skeletal muscles." Acta Physiol Scand **180**(3): 281-289.
Jacques, A., C. Bleau, et al. (2009). "Macrophage interleukin-6 and tumour necrosis factor-alpha are induced by coronavirus fixation to Toll-like receptor 2/heparan sulphate receptors but not carcinoembryonic cell adhesion antigen 1a." Immunology **128**(1 Suppl): e181-192.
Jayaraman, T. and A. R. Marks (1993). "Rapamycin-FKBP12 blocks proliferation, induces differentiation, and inhibits cdc2 kinase activity in a myogenic cell line." J Biol Chem **268**(34): 25385-25388.
Jin, X., J. G. Kim, et al. (2007). "Opposite roles of MRF4 and MyoD in cell proliferation and myogenic differentiation." Biochem Biophys Res Commun **364**(3): 476-482.
Jo, C., H. Kim, et al. (2005). "Leukemia inhibitory factor blocks early differentiation of skeletal muscle cells by activating ERK." Biochim Biophys Acta **1743**(3): 187-197.
Johnson, S. E. and R. E. Allen (1993). "Proliferating cell nuclear antigen (PCNA) is expressed in activated rat skeletal muscle satellite cells." J Cell Physiol **154**(1): 39-43.
Kadi, F., N. Charifi, et al. (2004). "Satellite cells and myonuclei in young and elderly women and men." Muscle Nerve **29**(1): 120-127.
Kadi, F. and E. Ponsot (2010). "The biology of satellite cells and telomeres in human skeletal muscle: effects of aging and physical activity." Scand J Med Sci Sports **20**(1): 39-48.
Kami, K. and E. Senba (2002). "In vivo activation of STAT3 signaling in satellite cells and myofibers in regenerating rat skeletal muscles." J Histochem Cytochem **50**(12): 1579-1589.
Karlsson, J. O., M. L. Yarmush, et al. (1998). "Interaction between heat shock and interleukin 6 stimulation in the acute-phase response of human hepatoma (HepG2) cells." Hepatology **28**(4): 994-1004.
Kataoka, Y., I. Matsumura, et al. (2003). "Reciprocal inhibition between MyoD and STAT3 in the regulation of growth and differentiation of myoblasts." J Biol Chem **278**(45): 44178-44187.
Keller, P., M. Penkowa, et al. (2005). "Interleukin-6 receptor expression in contracting human skeletal muscle: regulating role of IL-6." FASEB J **19**(9): 1181-1183.
Kikutani, H., T. Taga, et al. (1985). "Effect of B cell differentiation factor (BCDF) on biosynthesis and secretion of immunoglobulin molecules in human B cell lines." J Immunol **134**(2): 990-995.
Kim, H., C. Jo, et al. (2008). "Oncostatin M induces growth arrest of skeletal muscle cells in G1 phase by regulating cyclin D1 protein level." Cell Signal **20**(1): 120-129.
Kishimoto, T., Y. Hirai, et al. (1978). "Regulation of antibody response in different immunoglobulin classes. IV. Properties and functions of IgE class-specific" suppressor factor(s) released from DNP-mycobacterium-primed T cells." J Immunol **121**(5): 2106-2112.
Kitzmann, M. and A. Fernandez (2001). "Crosstalk between cell cycle regulators and the myogenic factor MyoD in skeletal myoblasts." Cell Mol Life Sci **58**(4): 571-579.
Klouche, M., S. Bhakdi, et al. (1999). "Novel path to activation of vascular smooth muscle cells: up-regulation of gp130 creates an autocrine activation loop by IL-6 and its soluble receptor." J Immunol **163**(8): 4583-4589.
Korzus, E., J. Torchia, et al. (1998). "Transcription factor-specific requirements for coactivators and their acetyltransferase functions." Science **279**(5351): 703-707.

Krebs, D. L. and D. J. Hilton (2001). "SOCS proteins: negative regulators of cytokine signaling." Stem Cells **19**(5): 378-387.
Lang, R., A. L. Pauleau, et al. (2003). "SOCS3 regulates the plasticity of gp130 signaling." Nat Immunol **4**(6): 546-550.
Langberg, H., J. L. Olesen, et al. (2002). "Substantial elevation of interleukin-6 concentration in peritendinous tissue, in contrast to muscle, following prolonged exercise in humans." J Physiol **542**(Pt 3): 985-990.
Leshem, Y., D. B. Spicer, et al. (2000). "Hepatocyte growth factor (HGF) inhibits skeletal muscle cell differentiation: a role for the bHLH protein twist and the cdk inhibitor p27." J Cell Physiol **184**(1): 101-109.
Levitt, D. G. (2003). "The pharmacokinetics of the interstitial space in humans." BMC Clin Pharmacol **3**: 3.
Levy, D. E. and J. E. Darnell, Jr. (2002). "Stats: transcriptional control and biological impact." Nat Rev Mol Cell Biol **3**(9): 651-662.
Li, J., S. A. Reed, et al. (2009). "Hepatocyte growth factor (HGF) signals through SHP2 to regulate primary mouse myoblast proliferation." Exp Cell Res **315**(13): 2284-2292.
Li, Y. P. (2003). "TNF-alpha is a mitogen in skeletal muscle." Am J Physiol Cell Physiol **285**(2): C370-376.
Li, Y. P. and R. J. Schwartz (2001). "TNF-alpha regulates early differentiation of C2C12 myoblasts in an autocrine fashion." FASEB J **15**(8): 1413-1415.
Longshaw, V. M., M. Baxter, et al. (2009). "Knockdown of the co-chaperone Hop promotes extranuclear accumulation of Stat3 in mouse embryonic stem cells." Eur J Cell Biol **88**(3): 153-166.
Mace, G., M. Miaczynska, et al. (2005). "Phosphorylation of EEA1 by p38 MAP kinase regulates mu opioid receptor endocytosis." EMBO J **24**(18): 3235-3246.
Marshall, C. J. (1995). "Specificity of receptor tyrosine kinase signaling: transient versus sustained extracellular signal-regulated kinase activation." Cell **80**(2): 179-185.
McFarland, D. C., J. E. Pesall, et al. (1993). "Comparison of the proliferation and differentiation of myogenic satellite cells derived from Merriam's and commercial varieties of turkeys." Comp Biochem Physiol Comp Physiol **104**(3): 455-460.
McKay, B. R., K. G. Toth, et al. (2010). "Satellite cell number and cell cycle kinetics in response to acute myotrauma in humans: immunohistochemistry versus flow cytometry." J Physiol **588**(Pt 17): 3307-3320.
Megeney, L. A., B. Kablar, et al. (1996). "MyoD is required for myogenic stem cell function in adult skeletal muscle." Genes Dev **10**(10): 1173-1183.
Megeney, L. A., R. L. Perry, et al. (1996). "bFGF and LIF signaling activates STAT3 in proliferating myoblasts." Dev Genet **19**(2): 139-145.
Miller, K. J., D. Thaloor, et al. (2000). "Hepatocyte growth factor affects satellite cell activation and differentiation in regenerating skeletal muscle." Am J Physiol Cell Physiol **278**(1): C174-181.
Miller, R. J. and G. I. Bell (1996). "JAK/STAT eats the fat." Trends Neurosci **19**(5): 159-161.
Minami, M., M. Inoue, et al. (1996). "STAT3 activation is a critical step in gp130-mediated terminal differentiation and growth arrest of a myeloid cell line." Proc Natl Acad Sci U S A **93**(9): 3963-3966.
Moldoveanu, A. I., R. J. Shephard, et al. (2000). "Exercise elevates plasma levels but not gene expression of IL-1beta, IL-6, and TNF-alpha in blood mononuclear cells." J Appl Physiol **89**(4): 1499-1504.
Myers, M. G., Jr. (2009). "Cell biology. Moonlighting in mitochondria." Science **323**(5915): 723-724.

Nagata, Y., H. Kobayashi, et al. (2006). "Sphingomyelin levels in the plasma membrane correlate with the activation state of muscle satellite cells." J Histochem Cytochem **54**(4): 375-384.
Narciso, L., P. Fortini, et al. (2007). "Terminally differentiated muscle cells are defective in base excision DNA repair and hypersensitive to oxygen injury." Proc Natl Acad Sci U S A **104**(43): 17010-17015.
Nieman, D. C., S. L. Nehlsen-Cannarella, et al. (1998). "Influence of mode and carbohydrate on the cytokine response to heavy exertion." Med Sci Sports Exerc **30**(5): 671-678.
Nishikawa, J., K. Sakuma, et al. (2005). "Increase of Cardiotrophin-1 immunoreactivity in regenerating and overloaded but not denervated muscles of rats." Neuropathology **25**(1): 54-65.
Okazaki, S., H. Kawai, et al. (1996). "Effects of calcitonin gene-related peptide and interleukin 6 on myoblast differentiation." Cell Prolif **29**(4): 173-182.
Olguin, H. C. and B. B. Olwin (2004). "Pax-7 up-regulation inhibits myogenesis and cell cycle progression in satellite cells: a potential mechanism for self-renewal." Dev Biol **275**(2): 375-388.
Ostrowski, K., C. Hermann, et al. (1998). "A trauma-like elevation of plasma cytokines in humans in response to treadmill running." J Physiol **513 (Pt 3)**: 889-894.
Ostrowski, K., T. Rohde, et al. (1999). "Pro- and anti-inflammatory cytokine balance in strenuous exercise in humans." J Physiol **515 (Pt 1)**: 287-291.
Otto, A., H. Collins-Hooper, et al. (2009). "The origin, molecular regulation and therapeutic potential of myogenic stem cell populations." J Anat **215**(5): 477-497.
Parganas, E., D. Wang, et al. (1998). "Jak2 is essential for signaling through a variety of cytokine receptors." Cell **93**(3): 385-395.
Park, K. S., N. G. Kim, et al. (1999). "Differential regulation of MAP kinase cascade in human colorectal tumorigenesis." Br J Cancer **81**(7): 1116-1121.
Penkowa, M., T. Moos, et al. (1999). "Strongly compromised inflammatory response to brain injury in interleukin-6-deficient mice." Glia **25**(4): 343-357.
Peterson, J. M., R. W. Bryner, et al. (2008). "Satellite cell proliferation is reduced in muscles of obese Zucker rats but restored with loading." Am J Physiol Cell Physiol **295**(2): C521-528.
Petrella, J. K., J. S. Kim, et al. (2006). "Efficacy of myonuclear addition may explain differential myofiber growth among resistance-trained young and older men and women." Am J Physiol Endocrinol Metab **291**(5): E937-946.
Puri, P. L., Z. Wu, et al. (2000). "Induction of terminal differentiation by constitutive activation of p38 MAP kinase in human rhabdomyosarcoma cells." Genes Dev **14**(5): 574-584.
Redshaw, Z., S. McOrist, et al. (2010). "Muscle origin of porcine satellite cells affects in vitro differentiation potential." Cell Biochem Funct **28**(5): 403-411.
Reich, N. C. (2009). "STAT3 revs up the powerhouse." Sci Signal **2**(90): pe61.
Robson-Ansley, P., E. Cockburn, et al. (2010). "The effect of exercise on plasma soluble IL-6 receptor concentration: a dichotomous response." Exerc Immunol Rev **16**: 56-76.
Rosenblatt, J. D., D. Yong, et al. (1994). "Satellite cell activity is required for hypertrophy of overloaded adult rat muscle." Muscle Nerve **17**(6): 608-613.
Rosendal, L., K. Sogaard, et al. (2005). "Increase in interstitial interleukin-6 of human skeletal muscle with repetitive low-force exercise." J Appl Physiol **98**(2): 477-481.
Rudnicki, M. A., F. Le Grand, et al. (2008). "The molecular regulation of muscle stem cell function." Cold Spring Harb Symp Quant Biol **73**: 323-331.
Sajko, S., L. Kubinova, et al. (2004). "Frequency of M-cadherin-stained satellite cells declines in human muscles during aging." J Histochem Cytochem **52**(2): 179-185.

Sato, N., T. Yamamoto, et al. (2003). "Involvement of heat-shock protein 90 in the interleukin-6-mediated signaling pathway through STAT3." Biochem Biophys Res Commun **300**(4): 847-852.
Schafer, K. A. (1998). "The cell cycle: a review." Vet Pathol **35**(6): 461-478.
Seale, P. and M. A. Rudnicki (2000). "A new look at the origin, function, and "stem-cell" status of muscle satellite cells." Dev Biol **218**(2): 115-124.
Seale, P., L. A. Sabourin, et al. (2000). "Pax7 is required for the specification of myogenic satellite cells." Cell **102**(6): 777-786.
Seidel, H. M., L. H. Milocco, et al. (1995). "Spacing of palindromic half sites as a determinant of selective STAT (signal transducers and activators of transcription) DNA binding and transcriptional activity." Proc Natl Acad Sci U S A **92**(7): 3041-3045.
Serrano, A. L., B. Baeza-Raja, et al. (2008). "Interleukin-6 is an essential regulator of satellite cell-mediated skeletal muscle hypertrophy." Cell Metab **7**(1): 33-44.
Setati, M. M., E. Prinsloo, et al. (2010). "Leukemia inhibitory factor promotes Hsp90 association with STAT3 in mouse embryonic stem cells." IUBMB Life **62**(1): 61-66.
Spangenburg, E. E. and F. W. Booth (2002). "Multiple signaling pathways mediate LIF-induced skeletal muscle satellite cell proliferation." Am J Physiol Cell Physiol **283**(1): C204-211.
Sun, L., K. Ma, et al. (2007). "JAK1-STAT1-STAT3, a key pathway promoting proliferation and preventing premature differentiation of myoblasts." J Cell Biol **179**(1): 129-138.
Taga, T. and T. Kishimoto (1997). "Gp130 and the interleukin-6 family of cytokines." Annu Rev Immunol **15**: 797-819.
Takahashi, T., H. Abe, et al. (2005). "Activation of STAT3/Smad1 is a key signaling pathway for progression to glomerulosclerosis in experimental glomerulonephritis." J Biol Chem **280**(8): 7100-7106.
Takai, Y., G. G. Wong, et al. (1988). "B cell stimulatory factor-2 is involved in the differentiation of cytotoxic T lymphocytes." J Immunol **140**(2): 508-512.
Takeda, K., T. Kaisho, et al. (1998). "Stat3 activation is responsible for IL-6-dependent T cell proliferation through preventing apoptosis: generation and characterization of T cell-specific Stat3-deficient mice." J Immunol **161**(9): 4652-4660.
Tauber, Z., V. Lichnovsky, et al. (1996). "[PCNA (proliferating cell nuclear antigen) in the tissues and organs of the human fetus. II]." Acta Univ Palacki Olomuc Fac Med **140**: 29-32.
Thiel, S., H. Dahmen, et al. (1998). "Constitutive internalization and association with adaptor protein-2 of the interleukin-6 signal transducer gp130." FEBS Lett **441**(2): 231-234.
Torres, J. and F. M. Watt (2008). "Nanog maintains pluripotency of mouse embryonic stem cells by inhibiting NFkappaB and cooperating with Stat3." Nat Cell Biol **10**(2): 194-201.
Tracey, K. J. and A. Cerami (1992). "Pleiotropic effects of TNF in infection and neoplasia: beneficial, inflammatory, catabolic, or injurious." Immunol Ser **56**: 431-452.
Trenerry, M. K., K. A. Carey, et al. (2007). "STAT3 signaling is activated in human skeletal muscle following acute resistance exercise." J Appl Physiol **102**(4): 1483-1489.
Trotter, J. A. and M. Nameroff (1976). "Myoblast differentiation in vitro: morphological differentiation of mononucleated myoblasts." Dev Biol **49**(2): 548-555.
Tseng, W. P., C. M. Su, et al. (2010). "FAK activation is required for TNF-alpha-induced IL-6 production in myoblasts." J Cell Physiol **223**(2): 389-396.
van der Bruggen, T., E. Caldenhoven, et al. (1995). "Interleukin-5 signaling in human eosinophils involves JAK2 tyrosine kinase and Stat1 alpha." Blood **85**(6): 1442-1448.
Velcheti, V. and R. Govindan (2006). "Insulin-like growth factor and lung cancer." J Thorac Oncol **1**(7): 607-610.
Velleman, S. G., X. Zhang, et al. (2010). "Changes in satellite cell proliferation and differentiation during turkey muscle development." Poult Sci **89**(4): 709-715.

Vindelov, L. L., I. J. Christensen, et al. (1983). "A detergent-trypsin method for the preparation of nuclei for flow cytometric DNA analysis." Cytometry **3**(5): 323-327.
Volonte, D., Y. Liu, et al. (2005). "The modulation of caveolin-1 expression controls satellite cell activation during muscle repair." FASEB J **19**(2): 237-239.
Wang, K., C. Wang, et al. (2008). "JAK2/STAT2/STAT3 are required for myogenic differentiation." J Biol Chem **283**(49): 34029-34036.
Wang, P., F. Zhu, et al. (2010). "Shear-induced interleukin-6 synthesis in chondrocytes: roles of E prostanoid (EP) 2 and EP3 in cAMP/protein kinase A- and PI3-K/Akt-dependent NF-kappaB activation." J Biol Chem **285**(32): 24793-24804.
Wang, X., H. Wu, et al. (2008). "Effects of interleukin-6, leukemia inhibitory factor, and ciliary neurotrophic factor on the proliferation and differentiation of adult human myoblasts." Cell Mol Neurobiol **28**(1): 113-124.
Webster, C. and H. M. Blau (1990). "Accelerated age-related decline in replicative life-span of Duchenne muscular dystrophy myoblasts: implications for cell and gene therapy." Somat Cell Mol Genet **16**(6): 557-565.
Wegrzyn, J., R. Potla, et al. (2009). "Function of mitochondrial Stat3 in cellular respiration." Science **323**(5915): 793-797.
Wei, Q. and B. M. Paterson (2001). "Regulation of MyoD function in the dividing myoblast." FEBS Lett **490**(3): 171-178.
Wen, Z., Z. Zhong, et al. (1995). "Maximal activation of transcription by Stat1 and Stat3 requires both tyrosine and serine phosphorylation." Cell **82**(2): 241-250.
White, J. D., M. Davies, et al. (2001). "Leukaemia inhibitory factor increases myoblast replication and survival and affects extracellular matrix production: combined in vivo and in vitro studies in post-natal skeletal muscle." Cell Tissue Res **306**(1): 129-141.
Wirt, S. E., A. S. Adler, et al. (2010). "G1 arrest and differentiation can occur independently of Rb family function." J Cell Biol **191**(4): 809-825.
Yang, C., S. P. Atkinson, et al. (2010). "Opposing Putative Roles for Canonical and Non-Canonical NFkappaB Signaling on the Survival, Proliferation and Differentiation Potential of Human Embryonic Stem Cells." Stem Cells.
Yang, J., X. Liao, et al. (2007). "Unphosphorylated STAT3 accumulates in response to IL-6 and activates transcription by binding to NFkappaB." Genes Dev **21**(11): 1396-1408.
Yang, Y., Y. Xu, et al. (2009). "STAT3 induces muscle stem cell differentiation by interaction with myoD." Cytokine **46**(1): 137-141.
Yu, Z., W. Zhang, et al. (2002). "Signal transducers and activators of transcription 3 (STAT3) inhibits transcription of the inducible nitric oxide synthase gene by interacting with nuclear factor kappaB." Biochem J **367**(Pt 1): 97-105.
Zimmerman, M. A., C. H. Selzman, et al. (2002). "Interleukin-11 attenuates human vascular smooth muscle cell proliferation." Am J Physiol Heart Circ Physiol **283**(1): H175-180.